2015

The Role of Central Metabolism and Electron Transport in Biofilm Formation by Vibrio fischeri

Jakob Michael Ondrey
Loyola University Chicago

LOYOLA UNIVERSITY CHICAGO

THE ROLE OF CENTRAL METABOLISM AND ELECTRON TRANSPORT IN BIOFILM FORMATION BY *VIBRIO FISCHERI*

A THESIS SUBMITTED TO

THE FACULTY OF THE GRADUATE SCHOOL

IN CANDIDACY FOR THE DEGREE OF

MASTER OF SCIENCE

PROGRAM IN MICROBIOLOGY AND IMMUNOLOGY

BY

JAKOB MICHAEL ONDREY

CHICAGO, IL

DECEMBER 2015

ACKNOWLEGEMENTS

I would like to thank my mentor, Dr. Karen L. Visick, for her patience, encouragement, and guidance. I would also like to thank all the past and present members of the Visick lab for their good advice and gracious help. Last, but not least, I would like to thank my family and friends for their encouragement and support.

For my wife, Jessica,
and my boys,
Calvin and Rhys

TABLE OF CONTENTS

LIST OF TABLES

LIST OF FIGURES

ABSTRACT

Biofilms protect bacteria from environmental threats, including antibiotics; thus, biofilms formed during infections pose an increasing threat to human health. A natural model used to study biofilm formation in the context of a host is the symbiosis between *Vibrio fischeri* and its host, the squid *Euprymna scolopes*. Successful colonization depends on the formation of a biofilm and genes involved in making the polysaccharide matrix component, *syp*. In culture, biofilm phenotypes, including the formation of wrinkled colonies, similarly depend on *syp*. However, little is known about other factors that contribute to this phenotype. To expand the utility of currently available genetic tools, I developed a Tn*5* transposon containing an outward facing *lac* promoter and a *V. fischeri* strain expressing *lacI* with which to control that promoter. To search for genes with previously uncharacterized roles in biofilm formation, I mutagenized the lacI-expressing biofilm-forming strain, and screened for mutants that failed to form wrinkled colonies. As expected, my screen for biofilm-defective smooth colonies yielded mutants of *syp* genes as well as other genes known to be required for biofilm formation. Several other mutants with disruptions in genes involved in central metabolism and electron transport we also isolated. Next, I shifted my attention to characterizing these mutant strains. Mutants lacking *glnA*, which encodes glutamine synthetase, exhibited a severe biofilm defect that could be rescued by the addition of glutamine, its product. A mutant defective for *mdh* (malate dehydrogenase) displayed an intermediate (diminished wrinkling) biofilm phenotype

which could also be rescued by the addition of glutamine. Mutants lacking *pck*, which encodes PEP carboxykinase, also exhibited a severe biofilm defect, displaying not only a smooth colony phenotype but also adhering to the agar surface. I was unable to identify conditions that fully rescued the biofilm defect, but the addition of gluconeogenic carbon sources such as glucose abrogated the adherence phenotype. An *sdhE* mutant formed smooth colonies with small divots after prolonged growth, and an independently isolated *sdhC* mutant was similarly biofilm-defective; both mutants have defects in production of the succinate dehydrogenase complex. Of note was the phenotypes of three electron transport system mutants with insertions within two *nqr* (Na^+-translocating NADH:ubiquinone oxidoreductase) genes and the *ubiG* (ubiquinone biosynthesis) gene: these mutants exhibited an extreme ability to strongly adhere attach to each other and/or the agar surface under biofilm-inducing conditions. The *nqr* phenotype required the production of Syp polysaccharide. Together, my work indicates a link between the metabolic state of the cell and biofilm formation.

CHAPTER ONE

LITERATURE REVIEW

I. Introduction

A bacterial biofilm is a community of microbes attached to a surface and encased within a protective extracellular matrix. This state, rather than the single-celled planktonic state, is thought to be the predominant form of the bacterial kingdom. One defining characteristic of a biofilm is the presence of an extracellular matrix consisting of some combination of a polysaccharide component, extracellular proteins, and extracellular DNA (eDNA) (Reviewed in (Flemming and Wingender, 2010)). Due, in part, to this matrix, bacteria within a biofilm have increased resistance to a number of external threats such as host defenses (Donlan and Costerton, 2002) and antimicrobials (Mah, 2012). Thus, understanding the regulation of this natural phenomenon has become an important area of research. While many model organisms are used in the laboratory to study biofilm formation and the role of the biofilm in animal infection, few exist in which *in vitro* phenotypes can readily predict the ability to form *in vivo* biofilms and productively colonize a host. One such model system is the symbiosis between the bacterium *Vibrio fischeri* and its host, the squid *Euprymna scolopes*. Research using the *Vibrio*-squid model system has uncovered many factors that promote biofilm formation (Visick and Skoufos, 2001, Yip, Grublesky et al., 2005, Morris, Darnell et al., 2011, Ray

and Visick, 2012, Norsworthy and Visick, 2015, Ray, Driks et al., 2015, Singh, Brooks et al., 2015). However, our current knowledge of this natural phenomenon is likely incomplete and it is likely that many important mediators of biofilm formation in *V. fischeri* remain to be identified.

While the body of my work revolves around genes required for the formation of the biofilm, and thus colonization initiation, the state of the symbiont within the light organ is, as yet, unknown and may well be biofilm-like. Therefore, it is possible that genes that affect biofilm formation but not colonization initiation could have roles in persistence of *V. fischeri*. In the following sections, I discuss the *V. fischeri*-squid symbiosis and then summarize some of the bacterial factors known to play a role in the initiation and persistence of this association. I then provide background information necessary to provide the reader with appropriate context to fully appreciate the additional factors identified, investigated, and discussed in the results and discussion sections.

II. The colonization of the squid *Euprymna scolopes* by the marine bacterium *Vibrio fischeri*

The *V. fischeri*-squid symbiosis is an excellent model system for the study of symbiosis and biofilm formation because the ability of *V. fischeri* to form a biofilm *in vitro* correlates with its ability to form a biofilm *in vivo* and to colonize its host. However, the strength of the system can only be appreciated after first understanding the colonization process and the stages *V. fischeri* cells must successfully navigate to establish and maintain a mutualistic association with the squid host (Fig. 1). These steps will be described here.

When juvenile squid hatch from their eggs, they lack their symbiont and must acquire it from the surrounding seawater (Wei and Young, 1989). This process is known to be extremely efficient: in their natural habitat, the coasts of Hawaii, no uncolonized squid has been captured (Stabb and Visick, 2013). Thus, researchers in the laboratory can control colonization by incubating eggs in seawater free of the symbiont, and subsequently adding *V. fischeri* (or mutant strains) to initiate colonization in an experimentally controlled manner.

Shortly after hatching, the squid begins to secrete mucus at the surface of its symbiotic organ, the light organ, which houses *V. fischeri* in colonized animals (Fig. 1) (Nyholm, Stabb et al., 2000, Altura, Heath-Heckman et al., 2013). This mucus, as well as surface-located cilia, promote the attachment of *V. fischeri* to the surface of the light organ (McFall-Ngai and Ruby, 1991). Little is known about the bacterial factors that mediate the initial attachment to the surface of the light organ, although the *V. fischeri* genome contains 10 pili loci that could play a role in this process. Initial studies into the mannose-sensitive hemagglutinin (Msh) adhesin showed that *V. fischeri* cells conditioned in mannose exhibited a squid colonization defect that the researchers suggested could be due to the non-productive binding of the adhesin to the soluble mannose rather than a host receptor based mannose (McFall-Ngai, Brennan et al., 1998). This hypothesis has never been confirmed, however, and a number of other pili exist that could also play a role in the initial attachment process.

After attachment to the surface of the light organ, *V. fischeri* cells form a biofilm (Nyholm, Stabb et al., 2000). The formation of this biofilm requires the activation of a sensory protein called RscS (Visick and Skoufos, 2001), the expression of the alternative

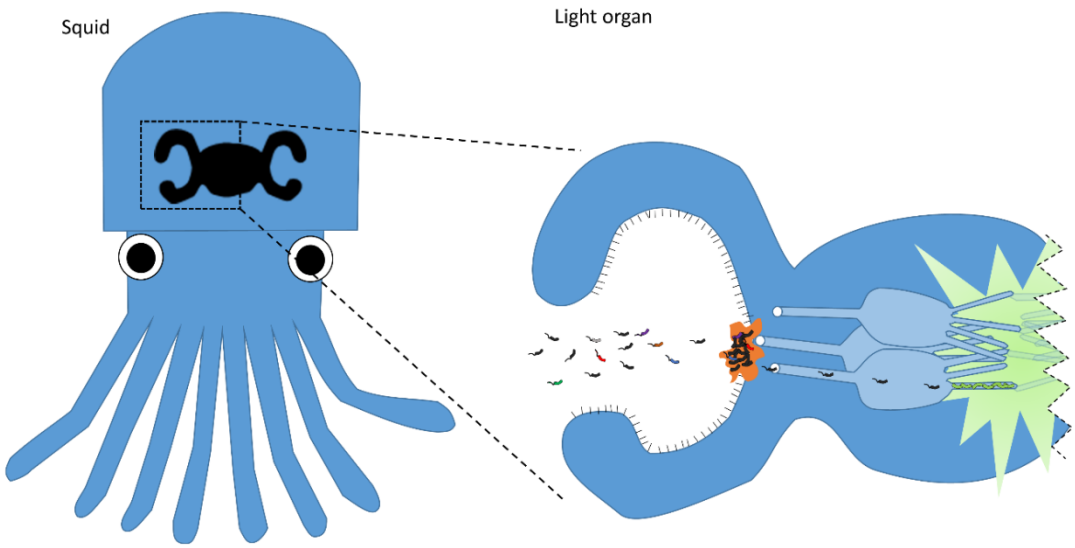

Figure. 1 - Colonization of *E. scolopes* by *V. fischeri*. The light organ (black structure) of *E. scolopes* is located under the mantle of the squid and is uncolonized upon hatching. After hatching, the squid begins secreting mucus (orange) onto the surface of the light organ near the pores. A variety of microbes are present in the seawater and a subset of them, including *V. fischeri* (Black cells) will encounter the mucus and cilia and attach to the cilia. It is here that *V. fischeri* form a biofilm and increase in number. *V. fischeri* cells then disperse from the biofilm and migrate into the pores, through the antechambers, and into the deep crypts (finger-like extensions) of the light organ. Once in the deep crypts, they grow and eventually reach a cell density sufficient to trigger bioluminescence.

sigma factor σ^{54} encoded by the *rpoN* gene (Wolfe, Millikan et al., 2004), and the expression of the symbiosis polysaccharide (*syp*) locus (Yip, Grublesky et al., 2005) (Fig. 2). The transcription and translation of the *syp* locus leads to the production of the Syp polysaccharide (Syp PS), a major component of the symbiotic biofilm (Yip, Geszvain et al., 2006, Shibata, Yip et al., 2012). *V. fischeri* strains unable to produce the Syp PS, due to mutations within the *syp* genes or the regulatory pathway that activates the locus, are unable to colonize squid, while strains that overproduce the Syp PS outcompete wild-type strains in competition assays (Yip, Geszvain et al., 2006). Recent work has also identified a requirement for the two genes *dnaJ* and *dnaK* in the formation of the Syp biofilm (Brooks, Gyllborg et al., 2014). The formation of a biofilm as a stage in a beneficial animal infection is one strength of this system in the study of biofilm formation. More details on the regulation of this vital step in biofilm formation and efficient colonization will be provided below.

After the biofilm forms, the bacteria must then disperse to reach the sites of colonization. In many microbes, the small molecule cyclic-di-GMP (c-di-GMP) is known to mediate the dispersal process. When the levels of c-di-GMP are high, genes with roles in biofilm formation are promoted and motility is inhibited while low levels of the molecule do the opposite and promote motility while repressing biofilm formation (Romling, Gomelsky et al., 2005). The regulatory process that induces bacteria to transition from the symbiotic biofilm is unclear in *V. fischeri*, but it is likely that c-di-GMP plays a role as disruption of genes promoting the production of c-di-GMP promote motility (O'Shea, Klein et al., 2006). σ^{54} (the sigma factor required for biofilm formation) is also required for the transcription of many of the genes required for motility and

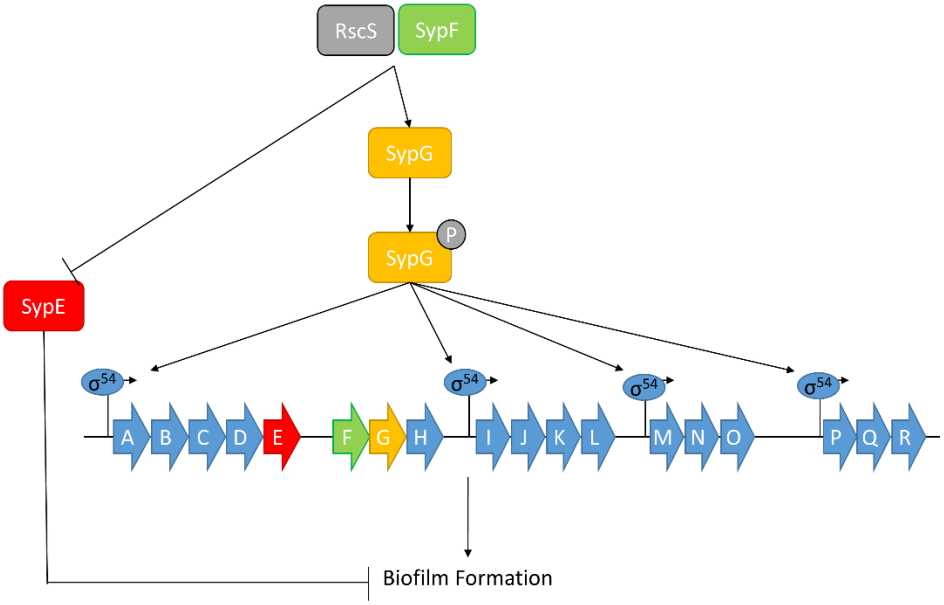

Figure 2 - The regulation of Syp polysaccharide production. The transmembrane sensor kinase protein RscS senses a signal, auto-phosphorylates, then donates its phosphoryl group to SypF. SypF then donates the phosphoryl group to either SypE or SypG. Phosphorylation deactivates the inhibitor (SypE) and activates transcription of the *syp* locus through SypG. Transcription of the *syp* locus also requires the sigma factor σ^{54}. The proteins of the *syp* locus are predicted to assemble and export the Syp PS, which is required for biofilm formation and squid colonization.

chemotaxis, behaviors that are hallmarks of dispersed cells. Thus, a molecule that could quickly mediate a switch between the biofilm and planktonic states is likely required and c-di-GMP is an exciting candidate for this role. The specific role of c-di-GMP has not been greatly studied in *V. fischeri* but remains an area of interest.

Once the cells have dispersed from the biofilm, they travel into the light organ through any of six pores (three pores are located on each side) and traverse through an antechamber to ultimately reach the deep crypts of the light organ. For this migration to occur, *V. fischeri* cells must be able to engage in a number of activities, including motility and chemotaxis. *V. fischeri* is motile through the use a tuft of flagella located at one of its poles (Ruby and Asato, 1993). Flagallar motility mutants are able to form a biofilm outside of the light organ, but do not efficiently colonize the host, likely because they lack the ability to migrate from the biofilm (Nyholm, Stabb et al., 2000). Similarly, chemotaxis mutants have a decreased ability to colonize the light organ of the squid (Hussa, O'Shea et al., 2007, Deloney-Marino and Visick, 2012). Chemotaxis is the process whereby bacteria direct their motion, typically away from threats or toward nutrients, via chemoreceptors that recognize specific molecules and subsequently modulate motility. Genome sequencing has identified nearly 40 chemoreceptors in *V. fischeri* (Ruby, Urbanowski et al., 2005) and research has shown that amino acids can serve as chemoattractants (DeLoney-Marino, Wolfe et al., 2003) as can other molecules (Nyholm, Stabb et al., 2000, DeLoney-Marino, Wolfe et al., , 2003, Mandel, Schaefer et al., 2012). A strain with a mutant allele of *cheY*, a regulator that modulates the transition from tumbles to runs, is unable to compete with wild-type strains in co-colonization assays (Hussa, O'Shea et al., 2007). While a full understanding of the regulation and roles

of motility and chemotaxis has not been attained, the necessity for these processes in squid colonization is clear.

As *V. fischeri* cells migrate deeper into the light organ, they encounter a number of host defense factors, including nitric oxide (NO), in the squid-secreted mucus (Davidson, Koropatnick et al., 2004) and host immune cells called hemocytes (Koropatnick, Engle et al., 2004). Davidson et al. showed that the addition to the seawater of rutin hydrate, an NO scavenging molecule, promoted the accumulation of non-*V. fischeri* cells in the squid-associated biofilm, suggesting that NO inhibits non-symbionts (Davidson, Koropatnick et al., 2004). More recent inquiries into the mechanism by which *V. fischeri* senses and responds to NO have identified the *hnoX* gene, which encodes a well-conserved NO sensing protein (Wang, Dufour et al., 2010). Wang et al. showed that HnoX bound NO and down-regulated a number of genes in response to activation; however, the genes identified had roles in iron sequestration rather than NO resistance (Wang, Dufour et al., 2010), suggesting a role for NO in priming *V. fischeri* cells for entry into the iron-limiting environment of the light organ.
E. scolopes' rudimentary immune system consists of hemocytes, a phagocytic cell type similar to a macrophage. The squid hemocytes regularly come into contact with *V. fischeri* cells both during their migration and throughout the life of the adult animal. However, the hemocytes show reduced binding to *V. fischeri* cells (Nyholm and McFall-Ngai, 1998, Nyholm, Stewart et al., 2009). Investigation into this phenomenon revealed that the outer membrane protein OmpU was vital to this process, as *V. fischeri* strains lacking OmpU were bound and engulfed by the hemocytes (Nyholm, Stewart et al.,

2009). Thus, the presence of OmpU is important for the recognition and prevention of phagocytosis of the *V. fischeri* cells by the hemocytes.

Once cells have completed their migration to the deep crypts, they begin prolific expansion as well as a reduction in cell size (Ruby and Asato, 1993). The enzymatic activity of *V. fischeri* isolated from colonized animals suggest that the cells are primarily utilizing anaerobic respiration (Proctor and Gunsalus, 2000). It was also shown by Graf and Ruby that the light organ of the squid is rich in amino acids (Graf and Ruby, 1998). These researchers hypothesized that squid-supplied amino acids serve as a major nutrient source for colonized *V. fischeri* cells. Indeed, a number of amino acid auxotrophs have been shown to be defective in squid colonization (Graf and Ruby, 1998). While it is clear that the ability to utilize an important nutrition source in the context of light organ would be vital to the ability of cells to grow in this niche, it is unclear what specific role these amino acids have in the colonization process. Further research will need to be conducted to identify the specific roles of these amino acids.

As their numbers grow, *V. fischeri* cells release pheromones, called autoinducers, which are sensed by neighboring cells and induce the activation of response pathways once the autoinducers reach a critical concentration. This system, called quorum sensing, regulates the induction of bioluminescence (Waters and Bassler, 2005). Once *V. fischeri* cells reach a high concentration within the light organ, the bioluminescence genes are induced and the cells begin to produce light. The direction and intensity of the light emitted from the light organ can likely be controlled through the use of various mechanisms such as a reflective surface and occlusion by ink from the squid's ink sac that surrounds the light organ (McFall-Ngai and Montgomery, 1990). This phenomenon

highlights another strength of this model system: colonization can be assessed without sacrificing the animal by measuring the luminescence of the squid (Ruby and Asato, 1993).

The predominant hypothesis as to how *E. scolopes* benefits from colonization by *V. fischeri* posits that the light emitted from the bacteria provides counter-illumination for the squid, thus preventing predation (Wei and Young, 1989, Jones and Nishiguchi, 2004, Stabb and Millikan, 2009). If this is so, *V. fischeri* cells with bioluminescence defects could be considered "cheaters" because they don't benefit the squid. Indeed, while luminescence mutant strains can colonize the light organ of the squid in single strain colonization experiments, colonization levels decrease over time (Visick, Foster et al., 2000, Whistler and Ruby, 2003) and the squid remains amenable for further colonization by additional *V. fischeri* cells (Koch, Miyashiro et al., 2014). Additionally, in competition experiments, bioluminescence-defective strains are quickly outcompeted and do not persist (Visick, Foster et al., 2000, Bose, Rosenberg et al., 2008). Researchers have investigated the mechanism by which the squid detects the presence of light in the light organ and findings such as the presence of light organ cells that express eye-specific genes are providing much needed insight into possible mechanisms (Peyer, Pankey et al., 2014). One intriguing microbe-centric explanation proposed for the increased fitness of bioluminescent-competent symbionts is the ability of the cells to remove oxygen (Visick, Foster et al., 2000). Increased oxygen concentrations within the environment or the cell can be detrimental to the health of the bacteria as the oxygen can be converted into H_2O_2 and/or other chemicals toxic to colonizing cells. There is evidence that the squid releases oxygen into the light organ (Ruby and McFall-Ngai, 1999). Utilization of

bioluminescence as a means to convert O_2 into inert molecules like H_2O could provide a fitness advantage to luminescence-competent cells.

Finally, once colonization has been established, the squid does not simply allow a high level of colonization for the remainder of its life. Rather, as it buries itself in the sand at dawn, it vents a large proportion of the bacteria out of its light organ (Ruby and Asato, 1993, Boettcher, Ruby et al., 1996), thus decreasing cell numbers below the levels needed for quorum-sensing and bioluminescence (Boettcher, Ruby et al., 1996), and decreasing the burden required to feed and maintain the culture. Furthermore, there is some evidence that following the venting, the host releases membrane bound "blebs" into the crypts of the light organ (Wier, Nyholm et al., 2010). Like many microbes that colonize animal hosts, *V. fischeri* must acquire iron within the iron-limited environment of its host and it has been hypothesized that these blebs could contain iron for the remaining *V. fischeri* cells (Septer, Wang et al., 2011). This hypothesis is supported by the observation that *V. fischeri* heme transport genes are also upregulated immediately after venting (Wier, Nyholm et al., 2010).

By leveraging the strengths of this model system, the ability to control the initiation of colonization, the requirement for a biofilm, and the ability to use luminescence as a colonization and persistence reporter, many strides have been made in identifying the bacterial genes that mediate biofilm formation and the initiation and persistence of colonization. In the following sections, I will discuss in greater detail the factors currently known to be important for biofilm formation, a key early stage in the colonization process.

III. Bacterial factors mediating biofilm formation

To colonize its squid host, *V. fischeri* first attaches to the surface of the light organ and forms a biofilm as described above. While there are a number of bacterial factors required or hypothesized to be required in this process, three are particularly important for my work: the Syp polysaccharide, the Bmp proteins, and the cysteine biosynthesis pathway. These factors will be described in greater detail here.

The Syp polysaccharide

The symbiosis polysaccharide locus (*syp*) is comprised of 18 genes, of which four encode regulatory proteins and 14 encode structural proteins responsible for the production and export of the Syp polysaccharide (Syp PS) (Fig. 2) (Yip, Grublesky et al., 2005, Yip, Geszvain et al., 2006, Shibata, Yip et al., 2012). This polysaccharide is secreted and is a major component of the extracellular matrix in *V. fischeri* biofilms. Production and secretion of the Syp PS is required for biofilm formation in the mucus near the pores of the squid's light organ and, as a consequence, *syp* mutant strains fail to colonize the squid. In addition to a defect in squid colonization, these mutants exhibit defects in biofilm phenotypes observed in culture, including the formation of wrinkled colonies on agar plates and pellicles at the air/liquid interface of static cultures (Yip, Geszvain et al., 2006, Darnell, Hussa et al., 2008, Hussa, Darnell et al., 2008, Shibata, Yip et al., 2012, Morris and Visick, 2013). The composition of the polysaccharide (the identity of the monosaccharides in the polysaccharide chain) is as yet unknown, but the presence of the polysaccharide promotes cell-cell associations: strains that overproduce the Syp PS exhibit a strong cohesive phenotype: when colonies formed by these strains are disturbed with a toothpick, the whole colony is displaced as a unit (Fig. 3) (Ray,

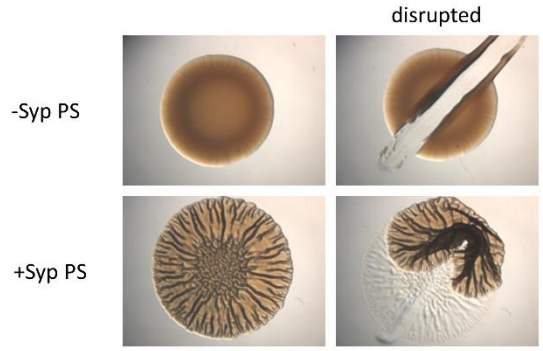

Figure 3 - Disruption of a *V. fischeri* biofilm. *V. fischeri* cells that do not produce the Syp PS do not wrinkle and are readily disrupted when a toothpick is drawn through a colony (top). In contrast, the production of the Syp PS results in a colony that forms a wrinkled phenotype and exhibits cell-cell cohesion when disrupted with a toothpick. Representative images are shown.

Driks et al., 2015). In contrast, non-biofilm-forming cells are not strongly cohesive, and their colonies are readily disrupted.

Increased transcription of the *syp* locus, and therefore increased production of the Syp PS, is activated by the transmembrane sensor kinase (SK) protein RscS (Yip, Geszvain et al., 2006). SK proteins auto-phosphorylate when they sense certain environmental signals and then donate that phosphoryl group to response regulator (RR) protein(s) to elicit a cellular response to that signal. While the identity of the environmental signal that activates RscS remains elusive, recent work has determined that RscS passes its phosphoryl groups to its RRs through an intermediary SK, SypF (Norsworthy and Visick, 2015). After receiving the phosphoryl group from RscS, SypF passes it to the two RRs that are encoded by the *syp* locus, SypE and SypG (Hussa, Darnell et al., 2008, Morris, Darnell et al., 2011, Norsworthy and Visick, 2015). When these two RRs are phosphorylated, SypE, an inhibitor of polysaccharide production, is deactivated, and SypG, a transcription factor, is activated to promote transcription of the *syp* locus and production of the Syp PS (Ray, Eddy et al., 2013). In *in vitro* cultures of *V. fischeri*, overexpression of *rscS* on a multi-copy plasmid also increases the production of the Syp PS, allowing researchers to study biofilm formation on a petri plate outside of the squid (Yip, Geszvain et al., 2006). In summary, activation of RscS leads to the production of Syp PS through the *syp* locus.

The role of the Bmp proteins in biofilm formation

In addition to promoting transcription of the *syp* locus, activated SypG also promotes transcription of three small operons, one of which is located adjacent to the *syp* locus. Each of these operons encode an extracellular biofilm maturation protein (Bmp)

and a putative biofilm associated lipopolysaccharide (Bal). The BmpA, B, and C proteins appear to have overlapping function (Ray, Driks et al., 2015). The loss of the Bmp proteins in a *bmpABC* triple mutant strain results in an *in vitro* biofilm that fails to exhibit the wrinkling phenotype characteristic of *V. fischeri* biofilms. However, the mutant strain maintains the cohesive properties of a Syp PS producing strain (Ray, Driks et al., 2015). Although the *bmpABC* mutant strain retains biofilm properties, these genes clearly play a role in the architecture of the biofilm: when *bmpABC* triple mutant cells are mixed with cells that do make and export the Bmp proteins, the mixture of the two strains exhibits biofilm phenotypes.

The role of cysteine biosynthesis in biofilm formation

Recently, researchers have uncovered a role for cysteine biosynthesis in biofilm formation and squid colonization. *V. fischeri* cells defective for the *cysK* gene, which encodes the protein responsible for the last step in cysteine biosynthesis, forms smooth colonies on agar plates unless the plates are supplemented with exogenous cysteine (Singh, Brooks et al., 2015). As expected of a smooth colony mutant, the *cysK* mutant strain also exhibits colonization initiation defects, although it could eventually colonize the light organ when given enough time. Experiments with the *cysK* mutant also found that cysteine is likely secreted by wild-type *V. fischeri* cells: when a *cysK* mutant strain induced to form a biofilm is mixed with a strain not induced to form a biofilm but possessing an intact cysteine biosynthesis pathway, a biofilm will form (Singh, Brooks et al., 2015). These results uncovered a new level of biofilm regulation in *V. fischeri*.

IV. Identifying additional factors required for biofilm formation

Outside of the factors described above, relatively little is known about the genetic requirements for biofilm formation by *V. fischeri*. Therefore, my thesis work focused on identifying and characterizing new factors that play a role in biofilm formation and potentially colonization by *V. fischeri*. The *V. fischeri* biofilm matrix contains a polysaccharide component (Syp PS) (Yip, Geszvain et al., 2006), extracellular proteins (Bmp) (Ray, Driks et al., 2015), and likely other extracellular proteins as well as eDNA. The physical complexity and function of components within of the matrix suggest that the decision to form a biofilm, and thus commit cellular resources, is a costly one. Thus, it is likely that mechanisms are present to determine whether cells should commit to this transition as well as biosynthetic pathways necessary to produce the matrix components. This level of complexity would likely require a number of potential as-yet undescribed mechanisms of biofilm control. In this thesis, I will describe the work that revealed the involvement of central metabolism and electron transport genes in biofilm formation. Here, I provide an overview of the central metabolism and electron transport pathways that will be important for understanding my findings.

Bacterial metabolism

For any organism to thrive, it must be capable of replicating, and thus, producing additional copies of the cellular machinery and all other components within the cell. To do this, its metabolic pathways must be able to synthesize the precursors and products that cannot be acquired directly from its environment. *V. fischeri* cells must be able to survive in two different environments, nutritionally dilute seawater, and relatively nutrient-rich squid light organ (Ruby and Asato, 1993, Graf and Ruby, 1998). When

present in either of these environments, *V. fischeri* likely senses its location and activates alternative signaling and metabolic pathways causing the cells to behave differently. Likewise, interruption of these processes and pathways can lead to altered behavior and morphology and inform us of the pathways required for key developmental events such as biofilm formation.

The TCA cycle

The Tricarboxylic Acid (TCA) cycle is a conserved metabolic pathway that consumes acetate and produces CO_2 as a byproduct (Fig. 4). This pathway is central to aerobic respiration and conserved in all organisms that utilize aerobic respiration. As carbon is oxidized through this pathway, NAD^+ is reduced to NADH and additional molecules, such as amino acid precursors, are generated as intermediates and can exit the cycle. Defects in the TCA cycle can cause changes in the behavior and fitness of a cell. For example, in *Salmonella enterica* serovar Typhi, disruption of TCA cycle genes, including malate dehydrogenase (*mdh*) and those of the succinate dehydrogenase complex (*sdhCDAB*), increases the ability of the mutant strains to survive in mouse macrophages (Bowden, Ramachandran et al., 2010). In contrast, deletion of *sdhB* in uropathogenic *E. coli* causes a 50-fold growth defect in the bladders of mice (Alteri, Smith et al., 2009). In addition to its role in virulence and pathogenicity, a relationship between the TCA cycle and biofilm formation has also been previously characterized. In some organisms, such as *Staphylococcus epidermidis*, biofilm formation is correlated with a decrease in TCA cycle activity (Sadykov, Hartmann et al., 2011). It is hypothesized that this is due to the transitioning of the biofilm forming cells from aerobic respiration to alternate forms of metabolism, such as fermentation, that they can utilize

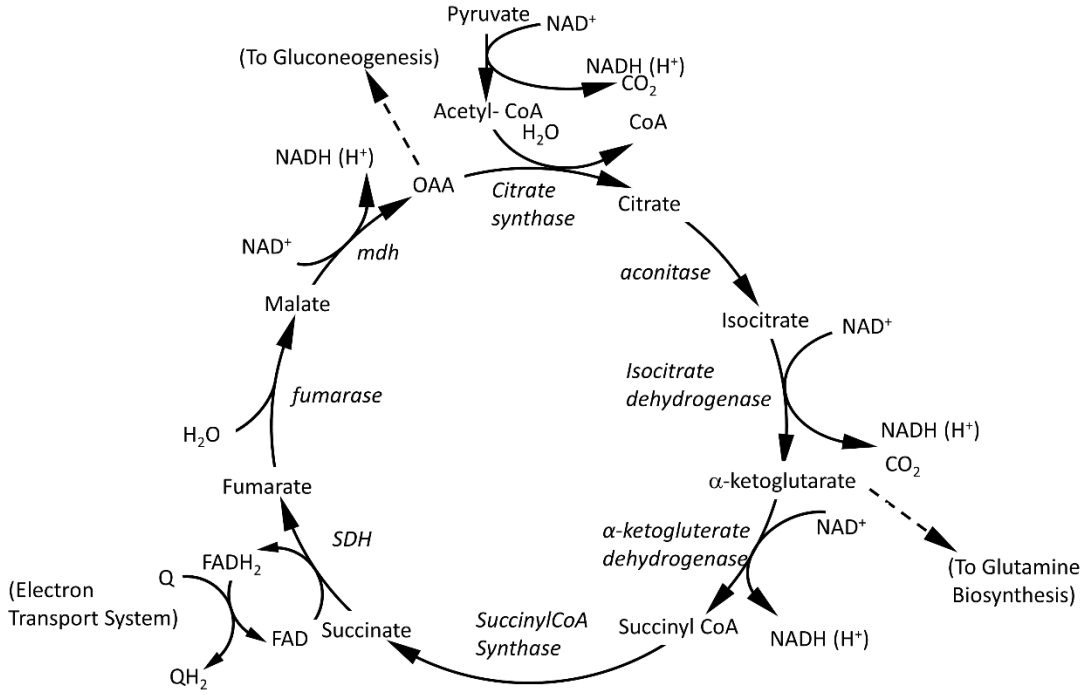

Figure 4 - The tricarboxylic acid (TCA) cycle. The TCA cycle is pictured. As pictured, acetate (from acetyl CoA) enters the TCA cycle as it is condensed with oxaloacetate into citrate. Relevant connected biosynthetic pathways, such as glutamine biosynthesis, electron transport, and gluconeogenesis, are indicated.

within the biofilm. Based on my work, I have identified a number of genes involved in the TCA cycle that play a role in biofilm formation by *V. fischeri*. Therefore, the following sections describe TCA cycle genes of interest.

The succinate dehydrogenase complex and *sdhE*

Succinate dehydrogenase (SDH) is the 5 protein complex that catalyzes the oxidation of succinate to fumarate, thus converting a flavin adenine dinucleotide (FAD) co-factor to $FADH_2$ (SDH) (Fig. 5) (Iverson, Luna-Chavez et al., 1999). In addition to its role in the TCA cycle, SDH also participates in the electron transport system as Complex II, where electrons from $FADH_2$ are removed from FAD and added to a ubiquinone molecule (Yankovskaya, Horsefield et al., 2003). Its specific role in electron transport will be elaborated on in a later section. The genes encoding the SDH complex are encoded in two separate operons. The first operon consists of *sdhCDAB* and encodes the catalytically active, membrane-associated components of the complex (Cecchini, Schroder et al., 2002). SdhC and SdhD are transmembrane proteins that function primarily in complex II's role in electron transport. SdhA is the subunit that serves as the primary TCA enzyme that catalyzes the oxidation of succinate to fumarate and the reduction of FAD to $FADH_2$. SdhB serves as a conduit through which electrons are shuttled from the $FADH_2$ molecule associated with SdhA to the ubiquinone associated with SdhC through three iron sulfur clusters.

The final component of the SDH complex is SdhE, which is encoded by a gene nearly 1.5 Mb away. SdhE has been shown in *Serratia* sp. to serve as a cytosolic activator of the membrane associated portion (McNeil, Clulow et al., 2012). For the Sdh complex to be active, SdhA must be loaded with the FAD co-factor that accepts protons as

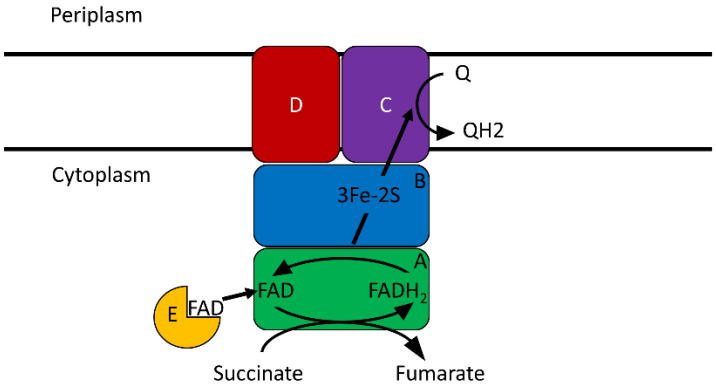

Figure 5 - The succinate dehydrogenase (SDH) complex. The SDH complex converts succinate to fumarate and is composed of 5 subunits; SdhA-D are membrane associated and SdhE is cytosolic. SdhE delivers a FAD co-factor to SdhA. The co-factor then serves as a proton acceptor as succinate is oxidized to fumarate and FAD is reduced to $FADH_2$. $FADH_2$ is then oxidized back into FAD as electrons are shuttled through iron-sulfur clusters in SdhB to SdhC where Q is reduced to QH_2.

succinate is oxidized. SdhE serves as the "flavinator" of the SDH complex. The genes regulating the activity of SdhE are unknown, as is the mechanism by which SdhE initially acquires its riboflavin molecule. SdhE is a promiscuous protein and has been shown recently to also activate the fumarase reductase complex (FRD), which catalyzes the reduction of fumarate to succinate (the reverse reaction of SDH) via the addition of the FAD co-factor (Fig. 6) (McNeil, Hampton et al., 2014). Deletion of *sdhE* in *Serratia* sp. results not only in an inability of cells to metabolize succinate and fumarate, but also causes additional phenotypes seemingly unrelated to these metabolic processes. These findings led to the hypothesis that SdhE may also provide FAD co-factors to other molecules (McNeil, Clulow et al., 2012). Identities of such "off target" proteins, other than FrdA, have not been described.

Malate dehydrogenase and *mdh*

Malate dehydrogenase (Mdh) catalyzes the oxidation of malate to oxaloacetate (OAA), reducing NAD to NADH in the process (Fig. 7) (van der Rest, Frank et al., 2000). OAA produced in this reaction can continue to cycle around the TCA cycle or exit the cycle along the gluconeogenic pathway (Fig. 8). The NADH produced in this reaction can be used by the electron transport system, which will be discussed in more detail shortly. Unlike the membrane bound SDH complex, Mdh is a single cytosolic protein that can also catalyze the reverse reaction. In *E. coli*, the Mqo protein has also been shown to catalyze the reaction, but bioinformatics searches could not identify a homolog of *mqo* in *V. fischeri*.

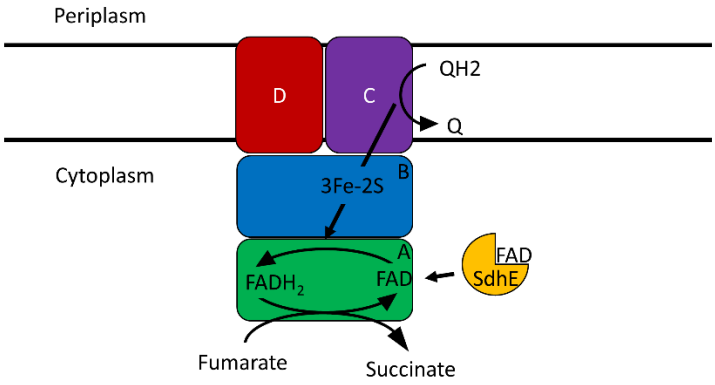

Figure 6 - The fumarate reductase (FRD) complex. The FRD complex reduces fumarate into succinate and is composed of 5 subunits; FrdA-D are membrane associated and SdhE (also a member of the SDH complex, is cytosolic. SdhE is hypothesized to provide the FAD co-factor to FrdA which can serve as an acceptor as electrons are shuttled through the Iron sulfur cluster of FrdB from the oxidation of QH_2. Once an $FADH_2$ is generated, fumatate can be reduced to succinate as $FADH_2$ is oxidized to FAD.

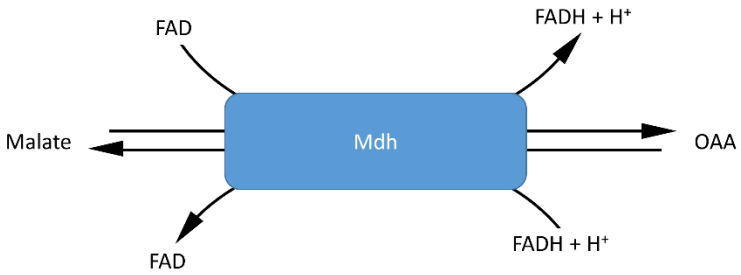

Figure 7 - Malate dehydrogenase (Mdh). Mdh is a cytosolic protein that catalyzes the oxidation of Malate to Oxaloacetate (OAA) as well as the reverse reaction. An FAD co-factor is reduced to $FADH_2$ in the process, or the reverse in the case of OAA reduction.

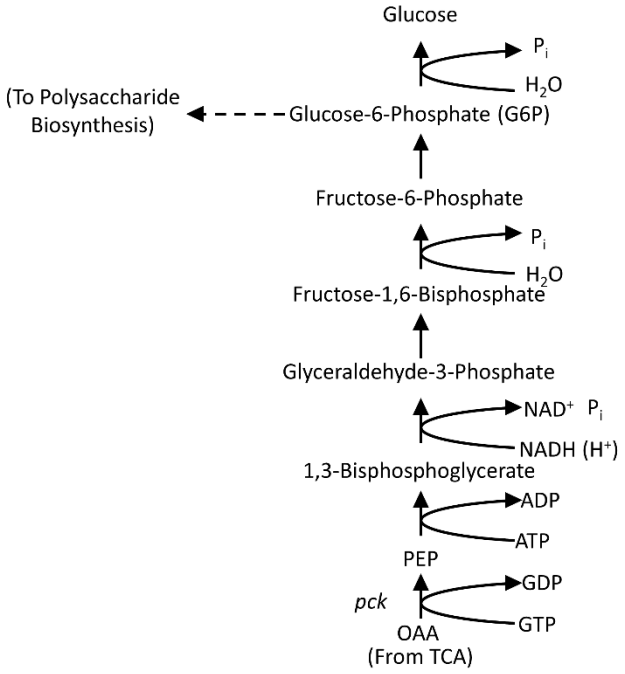

Figure 8 - Gluconeogenesis (GNG). Gluconeogenesis is the biosynthetic process of anabolizing glucose from TCA intermediates. Throughout this process, intermediates are hydrated and reduced. The GNG intermediate glucose-6-phosphate is necessary as an input in polysaccharide biosynthesis.

Gluconeogenesis

My work has identified a number of genes (including *mdh* described above) involved in gluconeogenesis (GNG) that also play a role in biofilm formation by *V. fischeri*. Additionally, other pathways known to be important in biofilm formation, such as polysaccharide production, likely also require GNG to generate precursor monosaccharides. Therefore, I will describe the hypothetical role of GNG in biofilm formation and then discuss the known functions of the GNG gene of interest.

GNG is the pathway responsible for the anabolism of glucose from smaller chains of carbon, such as amino acids or TCA cycle intermediates (Fig. 8). Organisms in nature are unlikely to find glucose in their environment and must synthesize it as a precursor to other vital molecules such as UDP- and ADP-glucose for polysaccharide biosynthesis. In the laboratory, *V. fischeri* is grown on LBS, a complex medium that primarily contains tryptone and yeast extract; therefore, amino acids serve as a primary carbon source (Dunlap and Kuo, 1992, Stabb, Reich et al., 2001). Thus, due to the role for GNG in the production of polysaccharide precursors from amino acids, this pathway should be vital to *in vitro* biofilm formation. In the squid, as well as seawater, *V. fischeri* cells are also not likely utilizing glucose as a primary nutrient source (Graf and Ruby, 1998) and, therefore, must anabolize the sugars required for Syp PS production and colonization.

Phosphoenolpyruvate carboxykinase (Pck)

The catalysis of OAA to phosphoenolpyruvate (PEP) pulls carbon out of the TCA cycle and begins the GNG pathway (Figs. 4 & 8). This reaction is mediated by the cytosolic enzyme phosphoenolpyruvate carboxykinase (Pck), encoded by the gene *pck*. The enzymatic activity of Pck utilizes the energy released by the hydrolysis of GTP to

GDP to decarboxylate and phosphorylate OAA (Fig. 9). This reaction is not reversible. The role of *pck* in PS production and biofilm formation by other bacteria has been previously described. For example, the activity of Pck is vital to the production of exopolysaccharide in *Myxococcus xanthus*, as this organism relies on sugars produced through gluconeogenesis rather than those present in its environment (Kim, Ramaswamy et al., 1999). As *M. xanthus* cultures exit exponential phase and enter stationary phase, Pck activity increases in conjunction with increases in polysaccharide production (Kim, Ramaswamy et al., 1999). Similarly, Osteras et al. described a decrease in root nodule formation, which involves another kind of symbiotic biofilm, during symbiosis of a number of plant species with a *pck* mutant strain of *Rhizobium* sp. (Osteras, Finan et al., 1991).

Electron transport system

I have also shown a number of genes involved in the electron transport system (ETS) to be important for biofilm formation by *V. fischeri*. In the following sections, I will describe the ETS and discuss the known functions of the identified ETS genes of interest.

Electron transport in bacteria occurs at the inner membrane and has the dual function of electron fixation to a terminal electron acceptor, such as oxygen, and the generation of an electrochemical gradient by the removal of protons from the cell. The electrochemical proton gradient is then used to drive ATP generation. In bacteria, the electron transport system generally consists of Complex I (an NADH:quinone oxidioreductase), Complex II (a succinate:quinone oxidioreductase), Complex III (a ubiquinol:cytochrome C reductase), Cytochrome C, Complex IV (a cytochrome C

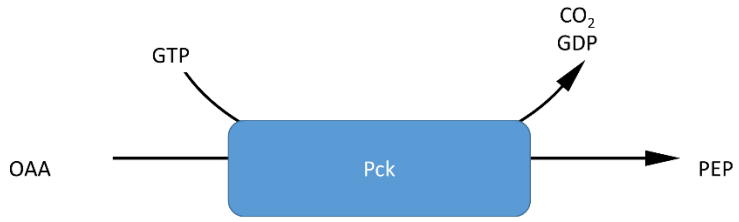

Figure 9 - Phosphoenolpyruvate carboxykinase (Pck). Pck is a cytosolic protein that decarboxylates and phosphorylates OAA, thus converting it to Phosphoenolpyruvate (PEP). To perform this activity, one molecule of GTP is hydrolyzed.

oxidase), and Complex V (an ATP synthase) (Keseler, Collado-Vides et al., 2011) (Fig. 10).

In the typical system, Complex I and Complex II transfer electrons from NADH and $FADH_2$, respectively, to ubiquinone (Q), resulting in ubiquinol (QH_2). QH_2 traffics to Complex III where QH_2 is oxidized, and the associated electrons are placed on molecules of Cytochrome C. The H^+ ions are pumped out of the cell, contributing to the proton gradient. The charged Cytochrome C molecules are then transferred to Complex IV where they are removed as Complex IV converts ½ O_2 and $2H^+$ions into H_2O and pumps out additional H^+ ions, further contributing to the proton gradient. Finally, all of the protons pumped out of the cell pass through the ATP synthase, resulting in the phosphorylation of ADP to ATP. This system is conserved in organisms that undergo aerobic respiration.

The role of SDH in electron transport

As noted above, the succinate dehydrogenase complex has roles in both the TCA cycle and electron transport. After the FAD cofactor is reduced to FADH, FADH is returned to its oxidized state and the associated electrons are shuttled through iron-sulfur bridges where they reduce Q to QH_2. QH_2 then traffics to Complex III and continues through the ETS, as described above, contributing to the proton gradient.

The role of ubiquinone biosynthesis in electron transport

One essential component of the electron transport system is the coenzyme ubiquinone (Q). Q is responsible for the trafficking of electrons from complexes I and II to complex III and without which the energy-generating potential of $NADH_2$ and FADH would be unrealized. Biosynthesis of Q (Fig. 11) requires the enzyme UbiG, a

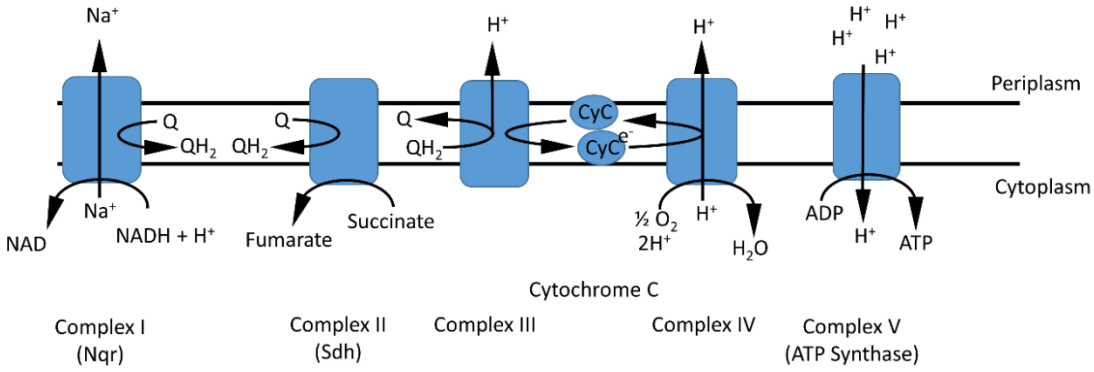

Figure 10 - The electron transport system (ETS). The ETS is composed of a number of membrane bound complexes, that generate an electrochemical gradient of protons by removing them from the cell. The system then uses that gradient to synthesize ATP. During this process, oxygen is used as an electron acceptor. Complex I of the ETS in *V. fischeri* is Na^+-NQR, which reduces ubiquinone (Q) to ubiquinol (QH_2) through the oxidation of NADH (and pumps Na^+ ions out of the cell in the process). Complex II (SDH) also generates molecules of QH_2, but does so through the oxidation of succinate. QH_2 molecules travel through the lipid center of the inner membrane to Complex III, which oxidizes QH_2, reduces cytochrome C (CyC), and pumps a proton out of the cell. Complex IV then oxidizes CyC by fixing the election onto oxygen, making water in the process, and removing an additional proton from the cell. Finally, the electrochemical gradient generated by the removal of protons from the cell is used to generate molecules of ATP as protons are allowed back into the cell.

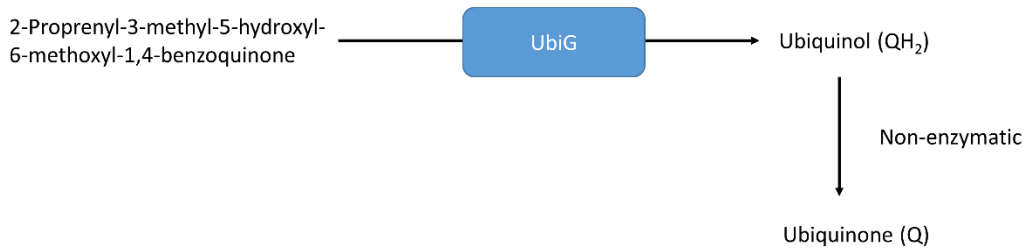

Figure 11 -The function of UbiG. UbiG mediates the final enzymatic reaction in ubiquinone (Q) biosynthesis by converting 2-Proprenyl-3-methyl-5-hydroxyl-6-methoxyl-1,4-benzoquinone to Ubiquinol (QH_2). The final step of Q biosynthesis is a non-enzymatic reaction that converts QH_2 to Q.

methyltransferase, for the final enzymatic reaction in the biosynthesis of Q (Poon, Barkovich et al., 1999, Meganathan, 2001). While a role for this pathway is not well studied in biofilm formation, research has established a role for Q, or more specifically a role for UbiG, in resistance to stress and longevity of cells. Briefly, *E. coli ubiG* mutants have increased resistance to oxidative stress and a delay in cell death after cultures enter stationary phase in an ArcA-dependent manner (Gonidakis, Finkel et al., 2011). Interestingly, ArcA, a transcription factor, modulates bioluminescence and quorum sensing in *V. fischeri* (Bose, Kim et al., 2007).

The role of the Na^+-Nqr in electron transport

In some marine bacteria, some of the functions of Complex I are carried out by Na^+-translocating NADH:quinone oxidoreductase complex (Na^+-Nqr) (Reyes-Prieto, Barquera et al., 2014) (Fig. 12). Na^+-Nqr is composed of 5 proteins, NqrA-F, that are encoded by the *nqr* locus. The enzymatic action of Na^+-Nqr begins as an NADH molecule binds to and is oxidized by NqrF and the associated electrons are transferred via an FAD molecule and two iron-sulfur bridges in NqrF to an FMN co-factor in NqrC. From there, the electrons are shuttled to an FMN, then to a riboflavin co-factor in NqrB, before finally reducing coenzyme Q. The free energy released by this reaction is used by NqrB, NqrD, and NqrE to pump Na^+ ions out of the cell. NqrA does not seem to play a catalytic role in the redox or Na^+-pumping roles of Na^+-Nqr, but appears to be vital for the assembly of the complex (Casutt, Huber et al., 2010).

As described above, rather than transporting H^+ ions out of the cell, as is common for most NADH:quinone oxidioreductase complexes, Na^+-Nqr transports Na^+ ions, contributing to the sodium motive force rather than the proton motive force. The Na^+

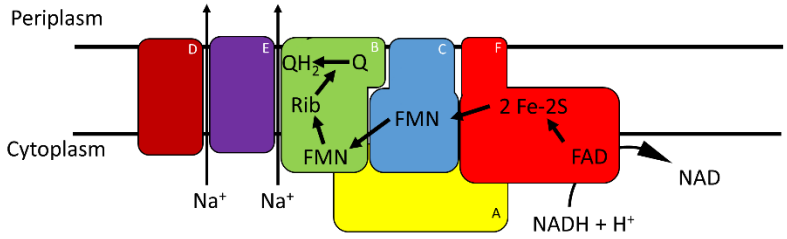

Figure 12 - The sodium translocating NADH:quinoneoxidioreductase (Na^+-NQR) complex. NADH is oxidized to NAD by NqrF and the electrons are shuttled via a FAD co-factor in NqrF to iron-sulfur bridges (also in NqrF). The electrons are then transported to a riboflavin co-factor in NqrB via FMN co-factors in NqrC and NqrB. They are used to reduce Q to QH_2. Energy released in the process is used to export sodium ions out of the cell.

motive force is responsible for driving flagellar motility in *V. cholerae* (Steuber, Halang et al., 2014). In addition, in this organism, reduction of the Na^+ motive force is correlated with increases in the production of virulence factors, such as Cholera Toxin (CT) and the Toxin Co-regulated Pilus (TCP) (Hase and Barquera, 2001). The role of Na^+-Nqr has not been described in *V. fischeri*, though all genes encoding the complex are present.

Amino acid and glutamine biosynthesis

I have identified one gene involved in the biosynthesis of the amino acid glutamine that plays a role in biofilm formation by *V. fischeri*. In many bacteria, glutamine serves as a nitrogen store and an important source of nitrogen in nitrogen-limiting conditions (Chandra, Basir et al., 2010). The synthesis of glutamine from its precursor, glutamate, is mediated by GlnA (Fig. 13). GlnA catalyzes the replacement of the hydroxyl in glutamic acid's side-chain with an amine group. A role for *glnA* and glutamine biosynthesis in *V. fischeri* has not been reported.

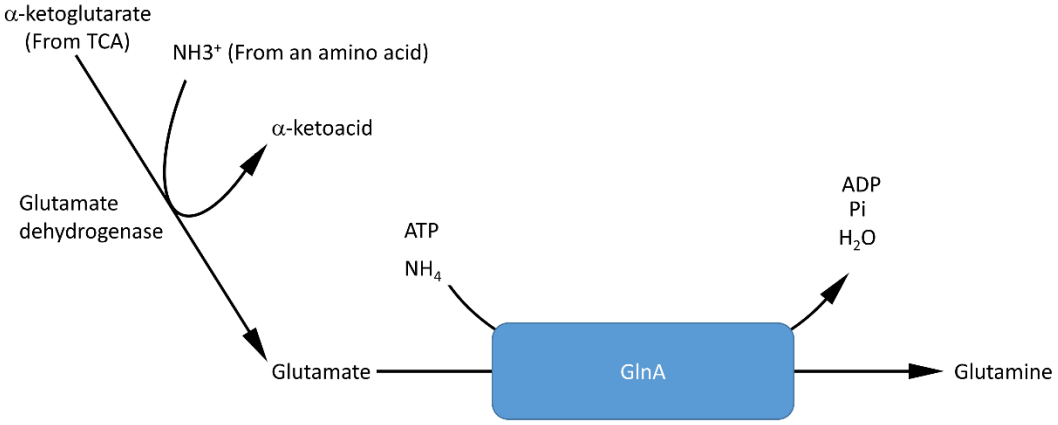

Figure 13 - Glutamine biosynthesis. To synthesize glutamine, α-ketoglutarate from the TCA cycle is converted to glutamate by glutamate dehydrogenase. Glutamate is then converted by GlnA into glutamine.

CHAPTER TWO

METHODS AND MATERIALS

Bacterial Strains and Media. The *V. fischeri* strains and plasmids constructed and/or used in this study are listed in Tables 1 and 2. Primers used in this study are listed in Table 3. *V. fischeri* strains ES114 and KV6576 were used as the parental strains for these studies. *V. fischeri* strains were grown in complex LB-salt (LBS) medium (Stabb, Reich et al., 2001), seawater tryptone (SWT) medium (Yip, Grublesky et al., 2005), HEPES-minimal medium (Ruby and Nealson, 1977), Tris-minimal medium (Brooks, Gyllborg et al., 2014), and tryptone broth-seawater (TB-SW) motility medium (DeLoney-Marino, Wolfe et al., 2003). We also used the *E. coli* strains GT115 (Invivogen, San Diego, CA), CC118, and π3813 (Le Roux, Binesse et al., 2007) for the purposes of cloning and conjugation. *E. coli* strains were grown using either LB (Bertani, 1951) or Brain-heart infusion (BHI) (Difco) medium. The following antibiotics were added, as appropriate, at the indicated final concentrations: chloramphenicol (Cm) at 1 to 5 μg/ml for *V. fischeri* and 25 μg/ml for *E. coli*; tetracycline (Tet) at 5 μg/ml for *V. fischeri* and 15 μg/ml for *E. coli*; kanamycin (Kan) at 100μg/ml for *V. fischeri* and 50 μg/ml for *E. coli*; erythromycin (Erm) at 5 μg/ml for *V. fischeri* and 150 μg/ml for *E. coli*; and ampicillin (Ap) at 100 μg/ml. Thymidine was added to a final concentration of 300 μM for the growth of π3813

Table 1: Strains used in this study.

Strains	**Genotype**	**Reference or Source**
E. coli		
GT115	F- *mcrA* Δ(*mrr-hsdRMS-mcrBC*) ϕ*80lacZ*Δ*M15* Δ*lacX74 recA1 endA1* Δ*dcm uidA*(Δ*MluI*)::*pir-116* Δ*sbcC-sbcD*	Invivogen
CC118	Δ(*ara-leu*) *araD* Δ*lac74 galE galK phoA20 thi-1 rpsE rpsB argE*(*am*) *recA l pir*	(Herrero, de Lorenzo et al., 1990)
π3813	*lacI*^{q} *thi-1 supE44 endA1 recA1 hsdR17 gyrA462 zei-298*::Tn*10* Δ*thyA*::(*erm-pir*) (Kan^{R} Erm^{R} Tet^{R})	(Le Roux, Binesse et al., 2007)
Tam1	*mcrA* Δ*(mrr-hsdRMS-mcrBC)* ϕ*80lacZ*Δ*M15* Δ*lacX74 recA1 araD139* Δ*(ara-leu)7697 galU galK rpsL endA1 nupG*	Active Motif
DH5α	*endA1 hsdR17* (*rK- mK+*) *supE44 thi-1 recA1 relA* Δ(*lacIZYA-argF*)*U169 phoA* [ϕ*80dlac*Δ(*lacZ*)*M15*]	Fermentas
V. fischeri		
ES114	Wild Type	
KV6576	IG (*yeiR-glmS*)::*lacI*^{q}	(Ondrey and Visick, 2014)
KV6873	IG (*yeiR-glmS*)::*lacI*^{q} *sdhE*::Tn*5*P Erm^{R}	This Study
KV6939	IG (*sypH-sypI*)::*erm* Erm^{R}	This Study
KV6940	IG (*sypH-sypI*)::*cm* Cm^{R}	This Study
KV6979	IG (*yeiR-glmS*)::*lacI*^{q} *nqrA*::Tn*5*P Erm^{R}	This Study
KV6983	IG (*yeiR-glmS*)::*lacI*^{q} *pck*::Tn*5*P Erm^{R}	This Study
KV6984	IG (*yeiR-glmS*)::*lacI*^{q} *glnA*::Tn*5*P Erm^{R}	This Study
KV6986	IG (*yeiR-glmS*)::*lacI*^{q} *pck*::Tn*5*P (2) Erm^{R}	This Study
KV6988	IG (*yeiR-glmS*)::*lacI*^{q} *ubiG*::Tn*5*P Erm^{R}	This Study
KV6990	IG (*yeiR-glmS*)::*lacI*^{q} *mdh*::Tn*5*P Erm^{R}	This Study
KV7029	IG (*yeiR-glmS*)::*lacI*^{q} Δ*sdhE*	This Study
KV7108	Δ*VF_2095*	This Study
KV7125	Δ*sdhE*	This Study
KV7138	Δ*sdhE* attTn*7*::*sdhE* Erm^{R}	This Study
KV7143	Δ*sdhE* attTn*7*::*erm* Erm^{R}	This Study
KV7422	IG (*yeiR-glmS*)::*lacI*^{q} *nqr*::Tn*5*P Erm^{R}	This Study
KV7432	IG (*yeiR-glmS*)::*lacI*^{q} IG (*VF_A0340-VF_A0341*)::Tn*5*P Erm^{R}	(Ondrey and Visick, 2014)
KV7433	IG (*yeiR-glmS*)::*lacI*^{q} *cheZ*::Tn*5*P Erm^{R}	(Ondrey and Visick, 2014)

KV7438	Δ*nqrA*	This Study
KV7439	IG (*yeiR-glmS*)::*lacI*^{q} Δ*nqrA*	This Study
KV7448	Δ*sypC nqrA*::Tn*5*P Erm^{R}	This Study
KV7449	Δ*sypE nqrA*::Tn*5*P Erm^{R}	This Study
KV7450	Δ*sypK nqrA*::Tn*5*P Erm^{R}	This Study
KV7451	Δ*sypQ nqrA*::Tn*5*P Erm^{R}	This Study
KV7452	Δ*VF_A1019* Δ*VF_A0120* Δ*VF_A0550 nqrA*::Tn*5*P Erm^{R}	This Study
KV7466	Δ*nqrA pck*::Tn*5*P Erm^{R}	This Study
KV7467	Δ*nqrA mdh*::Tn*5*P Erm^{R}	This Study
KV7468	Δ*nqrA sdhE*::Tn*5*P Erm^{R}	This Study
KV7469	Δ*sdhE pck*::Tn*5*P Erm^{R}	This Study
KV7470	Δ*sdhE mdh*::Tn*5*P Erm^{R}	This Study
KV7471	Δ*sdhE nqrA*::Tn*5*P Erm^{R}	This Study
KV7541	IG (*yeiR-glmS*)::*lacI*^{q} Tn7::*erm* Erm^{R}	This Study
KV7700	*nqrA*::Tn*5*P Erm^{R}	This Study
KV7701	*pck*::Tn*5*P Erm^{R}	This Study
KV7702	*mdh*::Tn*5*P Erm^{R}	This Study
KV7703	*glnA*::Tn*5*P Erm^{R}	This Study
KV7704	*ubiG*::Tn*5*P Erm^{R}	This Study
KV7705	*sdhE*::Tn*5*P Erm^{R}	This Study
KV7706	Δ*sdhE sdhC*::*erm* Erm^{R}	This Study
Temp	Δ*nqrA csgD*::*erm* Erm^{R}	This Study
KV5948	*mshA*::Tn*5* Erm^{R}	(Visick, Quirke et al., 2013)
KV4147	*csgD*::*erm* Erm^{R}	This Study
Temp	Δ*nqrA mshA*::Tn*5* Erm^{R}	This Study

Table 2: Plasmids used in this study

Name	Description	Reference
pARM7	*rscS* overexpression vector (Tet^R)	(Morris, Darnell et al., 2011)
pCA24n	*lacI*^{q} expression vector (Cm^R)	(Kitagawa, Ara et al., 2005)
pCLD46	*rscS* overexpression vector (Cm^R)	(Hussa, Darnell et al., 2008)
pCLD56	*sypG* overexpression vector (Tet^R)	(Morris and Visick, 2013)
pEVS107	Tn*7* delivery vector (Erm^R Kan^R)	(McCann, Stabb et al., 2003)
pEVS170	Tn*5* delivery plasmid (Kan^R Erm^R)	(Lyell, Dunn et al., 2008)
pJet1.2	PCR cloning vector (Amp^R)	Fisher
pJFB9	Vector carrying *tfoX* (Kan^R)	(Brooks, Gyllborg et al., 2014)
pJMO10	Tn*5* delivery plasmid containing an outward facing *lac* promoter near the mosaic end (Kan^R)	(Ondrey and Visick, 2014)
pJMO14	pJMO8 containing *lacI*^{q} at its NotI site (Cm^R)	(Ondrey and Visick, 2014)
pJMO22	pSW8197 containing *sypH*, a Cm^R cassette, and *sypI* (Kan^R Cm^R)	This Study
pJMO23	pKV363 containing *VF_2095* deletion construct (Cm^R)	This Study
pJMO27	pKV363 containing *sdhE* deletion construct (Cm^R)	This Study
pJMO32	pKV363 containing *nqrA* deletion construct (Cm^R)	This Study
pJMO33	*V. fischeri* expression vector (Tet^R Cm^R)	This Study
pJMO34	pJMO33 derived *rscS* overexpression vector (EcoRI) (Tet^R)	This Study
pJMO8	pKV363 containing the *V. fischeri* Tn*7* site and upstream NotI site (Cm^R)	(Ondrey and Visick, 2014)
pJMO9	pJMO8 containing *lacI* at its NotI site (Cm^R)	This Study
pKG11	pKV69 derived *rscS* overexpression vector (Cm^R Tet^R)	(Yip, Geszvain et al., 2006)
pKV282	pKV69 derived empty vector (Tet^R)	(Morris, Darnell et al., 2011)
pKV363	suicide plasmid (Cm^R)	(Shibata, Yip et al., 2012)
pKV37	expression vector (Amp^R Cm^R)	(DeLoney, Bartley et al., 2002)
pKV69	expression vector (Cm^R Tet^R)	(Visick and

		Skoufos, 2001)
pLosTfoX	Vector carrying *tfoX* (Cm^R)	(Pollack-Berti, Wollenberg et al., 2010)
pLS1	*V. fischeri* expression vector (Cm^R)	(Visick and Ruby, 1997)
pSS18	*sypI* expression vector (Cm^R)	(Shibata, Yip et al., 2012)
pSS23	*sypH* expression vector (Cm^R)	(Shibata, Yip et al., 2012)
pSW8197	suicide plasmid (Kan^R)	(Le Roux, Binesse et al., 2007)

Table 3: Primers used in this study

Primer	**Gene**	**Sequence (5' -3')**
1484	*VF_2371* F	CTT GAT TTA TAC AGC GAA GG
1485	*VF_2371* NotI R	TAG GCG GCC GCA CTT AGT ATG GTT TTG AAG AGT AAT TAA TGT TTA TTG
1486	*VF_2372* NotI F	CAT ACT AAG TGC GGC CGC CTA TAT TGT CTC TCT TAG AAC AAT TAT TC
1487	*VF_2372* R	GGT CGT GGG GAG TTT TAT CC
1488	*lacI* NotI F	GCG GCC GCG GGA TCA GGA GGA GAA GAT C
1489	*lacI* NotI R	GCG GCC GCC GCT CAC TGC CCG CTT TCC
1544	*lacI*^{q} NotI F	GCG GCC GCG ACA CCA TCG AAT GGT GCA AAA C
1700	*sdhE* Kpn F	GGTACC CAT CTT ATG ACT TTA GAT CAT GG
1701	*sdhE* Spe R	ACTAGT GT TCA GCG TTA TTT TAA CGT AAC
1702	*sdhE* SOE P1	GCC CAC CGA AGG TGA TCT C
1703	*sdhE* SOE P2	TAG GCG GCC GCA CTT AGT ATG ACT GTA CAT ACT GTC CCC TAG
1704	*sdhE* SOE P3	CAT ACT AAG TGC GGC CGC CTA GAT AAA ATC GTT GAG CAC AAC CTC
1705	*VF_2095* Spe R	ACTAGT CAA CAC GAC TAC TTT AAG AGC
1707	*VF_2095* SOE P2	TAG GCG GCC GCA CTT AGT ATG GTT CAG CGT TAT TTT AAC GTA AC
1708	*VF_2095* SOE P3	CAT ACT AAG TGC GGC CGC CTA CTC TTA AAG TAG TCG TGT TGT C
1709	*VF_2095* SOE P4	GCG GTG TAA TGG TTG ATA AAC
1805	P1 *nqrA* del Gib	GCG AGG CTG GCC GGC GTC GAC TAT GCA TAA CGT ACC TGA AGG
1806	P2 *nqrA* del Gib	GCT CAT CAA TTA CCC TTC CTT CTG CAT GTG TCC AGT ATT GAC
1807	P3 *nqrA* del Gib	GTC AAT ACT GGA CAC ATG CAG AAG GAA GGG TAA TTG ATG AGC
1808	P4 *nqrA* del Gib	CAG ACA ATT GAC GGC TCT AGA CTT TCG CTA CAA CAA CAC CG

E. coli cells. Isopropyl β-D-thiogalactopyranoside (IPTG) was generally added at 1.75 mM or at a range between 1.75 mM and 3.5 µM to induce promoter activity. Agar was added at a final concentration of 1.5% for solid media and 0.225% for the motility medium. For experiments utilizing LBS plates supplemented with an additional carbon source, a 20% stock solution of the indicated carbon source was prepared and filter sterilized. Plates were then prepared with a final concentration of 0.2% indicated carbon source.

Insertion of *lacI*^{q} into the ES114 chromosome. Plasmid pJMO14 was used to insert the *lacI*^{q} gene into the chromosome between *yeiR* and *glmS*, adjacent to the *att*Tn*7* site (Fig. 15). To generate pJMO14, upstream and downstream sequences (~500 bp) flanking the target insertion site were first amplified from the ES114 chromosome by PCR using primers 1484 and 1485 and primers 1486 and 1487, then joined using overlap extension PCR (Ho, Hunt et al., 1989, Shibata and Visick, 2012). The resulting DNA fragment, which consisted of the flanking sequences joined by non-native sequences including a NotI site, was ligated into suicide vector pKV363 to generate pJMO8. Finally, the *lacI*^{q} gene, which was amplified using PCR with pCA24N as a template and primers 1544 and1489, was cloned into the PCR cloning vector pJET1.2, then sub-cloned into NotI-digested pJMO8 to generate pJMO14. To insert *lacI*^{q} into the chromosome, the method of Le Roux *et al.* (Le Roux, Binesse et al., 2007) was used as described previously (Shibata and Visick, 2012). The insertion of *lacI*^{q} into ES114, generating KV6576, was confirmed using PCR with primers 974 and 975.

Construction of Tn*5*P. Plasmid pJMO10, which was used to deliver the Tn*5* + promoter (Tn*5*P) for transposon mutagenesis, was constructed as follows. Oligonucleotides 1439

and 1440, which contained sequences for the LacI-repressible PA1/34 promoter (Lanzer and Bujard, 1988, Bose, Rosenberg et al., 2008), were annealed and ligated into the ApaI/SpeI-digested Tn*5* delivery plasmid pEVS170 (Lyell, Dunn et al., 2008). The insertion of the promoter into Tn*5* was confirmed by sequencing.

Deletion of *sdhE* from the chromosome. Plasmid pJMO27 was used to delete the *sdhE* gene from the chromosome. To generate pJMO27, upstream and downstream sequences (~500 bp) flanking the gene but including the first 9 and last 39 bases of the *sdhE* reading frame were first amplified from the ES114 chromosome by PCR using primers 1702 and 1703 and primers 1704 and 1709, then joined using overlap extension PCR (Ho, Hunt et al., 1989). The resulting DNA fragment consisted of an allele of *sdhE* encoding only the first 3 and last 12 amino acids; downstream gene *VF_2095* overlaps the end of *sdhE* so making a larger deletion that would not also disrupt *VF_2095* was not possible. This fragment was ligated into the PCR cloning vector pJET1.2, then sub-cloned into ClaI/XhoI-digested suicide vector pKV363 to generate pJMO27. To delete *sdhE* from the chromosome, the method of Le Roux *et al.* (Le Roux, Binesse et al., 2007) was used as described previously (Shibata and Visick, 2012). The deletion of *sdhE* from ES114, generating KV7125, was confirmed using PCR with primers 1702 and 1709.

Deletion of *VF_2095* from the chromosome. Plasmid pJMO23 was used to delete the *VF_2095* gene from the chromosome. To generate pJMO23, upstream and downstream sequences (~500 bp) flanking the gene, as well as the first 42 and last 6 bases of the *VF_2095* reading frame, were first amplified from the ES114 chromosome by PCR using primers 1702 and 1707 and primers 1708 and 1709, then joined using overlap extension PCR (Ho, Hunt et al., 1989, Shibata and Visick, 2012). The resulting DNA fragment

consisted of an allele of *VF_2095* encoding only the first 14 and last 3 amino acids; upstream gene *sdhE* overlaps the end of *VF_2095* so a larger deletion that would not also disrupt *sdhE* was not possible. This fragment was ligated into the PCR cloning vector pJET1.2, then sub-cloned into ClaI/XhoI-digested suicide vector pKV363 to generate pJMO23. To delete *VF_2095* from the chromosome, the method of Le Roux *et al.* (Le Roux, Binesse et al., 2007) was used as described previously (Shibata and Visick, 2012). The deletion of *VF_2095* from ES114, generating KV7108, was confirmed using PCR with primers 1702 and 1709.

Deletion of *nqrA* from the chromosome. Plasmid pJMO32 was used to delete the *nqrA* gene from the chromosome. To generate pJMO32, upstream and downstream sequences (~500 bp) flanking the gene, as well as the first 6 and last 12 bases of the *nqrA* reading frame were first amplified from the ES114 chromosome by PCR using primers 1805 and 1806 and primers 1807 and 1808. The two fragments were joined together and inserted into XbaI/SalI cut suicide vector pKV363 using Gibson Assembly (New England Biolabs). The resulting plasmid, pJMO32, consisted of an allele of *nqrA* encoding only the first 2 and last 3 amino acids. To delete *nqrA* from the chromosome, the method of Le Roux *et al.* (Le Roux, Binesse et al., 2007) was used as described previously (Shibata and Visick, 2012). The deletion of *nqrA* from ES114, generating KV7438, was confirmed using PCR with primers 1805 and 1809.

Insertion of a Cm resistance cassette into *syp* locus. Plasmid pJMO22 was used to insert the Cm resistance cassette gene into the chromosome between *sypH* and *sypI* (Fig. 20). To generate pJMO22, *sypH* was amplified from pSS23 using primers 1720 and 1721, *sypI* was amplified from pSS18 using primers 1724 and 1725, and the Cm resistance

cassette was amplified from pKV37 using primers 1722 and 1723. The three fragments were joined together and inserted into XbaI/SalI cut suicide vector pSW8197 using Gibson Assembly (New England Biolabs). The resulting plasmid, pJMO22 contained the Cm resistance cassette flanked by *sypH* and *sypI*. To insert the Cm resistance cassette into the chromosome, the method of Le Roux *et al.* (Le Roux, Binesse et al., 2007) was used as described previously (Shibata and Visick, 2012). The insertion of the chloramphenicol resistance cassette into ES114, generating KV6940, was confirmed using PCR with primers 1720 and 1725.

Transposon Mutagenesis. Parental strain KV6577 (KV6576 containing pRscS plasmid pARM7) was mutagenized with Tn*5*P by performing a tri-parental conjugation (Stabb and Ruby, 2002) with two *E. coli* strains, one carrying pJMO10 (Ondrey and Visick, 2014) and other carrying pEVS104 (Stabb and Ruby, 2002) and selecting for the insertion of the transposon using Erm-, Tet-, and IPTG-containing LBS (LBS-Erm/Tet/IPTG) plates. After 72 h, the morphology of the colonies was evaluated. Smooth colonies were re-streaked two additional times on LBS-Erm/Tet/IPTG plates and allowed to grow for an additional 72 h to verify their phenotype.

Identification of pRscS Mutants. Smooth mutants were grown non-selectively on LBS until they were cured of the Tet^R plasmid pARM7. Tet^S strains were then placed on LBS-Erm and LBS plates not containing antibiotic to assess whether the strain maintained the Erm^R marker contained within Tn*5*P.

Gene Mapping. KV6940 cells containing pJFB9 were made competent by growing them in TMM supplemented with 0.2% NAG as described by Brooks *et al.* (Brooks, Gyllborg et al., 2014). Chromosomal DNA samples harvested from putative biofilm mutant strains

were then used to transform competent cells (Brooks, Gyllborg et al., 2014). Linkage between the Cm^R cassette in KV6940 and the Erm^R cassette within Tn*5*P was then assessed by the loss or maintenance of the Cm^R cassette.

Identification of Tn*5*P Insertion Site. Chromosomal DNA was isolated from transposon-insertion mutants and digested using the HhaI restriction enzyme as previously described (Lyell, Dunn et al., 2008). Digested DNA was then self-ligated and used to transform CC118 *E. coli* cells, and clones were selected on Erm-containing BHI agar. The resulting plasmids were sequenced using primer 908 or 549.

Wrinkled Colony Assays. Strains were grown overnight in LBS containing an appropriate antibiotic at 28°C with agitation, then subcultured into fresh medium and grown until they reached exponential phase. Cultures were then diluted to an optical density at 600 nm (OD_{600}) of 0.2, concentrated by centrifugation, and re-suspended in fresh medium. 10 µl aliquots of each culture were spotted onto an agar plate and incubated at room temperature and wrinkled colony development was monitored.

Pellicle Assays. Strains were grown overnight at 28°C with agitation in a liquid medium of LBS, SWT, or Hepes minimal medium. The OD_{600} of each strain was then measured and used to standardize the cell concentration for subsequent sub-culturing into 2 ml of LBS or Minimal medium in 24-well microtiter plates at the final OD of 0.1-0.4, depending on the experiment. Plates were then placed at 24°C to allow pellicles to form. Pellicles were disrupted with a pipette tip at the time indicated to more readily visualize the pellicle.

Motility Assays. Strains were grown overnight in LBS and the cultures were diluted to an OD_{600} of 0.4. Cells were pelleted, washed, and re-suspended in LBS and 5 µl aliquots

were inoculated on the surface of TB-SW motility plates lacking or containing IPTG (in the range of 1.75 mM to 3.5 µM). Representative images were captured and the diameters of the outer ring of the swimming cells were measured using a ruler.

Squid Colonization Assays. Strains used for squid colonization were grown statically in SWT at 28°C for at least 3 hours prior to use in the assay. The OD_{600} of each sample was assessed and bacterial samples at a concentration of 1,000 – 32,000 per ml were inoculated into 50 ml of ASW. The inoculum was then added to glass bowls and freshly hatched squid were introduced to the bowls. At 3 h or 18 h post inoculation, squid were removed from the inoculum and washed in fresh ASW. Animals in the 3 h inoculation condition were maintained in fresh ASW until the 18 h time point. Animals were then moved to glass scintillation vials and luminescence was assessed using a scintillation counter. Once animals exposed to WT *V. fischeri* exhibited luminescence, all animals were homogenized. Homogenates were then diluted and spread onto SWT plates, and the plates were then incubated at 28°C. The following day, colonies were counted and total CFU/squid were calculated.

Growth assays. Strains were grown overnight with agitation at 28°C in LBS. Then, the OD_{600} of each strain was measured and 25 ml of fresh LBS was inoculated to a final OD_{600} of 0.01 in a 250 ml beveled flask. Flasks were then incubated at 28°C with agitation. Growth of the cultures was monitored by assessing OD_{600} over time.

Cohesion and adherence assays. To assess cohesion and adherence, a flat ended toothpick was drawn through the center of a developed colony (Ray, Driks et al., 2015). Cohesion is a qualitative measure of cell-cell associations and was characterized by the ability of the colony to self-associate via the production of a matrix and be moved as a

single unit when disrupted. Adherence is a qualitative measure of cell-surface association and was characterized by the colony being resistant to disassociation from the agar surface when disrupted, i.e., a portion of the colony sticks to the agar surface. Special care was taken to use consistent pressure and speed as spots were disrupted.

Natural transformation. The method of Brooks et al. (Brooks, Gyllborg et al., 2014) was used to transform *V. fischeri* cells, with the following alterations. 1) *V. fischeri* cells containing a *tfoX* over-expression plasmid were grown overnight in LBS at 28°C prior to being subcultured into LBS and grown at 25°C during the day. Late in the afternoon, strains were subcultured into TMM and grown at 25°C; 2) *V. fischeri* cells containing a TfoX plasmid were taken from frozen glycerol stocks and inoculated into 1 ml LBS in the morning and grown with shaking under selection at 28°C. Late in the afternoon, strains were subcultured into TMM and grown at 25°C; 3) Chromosomal DNA was prepped as described by Singh et al. (Singh, Brooks et al., 2015); 4) In some cases, such as transformation of strains exhibiting growth defects, more of the transformation mixture was plated after the recovery phase; and 5) Verification of successful natural transformation in back-crossed strains was achieved by using a PCR reaction with primers on both sides of the insertion site and observing a shift in the size of the Tn*5*P insertion compared to a wild-type control.

CHAPTER THREE

RESULTS

I. Missing regulatory and structural determinants of biofilm formation in *V. fischeri*

Biofilm formation in *V. fischeri* depends upon an intricate regulatory process that involves the interplay of positive and negative regulators such as SypG and SypE, and has as its end result a complex macromolecular structure, such as a wrinkled colony. As described in the literature review, a number of genes are required for the production of the polysaccharide and protein components, but it is unlikely that our current knowledge of the structural and regulatory genes required for wrinkled colony formation is complete. Thus, the goal of this project was to identify additional determinants of biofilm formation of *V. fischeri*, and increase our understanding of this important phenomenon.

Nearly all of the genetic determinants of biofilm formation identified in *V. fischeri* are positive regulators of biofilm formation, i.e., the presence and activity of their gene products are required for the formation of the biofilm. There are methods currently used in *V. fischeri* to identify negative regulators of phenotypes, but they have certain caveats that reduce their effectiveness. For example, plasmid libraries containing fragments of digested *V. fischeri* DNA could be used with the goal of identifying a negative determinant present within one of the plasmids, but this approach is severely limited by the completeness of the existing libraries. Thus, to be able to conduct a

saturating screen for negative, as well as positive, determinants of biofilm formation in *V. fischeri*, I first developed a better genetic tool by combining the power of the transposon mutagenesis, a method normally used to disrupt genes and identify positive regulators, with the addition of an outward facing promoter just within the transposon end, to promote the expression of negative regulators. I then generated a strain in which I could control promoter activity, and demonstrated that this new tool worked to obtain specific classes of mutants. Finally, I used it to search for positive and negative regulators of biofilm formation.

II. Tn*5*P, a mutagenesis tool for the combined identification of positive and negative regulators

To develop a genetic tool for identifying positive and negative regulators of biofilm formation, I chose to introduce an inducible promoter into a transposon that could function in *V. fischeri*. For the inducible promoter, I used the LacI-repressible promoter A1/34 (Bose, Rosenberg et al., 2008). This promoter contains two LacI binding sites, one between the -35 and -10 sites and another that overlaps the transcriptional start site (Fig. 14), and has been shown previously to function as a strong promoter in *V. fischeri* when it was inserted directly upstream of an operon (Bose, Rosenberg et al., 2008). I then engineered the mini-Tn*5* delivery vector pEVS170 (Lyell, Dunn et al., 2008) to contain this promoter within the transposable element in an outward-facing position (Fig. 15); the insertion of the promoter was confirmed by sequencing. This transposon will be referred to as Tn*5*P, for Tn*5* plus Promoter.

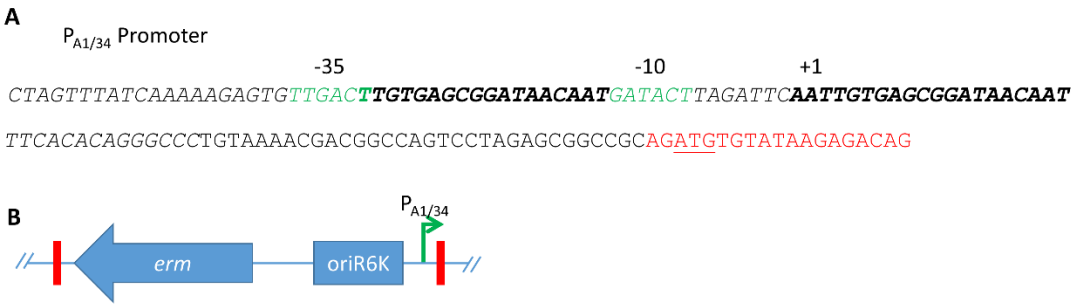

Figure 14 - Construction of pJMO10 and the Tn*5*P transposon. (A) The $P_{A1/34}$ promoter region (italics) contains two LacI binding sites (bold). The binding of LacI to these sites hinders access to the -35 and -10 sites (green), thus repressing transcription. The Tn*5* end (red) contains a start codon (underlined). B) The $P_{A1/34}$ promoter region described above was introduced to the Tn*5* from pEVS170 which contains an erythromycin resistance gene and an origin of replication (blue arrow and box) within the Tn*5* ends (red rectangles). Thus, pJMO10, the modified pEVS170, contains an outward-facing, LacI-repressible/IPTG-inducible promoter, $P_{A1/34}$ (green arrow).

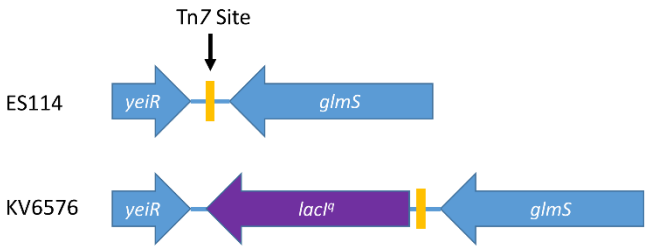

Figure 15 - Construction of a *lacI*-expressing *V. fischeri* strain. ES114 contains a Tn*7* site (yellow rectangle) between *yeiR* and *glmS*. KV6576 was engineered to contain the *lacI* overexpression allele (*lacI*^{q}, purple arrow) near, but not disrupting, the Tn*7* site.

III. Insertion of the *lacI* gene into *V. fischeri* and phenotypic assessment

V. fischeri does not contain the *lacI* repressor gene. Therefore, to control expression from the promoter within Tn*5*P, it was necessary to introduce the *lacI* gene into *V. fischeri*. One location traditionally used to insert genes within the *V. fischeri* genome is the Tn*7* site, which is positioned between *yeiR* and *glmS* (Fig. 15) (Lichtenstein and Brenner, 1982, McCann, Stabb et al., 2003). However, because this site is heavily utilized for single copy complementation (*e.g.*, (Morris, Darnell et al., 2011)), I chose to leave this site intact for future manipulations. Instead, I targeted the insertion of $lacI^q$, a more highly transcribed allele of the *lacI* gene, to a region immediately adjacent to the Tn*7* site (between *yeiR* and the Tn*7* site) (Fig. 15). The result was a strain, KV6576, which contains $lacI^q$, retains an intact Tn*7* site, and remains unmarked, allowing for the use of an antibiotic resistance marker in future manipulations. I also generated an identically constructed *lacI* containing strain, KV6056, for use in future experiments in which less LacI is required for promoter repression (Table 1).

With the generation of the $lacI^q$-containing *V. fischeri*, two questions arose: (i) Is the $lacI^q$ allele functional (*e.g.*, does it control gene expression in *V. fischeri*?); and (ii) is the Tn*7* site, which is adjacent to the site of insertion of the $lacI^q$ gene, still permissive for insertion events? To assess whether the $lacI^q$ allele in KV6576 was functional, I investigated the ability of this strain to impact expression of a *lac* promoter-controlled gene. Specifically, we introduced into KV6576 a plasmid, pCLD46, which contains the *rscS* gene driven by the *lac* promoter, or pVSV105, the empty vector from which pCLD46 was derived. When pCLD46 is introduced into wild-type *V. fischeri*, RscS protein is made and induces biofilm formation (Hussa, Darnell et al., 2008). One biofilm

phenotype that can be readily assessed is the formation of wrinkled colonies. I anticipated that, if the *lacI*^{q} allele in KV6576 were functional, then LacI would repress expression of *rscS*, resulting in a strain that either fails to form wrinkled colonies or does so after a delay. Indeed, I found that this strain failed to wrinkle after 24 hours of growth in the absence of IPTG (Fig. 16). Moreover, when I grew the strain in the presence of IPTG, which should inactivate LacI, wrinkled colonies developed with a timing indistinguishable from the control (Fig. 16 and data not shown). These data indicate that functional LacI was made and was responsive to IPTG. I note, however, that the repression of *rscS* expression from pCLD46 was not complete: at later times, the strain exhibited a modest wrinkling phenotype in the absence of IPTG (Fig. 16). I attribute this result to the inability of LacI expressed from the chromosome to fully repress a promoter present on a multi-copy plasmid. I further note that this should not be a factor in the event of a mutagenesis with Tn5P, as this promoter will be in single copy as it inserts within the chromosome.

To verify that the Tn*7* site near the site of *lacI*^{q} insertion in KV6576 remained amenable to manipulation, I used pEVS107, a Tn*7* delivery vector that targets the Tn*7* site (McCann, Stabb et al., 2003), to introduce an Erm resistance cassette at that location. pEVS107 contains an Erm resistance cassette within the Tn*7* ends and a kanamycin resistance cassette outside. Erythromycin-resistant strains were readily isolated and exhibited sensitivity to kanamycin, as expected when the Tn*7* cassette inserts at the Tn*7* site (data not shown).

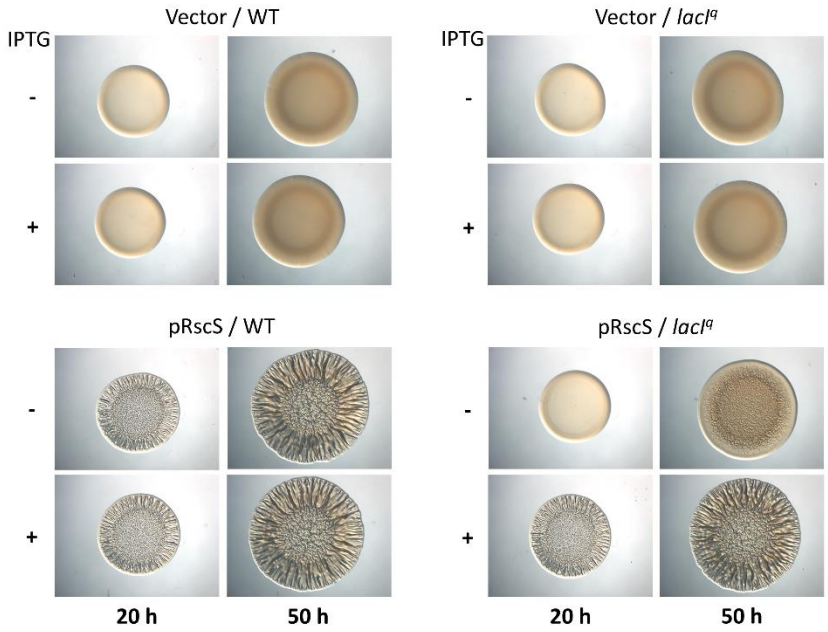

Figure 16 - *lac* promoter-driven biofilm formation by WT and *lacI* expressing strains. Cultures of wild-type (ES114) and *lacI*^{q} (KV6576) strains containing either the empty vector pVSV105 or RscS expression plasmid pCLD46 were grown in LBS containing Cm. Aliquots were diluted to an OD600 of 0.2, spotted onto LBS-Cm medium containing or lacking 1.75 mM IPTG, and incubated at room temperature. Wrinkled colony formation was assessed at 20 and 50 h post inoculation.

IV. Identification of motility mutants

My data above indicate that the *lacI* gene inserted into the chromosome is functional to repress transcription of a *lac* promoter-controlled gene. However, the question remained, does the *lacI*^{q} allele control transcription from the $P_{A1/34}$ promoter contained within Tn*5*P? Specifically, I wondered whether I could induce or repress native *V. fischeri* genes in KV6576 containing insertions of Tn*5*P. To address this question, I chose to evaluate a readily assessable phenotype, motility, prior to performing a larger study of biofilm formation. *V. fischeri* contains a number of genes known (Millikan and Ruby, 2003, Millikan and Ruby, 2004, Wolfe, Millikan et al., 2004, Brennan, Mandel et al., 2013) or predicted (Wolfe and Visick, 2010) to impact motility. I hypothesized that Tn*5*P insertions upstream of such genes could result in strains with inducible or repressible motility. I thus introduced Tn*5*P into KV6576 and assessed mutant motility on soft agar plates that contained or lacked IPTG. From a screen of about 2000 mutants, we identified about 20 strains with potential IPTG-dependent motility phenotypes and confirmed the phenotypes of a subset of these mutants. Of these, my focus was drawn to two strains with opposing phenotypes (Fig. 17). One strain, KV7432, had IPTG-repressible motility: it exhibited near wild-type motility in the absence of IPTG but greatly diminished motility in the presence of IPTG (Fig. 17B). In contrast, IPTG did not impact motility of the control strain (Fig. 17A). The second strain of interest, KV7433, had IPTG-inducible motility: it was non-motile in the absence of IPTG but regained a wild-type motility phenotype in the presence of IPTG (Fig. 17C). Because of their strong yet opposite phenotypes, I chose these two strains for additional characterization.

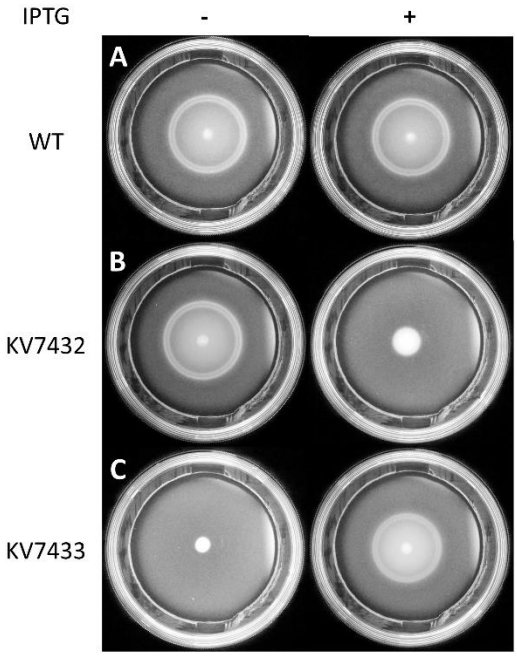

Figure 17 - Migration of mutant strains on soft agar. KV6576 (A), KV7432 (B), and KV7433 (C) were grown overnight in LBS. Cultures were diluted to an OD600 of 0.4 prior to inoculation on TB-SW motility medium containing or lacking 1.75 mM IPTG. The images depict migration after 5.5 h of incubation at 28°C.

I first identified the sites of insertion of Tn*5*P as described in Materials and Methods. The mutant with IPTG-repressible motility, KV7432, contained an insert within the intergenic region between *VF_A0340* and *VF_A0341*, with the promoter of Tn*5*P oriented toward *VF_A0341* (Fig. 18A). In this orientation, the promoter appears positioned to drive expression of the nearby three-gene operon consisting of *VF_A0342*, *VF_A0343*, and *VF_A0344*. These three genes are predicted to encode proteins with GGDEF or EAL domains. These domains are found in diguanylate cyclase and phosphodiesterase proteins, which synthesize and degrade, respectively, the second messenger cyclic-di-GMP (c-di-GMP) (Wolfe and Visick, 2010). High levels of cellular c-di-GMP inhibit motility in a variety of bacteria (Romling, Gomelsky et al., 2005). Therefore, I hypothesize that IPTG-mediated expression from the transposon promoter increases the levels of c-di-GMP in the cell and thus, inhibits motility. It also remains possible that expression from the Tn*5*P promoter decreases the expression of *VF_A0341*, which encodes a hypothetical protein with no conserved domains.

The mutant with IPTG-inducible motility, KV7433, carried the Tn*5*P insertion within the *cheZ* gene, with the transposon's promoter oriented with the *che* operon (Fig. 18B). In the absence of IPTG, the transposon insertion should interrupt transcription of *cheZ* as well as the downstream *che* genes, which coordinate chemotaxis and are required for motility in *V. fischeri* (Brennan, Mandel et al., 2013). Thus, it was not surprising that, in the absence of IPTG, this mutant exhibited a motility defect. Given that the Tn insertion was within the *cheZ* gene, however, it was unexpected that the addition of IPTG would restore near wild-type motility (Fig. 17). Upon closer investigation of the insertion site, I noted that (1) the Tn is inserted near the beginning of *cheZ*, and (2) an ATG start

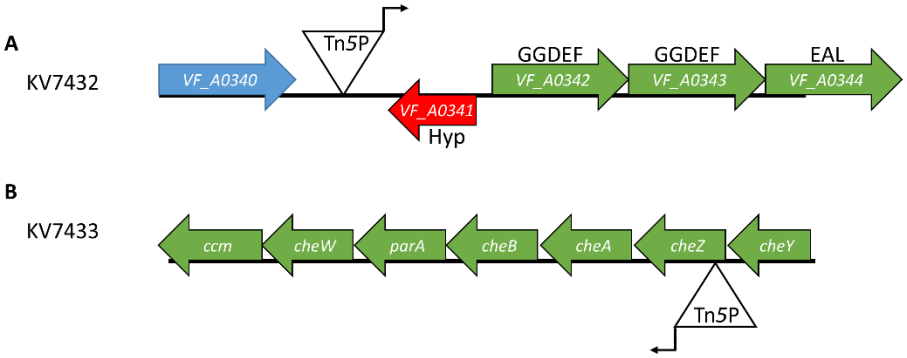

Figure 18 - The location and orientation of the Tn*5*P insertions in two motility mutants. The insertion in KV7432 is located in the intergenic region between *VF_A0340* and *VF_A0341* with the A1/34 promoter oriented toward *VF_A0341* (A). The insertion in KV7433 is located within the 5' end of *cheZ* with the A1/34 promoter oriented toward *cheA* (B).

codon within the Tn*5*P transposon end is in frame with the *cheZ* open reading frame (Fig. 14A and data not shown). Based on these observations, I hypothesize that expression from the transposon's promoter and translation from the ATG within the transposon end results in the production of a hybrid CheZ protein with an altered N-terminus that is functional to promote motility.

Assessment of IPTG induction

My previous experiments used a single concentration of IPTG, 1.75 mM, to induce transcription from the Tn*5*P promoter. However, it was unclear whether this high amount of IPTG was necessary to obtain full repression/induction of motility by our strains. Thus, to determine the sensitivity of the Tn*5*P promoter to IPTG, I assessed the mutants' motility phenotypes in the presence of a range of IPTG concentrations. KV7433 exhibited a dose-dependent increase in motility within a wide range of IPTG concentrations between 3.5 μM and 175 μM IPTG that was not further increased with additional IPTG (Fig. 19). The other mutant, KV7432, similarly exhibited a dose-dependent change. In this case, the impact on motility required higher IPTG concentrations, above 35 μM; at the highest amount tested, 1.75 mM, motility was not fully repressed (Fig. 19). These data further support my conclusion that expression from the Tn*5*P promoter is induced by the addition of IPTG. Additionally, because I obtained different ranges of IPTG addition required for a transition from the motile to non-motile phenotype in the two strains, I conclude that it may be necessary to experimentally determine the optimal expression of a particular gene obtained using this experimental set-up (*lacI*^{q}/Tn*5*P) by titrating the concentration of IPTG in the medium against the phenotype being tested.

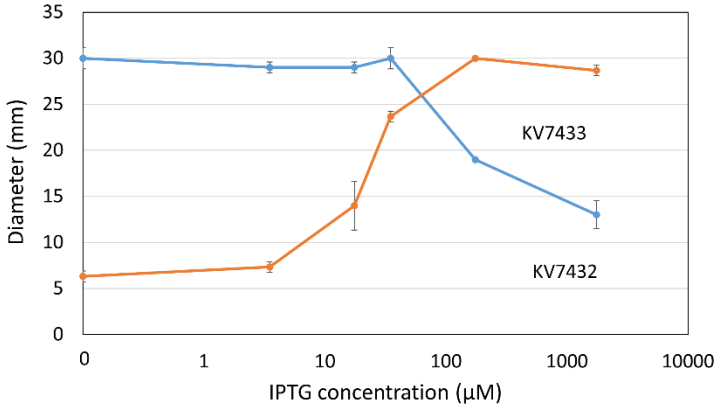

Figure 19 - Dependence of mutant motility phenotypes on IPTG. Motility mutants KV7432 and KV7433 were grown at 28°C in TB-SW motility medium containing the indicated concentrations of IPTG. The average diameter of migration of triplicate samples after 5 hours is shown. Standard deviation is indicated by error bars. Error bars smaller than the plotted points are occluded by the points and not visible.

V. Identification of Biofilm Mutants

Having demonstrated that the *lacI*^{q}/Tn*5*P mutagenesis system was capable of identifying regulators of phenotypes through induction with the promoter, I applied this technique to the identification of genetic determinants of biofilm formation in *V. fischeri*. I hypothesized that I would be able to identify genes whose increased expression driven by the Tn*5*P promoter caused a decrease in biofilm formation in addition to Tn*5*P disrupted genes required for biofilm formation. Therefore I introduced the Tn*5*P to a *lacI*^{q} expressing biofilm forming strain (KV6576 containing *rscS*-overexpression plasmid pARM7), selected for insertional mutants and screened for smooth colonies on plates containing IPTG. Over the course of 15 independent mutagenesis experiments, I screened approximately 47,000 mutants, and identified approximately 270 mutants displaying a smooth phenotype in the presence of IPTG.

VI. Elimination of Characterized Mutants

As I noted in the literature review, there are many known and characterized genetic determinants of biofilm formation in *V. fischeri*, including *syp*, *rscS* and *rpoN*. Indeed, due to the large size of the *syp* locus, it was likely that many of my smooth mutant strains would have insertions within this locus. Because my goal was to identify new factors involved in biofilm formation, I first sought to rule out strains with insertions within the plasmid borne *rscS* gene, the chromosomally encoded *rpoN* gene, and the chromosomally encoded *syp* locus.

Identification and elimination of insertions within pRscS

Insertions within chromosomal *rscS* would be unlikely to cause a defect in biofilm formation due to the multiple copies of the *rscS* plasmid pARM7 also present within

these strains. However, an insertion of Tn*5*P into the pARM7-borne *rscS* allele could result in a smooth phenotype. If a mutant strain contains the Tn*5*P insertion within the pARM7 plasmid, then the same strain cured of its plasmid would lose the Tn*5*P associated Erm^R cassette and be Erm^S. To identify mutants with insertions within the plasmid borne *rscS* allele, I cured all of the mutant strains of the pARM7 plasmid and then assessed the plasmid-less strains for their ability to grow on medium containing Erm. 143 Tet^S strains that remained Erm^R were determined to contain insertions elsewhere (NOT within the plasmid borne *rscS* allele); those strains were maintained and others were set aside. Nearly half of the mutant strains contained Tn*5*P insertions within the *rscS* plasmid (Table 4).

Identification and elimination of insertions within *rpoN*

Next, I sought to identify mutant strains with insertions within the *rpoN* gene, which encodes the sigma factor required for biofilm formation and motility (Wolfe, Millikan et al., 2004). I leveraged *rpoN*'s dual role by utilizing a motility assay to identify insertions likely within this gene. If the strain is both non-motile and has a biofilm defect, there is likely an insertion within *rpoN*. To do this, I grew each of the mutant strains in TB-SW motility medium and assessed the ability of the mutants to migrate through the agar. 13 mutant strains were non-motile and were set aside as putative *rpoN* mutant strains (Table 4). Motile strains were considered to have the Tn*5*P insertion not within *rpoN* and were further analyzed. While additional uncharacterized genes could perform dual roles in both motility and biofilm formation, it was deemed more likely that such mutants would have insertions within *rpoN*. Indeed, a number of putative *rpoN* mutants were later confirmed as such.

Table 4: Mutants

Mutant Type	**Number of mutants (remaining)**
Total smooth mutants	270
Putative Tn*5*P insertions within pRscS	127 (143)
Putative Tn*5*P insertions within *rpoN*	13 (130)
Putative Tn*5*P inserts within *syp*	103 (27)
Mutants with severe growth defects	5 (22)
Identified novel Tn*5*P insertions	8 (14)
Unidentified Tn*5*P insertions	14

Identification and elimination of insertions within the *syp* locus

Lastly, I sought to identify and eliminate mutants with insertions within the genes of the *syp* locus. Insertions within almost any of these genes will result in an inability to form biofilms (Yip, 2005; Shibata, 2012). To identify putative *syp* mutants, I developed a linkage assay described in Methods and Materials (Fig. 20). Briefly, by transforming chromosomal DNA from my mutant strains containing the Erm^R Tn*5*P into a *syp*-Cm strain, I could assess for linkage between the Tn*5*P and *syp* (between the Erm and Cm antibiotic markers). 103 of the remaining mutant strains exhibited Cm sensitivity (thus linkage) (Table 4) and were eliminated from further consideration. The remaining mutants were retained for further study. While I was able to utilize this method to quickly identify Tn*5*P insertion sites within the *syp* locus, it is also possible that some of the mutants were not within but rather near the *syp* locus. This is of relatively little concern, however, as many of the genes adjacent to the *syp* locus have already been assessed and do not cause a smooth colony phenotype when disrupted (Yip, Grublesky et al., 2005, Ray, Driks et al., 2015).

Ruling out a role for second site mutations in the smooth mutant strains

Of the remaining smooth mutants, 8 were selected for further characterization (Table 4). However, there remained a possibility that the smooth phenotype was due to a mutation at a site secondary to the Tn*5*P insertion site. To confirm that the Tn*5*P insertion could be responsible for the smooth phenotype, I used natural transformation to backcross the Tn*5*P and surrounding DNA into the parent strain. Once a backcrossed strain was obtained, pJMO34, a plasmid containing *rscS* driven by the *cat* (chloramphenicol acetyltransferase) promoter (thus not LacI-repressible) was introduced

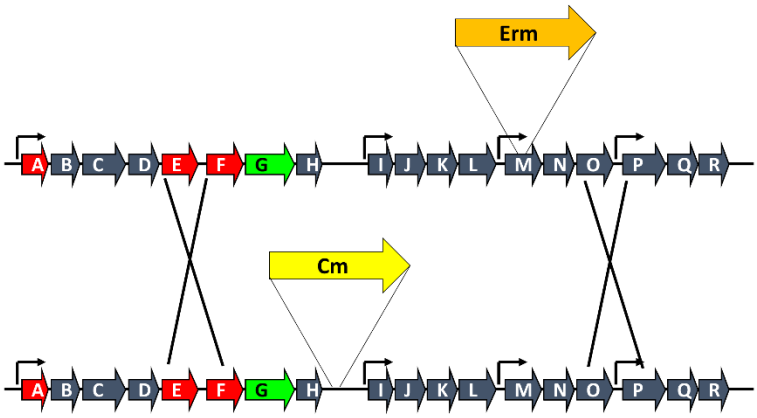

Figure 20 - Establishing linkage between the *syp* locus and Tn*5*P insertion sites. A recipient strain was generated by introducing a Cm^R cassette to the center of the *syp* locus between *sypH* and *sypI*. DNA from the biofilm defective mutant strains was transformed into the recipient strain and recombinant cells were selected by growth on Erm containing medium. Linkage between the Tn*5*P insertion site and the center of the *syp* locus was then determined by assessing Erm^R strains for sensitivity to Cm. Strains that exhibited sensitivity to Cm in more than 1 out of 10 transformants was considered to contain a Tn*5*P insertion within the *syp* locus by virtue of the linkage between the Tn*5*P and the Cm cassette within the *syp* locus.

to the mutant and the strain was reassessed for wrinkled colony formation. Mutants that maintained a smooth or severely delayed wrinkling phenotype were retained and further analyzed to identify the site of insertion as described in Materials and Methods.

VII. Characterization of the biofilm mutants

In the following sections, I will describe the individual biofilm-defective mutant strains I obtained and my approaches to test specific hypotheses that could explain why the loss of a given gene could inhibit or impair the ability of the strain to form a biofilm. This work provides a broad overview of the roles of central metabolism and the electron transport system in wrinkled colony formation in *V. fischeri* and possible mechanisms by which central metabolism and electron transport may modulate the process.

The role of *glnA* on wrinkled colony formation by *V. fischeri*

Introduction

The biosynthesis of amino acids is vital to the health and growth of the cell. In *V. fischeri*, a number of amino acid auxotrophs either fail to form wrinkled colonies (Singh, Brooks et al., 2015), fail to colonize (Graf and Ruby, 1998), or both (Singh, Brooks et al., 2015). Cysteine auxotrophs, specifically mutants of the *cysK* gene, are unable to form wrinkled colonies unless the growth medium is supplemented with cysteine or the mutants are grown together with a different strain that is able to synthesize cysteine (Singh, Brooks et al., 2015). While the mechanism for the role of cysteine in *V. fischeri* biofilm formation has not been uncovered, the requirement for the amino acid is certain.

One of the smooth mutants I collected from my screen contained an insertion within the *glnA* gene. As described in the literature review, the GlnA protein encoded by this gene is responsible for replacing the hydroxyl in glutamic acid's side-chain with an

amine group, thus generating glutamine. In the following section, I will describe the phenotype of the *glnA* mutant and test a number of hypotheses that could explain why the loss of glutamine synthesis inhibits biofilm formation in *V. fischeri.*

The *glnA* Tn*5*P mutant strain

From my screen of wrinkled colony defective mutants, I isolated one mutant with an insertion in *glnA* (*VF_0098*). The Tn*5*P insertion was positioned on chromosome I between bases 115,019 and 115,020, and the Tn*5*P promoter was oriented upstream, in the orientation opposite to *glnA* transcription (Fig. 21). Whereas the parent strain formed wrinkled colonies within 18 h, the *glnA* mutant strain exhibited a severe defect in wrinkled colony formation: the mutant colonies remained smooth even after 77 h of growth (Fig. 22). These results suggest a role for *glnA* and glutamine biosynthesis in biofilm formation by *V. fischeri*.

The role of Tn*5*P promoter and polar effects on biofilm formation in the *glnA*::Tn*5*P mutant strain

Based solely on the position and orientation of the Tn*5*P insertion (Fig. 21), it is possible the Tn could cause dysregulation of a number of genes other than *glnA* that could mediate the observed phenotype. For example, it is possible that the defect in biofilm formation is caused by the Tn*5*P promoter driving expression of *typA*, a putative GTP binding protein. If this were the case, I would expect that the smooth colony phenotype would depend on the presence of IPTG in the medium. However, this was not the case as many experiments, including those in Figure 22, were conducted in the absence of IPTG, and therefore the absence of expression from the Tn*5*P promoter.

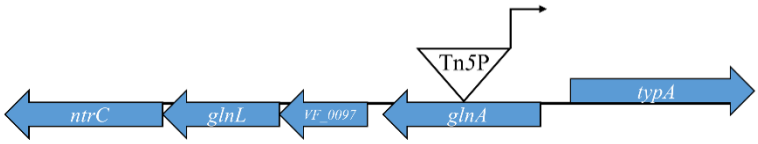

Figure 21 - The location and orientation of the Tn*5*P insertion in the *glnA* mutant strain. The insertion in *glnA*::Tn*5*P is located in *glnA* on chromosome I between bases 115,019 and 115,020 with the A1/34 promoter oriented opposite of *glnA* transcription.

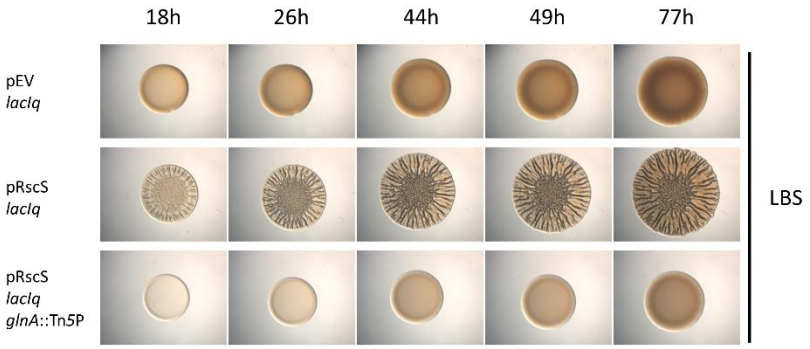

Figure 22 - The biofilm phenotype of the *glnA*::Tn*5*P mutant strain. The ability of the *glnA*::Tn*5*P mutant strain to wrinkle was assessed using the wrinkled colony assay. A parental strain carrying an empty vector (pJMO33) does not exhibit wrinkling or any colony architecture even after 77 h when grown on LBS. Parental strains carrying an *rscS* overexpression vector (pJMO34) have begun to wrinkle by 18 h and maintain a wrinkled morphology. The *glnA*::Tn*5*P mutant strain carrying pJMO34 does not wrinkle even after 77 h of growth. This figure is representative of at least 3 independent experiments.

It is also possible that the Tn*5*P insertion exerts polar effects on these downstream genes. However, it is unlikely based on the relatively large gap (250 bp) between the end of *glnA* and the beginning of the next gene on the chromosome, *VF_0097* (which encodes a hypothetical protein). Additionally, based on the role of *glnA* in glutamine biosynthesis, my investigations into this mutant described below, it is unlikely that polar effects account for the disruption in biofilm formation of this mutant.

The role of GlnA substrate accumulation in biofilm formation

One potential reason for the defect in biofilm formation of the *glnA* mutant strain is the accumulation of the GlnA substrates, glutamate or NH_3 (Fig. 13). If the *glnA* smooth phenotype is mediated by the accumulation of glutamate, then the addition of glutamate should delay or inhibit wrinkling by the parental strain. To test this possibility, I inoculated the parental strain onto a medium containing 0.2% glutamic acid and assessed wrinkled colony formation. No differences in wrinkling were observed at the times assessed (Fig. 23), though the start of wrinkling was not captured. Given the extreme nature of the *glnA* mutant defect, these results suggest that the accumulation of glutamate in the *glnA* mutant is not responsible for the defect in biofilm formation.
One of the functions of glutamine is to store nitrogen in the form of the amine group on its side-chain (Chandra, Basir et al., 2010). Therefore, the activity of GlnA removes NH_3 from its soluble form in the cell and stores it for times of nitrogen limitation. I thus hypothesized that the *glnA* mutant may have increased levels of NH_3 that could cause its biofilm defect. If increased levels of NH_3 are responsible for the inability of the *glnA* mutant to form wrinkled colonies, then the addition of ammonia should delay or inhibit the ability of the parental strain to form a wrinkled colony. To test this possibility, I

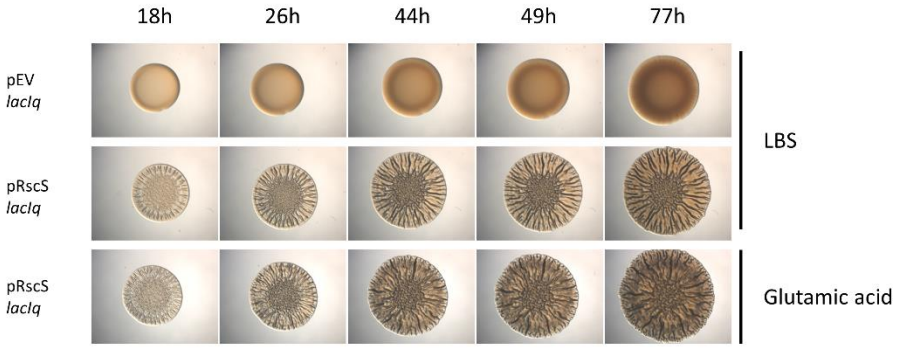

Figure 23 - The phenotype of a parental strain grown in the presence of supplemented glutamic acid. The role of GlnA substrate accumulation on biofilm formation was assessed by growing the parental strain in LBS medium supplemented with 0.2% glutamic acid. Compared to the parental strain grown on LBS with no extra nutrient added, the parental strain grown in LBS + glutamic acid does not appear to exhibit a biofilm defect that would be expected if glutamate accumulation contributed to the inability of the *glnA*::Tn*5*P mutant to form a biofilm. The empty vector, pEV, is pJMO33. The RscS plasmid, pRscS, is pJMO34. This figure is representative of at least 2 independent experiments.

inoculated the parental strain onto LBS medium supplemented with 0.2% ammonium chloride and assessed wrinkled colony formation. No differences in wrinkled colony formation were observed at the times assessed (Fig. 24). These results suggest that any accumulation of NH_3 that may occur in the *glnA* mutant is not responsible for the defect in biofilm formation.

The role of GlnA product loss in biofilm formation

The function of GlnA is the synthesis of glutamine from glutamate and ammonia. The decrease in availability of glutamine in the *glnA* mutant strain may contribute to the inability of the strain to form a wrinkled colony. If the *glnA* smooth phenotype is mediated by the loss of the GlnA product, then the addition of glutamine, the product of GlnA, should restore the wrinkling phenotype. To test this possibility, I inoculated the *glnA* mutant onto medium supplemented with 0.2% glutamine and assessed wrinkled colony formation. Even at the earliest time points assessed, the exogenous addition of glutamine to the *glnA* mutant strain restored the ability of the mutant to form wrinkled colonies (Fig. 25). While the phenotype of the parental strain was altered when grown in the presence of 0.2% glutamine compared to LBS, the ability of the *glnA* mutant to form wrinkled colonies was clearly restored. This demonstrates that glutamine is required for biofilm formation by *V. fischeri*. Further, it suggests that even if there are polar effects of the Tn insertion, they do not significantly impact biofilm formation. Additionally, this result rules out a role for second site mutations in the phenotype of the *glnA* mutant.

V. fischeri amino acid auxotrophs are capable of being complemented by growth in close proximity to non-auxotrophic cells. An investigation into the role of cysteine in *V. fischeri* biofilm formation by Singh et al. demonstrated that co-inoculating cysteine

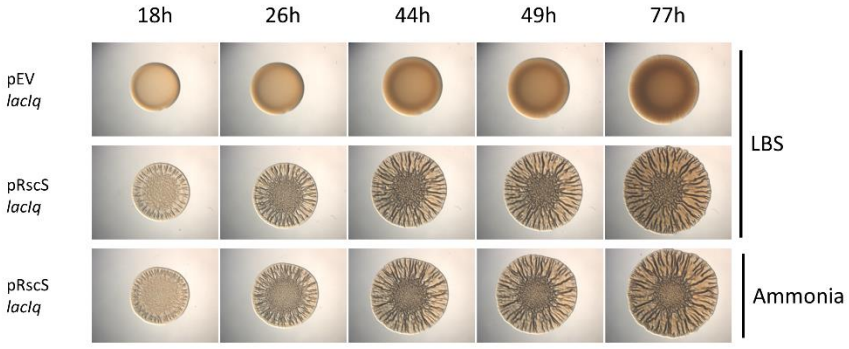

Figure 24 - The phenotype of a parental strain grown in the presence of supplemented ammonia. The role of GlnA substrate accumulation on biofilm formation was assessed by growing the parental strain in LBS medium supplemented with 0.2% ammonium chloride. Compared to the parental strain grown on LBS with no extra nutrient added, the parental strain grown in LBS + ammonia does not appear to exhibit a biofilm defect that would be expected if ammonia accumulation contributed to the inability of the *glnA*::Tn*5*P mutant to form a biofilm. The empty vector, pEV, is pJMO33. The RscS plasmid, pRscS, is pJMO34. This figure is representative of at least 2 independent experiments.

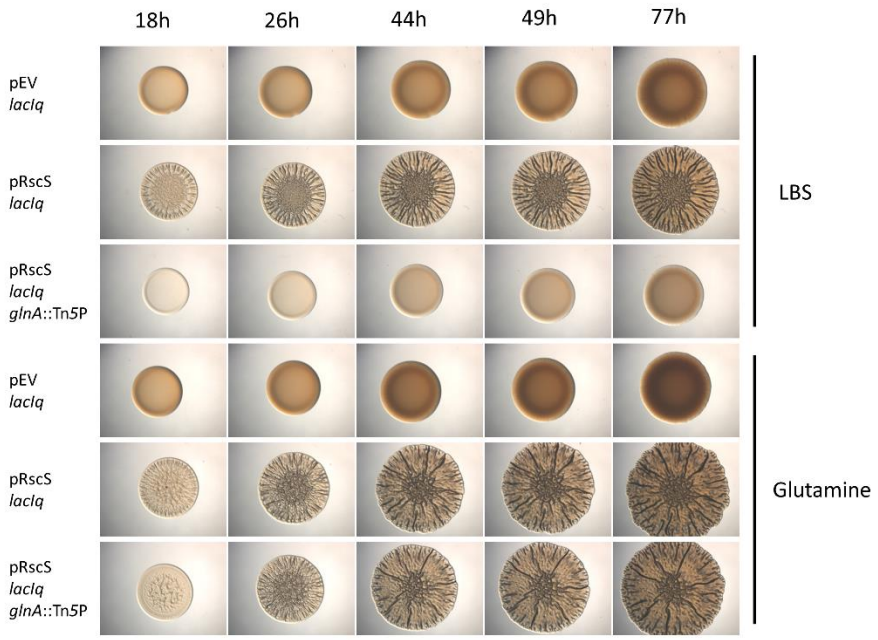

Figure 25 - The phenotype of a parental and *glnA* mutant strains grown in the presence of supplemented glutamine. The role of GlnA product loss on biofilm formation was assessed by growing the *glnA*::Tn*5*P mutant strain in LBS medium supplemented with 0.2% glutamine. No change in phenotype was noted between the parental strain containing the control vector grown in with LBS or LBS supplemented with glutamine. The empty vector, pEV, is pJMO33. The RscS plasmid, pRscS, is pJMO34. This figure is representative of at least 3 independent experiments.

biosynthesis-competent but non-biofilm forming *V. fischeri* strains with a *cysK* mutant strain restores the ability of the *cysK* mutant to form wrinkled colonies (Singh, Brooks et al., 2015). Presumably, this is because the strain competent in cysteine biosynthesis exports enough of the amino acid to complement the defect of the *cysK* mutant strain. Thus, I next asked whether the defect of the *glnA* mutant strain could be restored by co-incubation with non-biofilm forming, but glutamine-synthesizing strain. However, the mixture of the *glnA* mutant strain with a *sypL* mutant strain was not sufficient to restore wrinkling to the *glnA* mutant (Fig. 26). One possibility for this is that glutamine may not be exported like cysteine (Dassler, Maier et al., 2000, Franke, Resch et al., 2003).

The role of GlnA in Syp PS production

While a role for glutamine in biofilm formation has now been established, there remains the question of what that role is and whether it impacts pathways known to be involved in wrinkled colony formation, such as Syp PS production. *V. fischeri* strains that produce the Syp PS exhibit increased cell-cell associations and, as a consequence, the disruption of a colony with a toothpick results in the entire colony being moved as a unit (Ray, 2015). I will refer to this phenotype as "cohesion" (Fig. 27A). *V. fischeri* cells not induced to produce Syp PS do not show cohesion: the toothpick readily penetrates the spot without disrupting the entire colony (Fig. 27B). To assess the ability of the *glnA* mutant strain to produce the Syp PS, the *glnA* mutant strain was inoculated onto LBS medium and the resulting spot was disrupted after 77 h of growth. Unlike the parental strain, colonies of the *glnA* mutant strain could not be moved as a single unit (Fig. 27). These results suggest that the *glnA* mutant strain does not produce Syp PS at all, or does

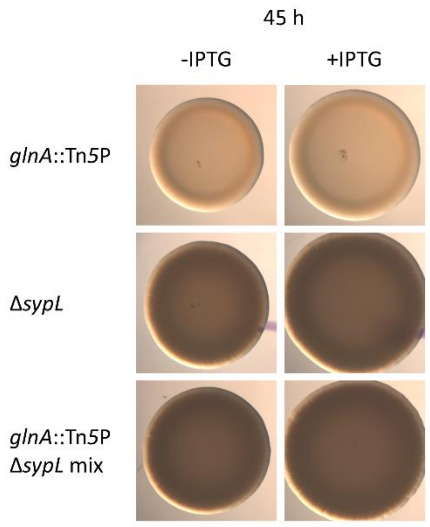

Figure 26 - The biofilm phenotype of the *glnA* mutant strain mixed with a glutamine biosynthesis competent strain. Some biofilm defects can be restored by mixing the defective strain with a second strain possessing an intact pathway for which the first strain is defective. To test whether the *glnA* mutant strain's biofilm defect can be restored in this manner, the mutant was mixed with a glutamine biosynthesis^{+} strain (Δ*sypL*) and assessed using a wrinkled colony assay. In both the presence and absence of IPTG, mixture with the Δ*sypL* strain was unable to restore the biofilm defect of the *glnA* mutant strain. This experiment was conducted once.

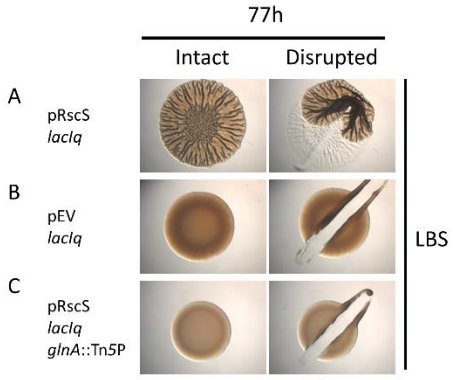

Figure 27 - The agar adherence phenotype of the *glnA*::Tn*5*P mutant strain. Strains were spotted and allowed to develop a biofilm for 77 h and then disrupted with a wooden toothpick by dragging the toothpick across the colony. When the parental strain carrying *rscS* overespression plasmid pJMO34 is disrupted, the wrinkled colony maintains cell-cell cohesion and gathers into a bunch A). The parental strain carrying an empty vector is easily disrupted and exhibits no cohesion due to a lack of Syp polysaccharide production B). The *glnA*::Tn*5*P mutant strain, like the parent strain carrying the control vector, exhibited no cell-cell cohesion. The empty vector, pEV, is pJMO33. The RscS plasmid, pRscS, is pJMO34. This figure is representative of at least 2 independent experiments.

not produce the PS in sufficient quantities to promote wrinkled colony formation. The role that glutamine has in PS production is unclear.

The biofilm phenotype of the *glnA* mutant strain grown on LBS containing glucose

As part of work performed with other mutants described below, I tested the impact of a number of other carbon sources on the *glnA* mutant phenotype (Methods and Materials). The wrinkled colony and Syp PS defects of the *glnA* mutant strain remained unaltered, with one exception: the addition of 0.2% glucose resulted in increased cohesion of the strain (Fig. 28). This result suggests that glucose causes increased production of the Syp PS in the *glnA* mutant. However, the addition of glucose also caused a delay in wrinkling of the parent strain (Fig. 28). My current data do not permit me to determine if the delayed wrinkling stems from delayed PS production or from a defect in the production of Bmp or another matrix protein required for wrinkled colony formation. The impact of glucose on the ability of both the *glnA* mutant and the wild-type strain to form a biofilm merits further investigation.

Summary

In summary, my screen for mutants unable to form wrinkled colonies yielded a mutant with a Tn*5*P insertion within the *glnA* gene. Investigations into the role of *glnA* in wrinkled colony formation showed that the defect in biofilm formation was not due to either activity of the Tn*5*P promoter or polar effects of the insertion. Instead, my data indicate that the *glnA* mutant strain is unable to form a wrinkled colony due, at least in part, to its inability to produce sufficient levels of Syp PS. However, there remains another underlying defect, as Syp PS production, but not wrinkled colony development,

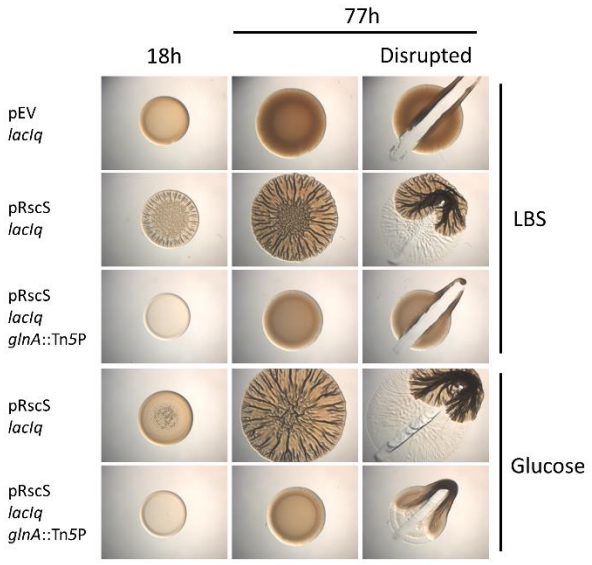

Figure 28 - The biofilm phenotype of the *glnA*::Tn*5*P mutant in response to glucose. The addition of glucose promoted an increase in colony size of the parental strain carrying pJMO34 but delayed wrinkled colony formation (18 h timepoint). The *glnA* mutant strain transitioned from a non-cohesive phenotype in LBS to a cohesive phenotype in the presence of glucose. The empty vector, pEV, is pJMO33. The RscS plasmid, pRscS, is pJMO34. This figure is representative of at least 2 independent experiments.

was restored when *glnA* mutants were exposed to glucose. These data demonstrate a specific requirement for glutamine in the formation of a wrinkled colony by *V. fischeri*.

The role of *mdh* on wrinkled colony formation by *V. fischeri*

Introduction

One of the smooth mutants I collected in my screen was a strain with an insertion within the TCA cycle gene, *mdh*. Mdh catalyzes the oxidation of malate into oxaloacetate (OAA) with the coincident reduction of NAD to NADH (Fig. 7), as well as the reverse reaction. In the following section, I describe the phenotype of the *mdh* mutant and test a number of hypotheses that could explain why the loss of Mdh function contributes to a defect in biofilm formation by *V. fischeri*.

The *mdh*::Tn*5*P mutant strain

From my screen of wrinkled colony defective mutants, I isolated one mutant with an insertion in *mdh* (*VF_0276*). The Tn*5*P insertion was positioned on chromosome I between bases 283,689 and 283,690 with the Tn*5*P promoter oriented upstream, in the opposite orientation to *mdh* transcription (Fig. 29). The *mdh* gene does not appear to be a part of a larger operon, suggesting that the wrinkled colony defect is not due to polar effects. Using the spotted colony time course assay, I found that the *mdh* mutant exhibited a severe defect in wrinkled colony formation: whereas the parent strain formed wrinkled colonies within 18 h, the *mdh*::Tn*5*P mutant strain exhibited a severe delay in biofilm formation: the mutant colonies began to show signs of wrinkling only after around 42 h of growth (Fig. 30). Moreover, it never developed a normal wrinkled colony morphology, but instead exhibited a divoting phenotype (Fig. 30). When I disrupted the *mdh* mutant spot with a toothpick after 77 h, I found that the center adhered strongly to

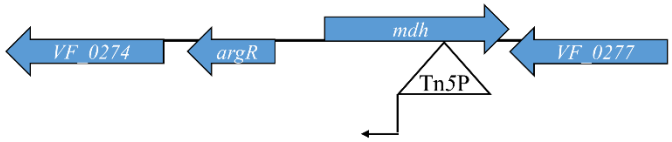

Figure 29 - The location and orientation of the Tn*5*P insertion in the *mdh* mutant strain. The insertion in *mdh*::Tn*5*P is located in *mdh* on chromosome I between bases 283,689 and 283,690 with the A1/34 promoter oriented opposite of *mdh* transcription.

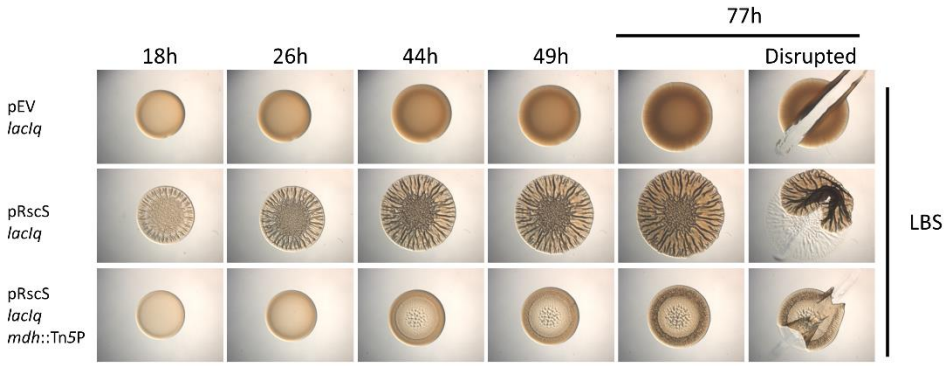

Figure 30 - The biofilm phenotype of the *mdh*::Tn*5*P mutant strain. The ability of the *mdh*::Tn*5*P mutant strain to wrinkle was assessed using the wrinkled colony assay. A parental strain carrying an empty vector (pJMO33) does not exhibit wrinkling or any colony architecture even after 77 h when grown on LBS. Parental strains carrying an *rscS* overexpression vector (pJMO34) have begun to wrinkle by 18 h and maintain a wrinkled morphology. The *mdh*::Tn*5*P mutant strain carrying pJMO34 begins to exhibit a divoting colony morphology at 44 h but never exhibits a WT wrinkling phenotype. When disrupted at 77 h, the *mdh*::Tn*5*P mutant strain exhibits colony cohesion at its edges, but adheres to the plate at its divoted center. The empty vector, pEV, is pJMO33. The RscS plasmid, pRscS, is pJMO34. This figure is representative of at least 3 independent experiments.

the agar surface, rather than being moved as a single unit, as has been observed for the parent. I will describe this novel phenotype in more detail below. Finally, to determine if the promoter within Tn*5*P contributed to the observed phenotype, I performed the same experiment in the presence of IPTG, but was unable to distinguish phenotypic differences between mutants grown in the presence or absence of IPTG (data not shown). I conclude that neither polar nor Tn*5*P promoter effects are contributing to the smooth phenotype of the *mdh*::Tn*5*P mutant strain.

The role of Mdh substrate accumulation in biofilm formation

One potential cause for the delay in biofilm formation by the *mdh*::Tn*5*P mutant strain is an accumulation of the Mdh substrate, malate, as carbon is cycling around the TCA cycle. If the *mdh*::Tn*5*P mutant strain's delay in wrinkling is mediated by the accumulation of this Mdh substrate, the addition of malate should also delay wrinkling by the parental strain. To test this possibility, I inoculated the parental strain onto LBS medium supplemented with 0.2% malic acid and assessed the formation of wrinkled colonies. Unfortunately, the addition of malic acid to the medium resulted in *V. fischeri* strains that failed to grow (data not shown). This effect was not caused by an acidic pH, as the medium used, LBS, was a Tris-buffered medium and the pH of the agar plates remained near 7.5, the pH of the buffer. Thus, a role for malate accumulation in the inhibition of biofilm formation cannot be ruled out.

The role of OAA, the Mdh product, in biofilm formation and Syp PS production

Another potential cause for the delay in biofilm formation by the *mdh*::Tn*5*P mutant strain is that there may be a lack of the Mdh product, OAA. If a lack of OAA contributes to the delay and/or defect in biofilm formation by the mutant, then the

addition of OAA to the growth medium of an *mdh* mutant should restore a more normal timing or pattern of wrinkling. To test this possibility, I inoculated the *mdh*::Tn*5*P mutant strain and its parent onto LBS medium supplemented with 0.2% OAA and assessed wrinkled colony formation. When grown in the presence of OAA, the parent strain exhibited a modest delay (~10 h) in wrinkled colony formation compared to its growth in LBS (Fig. 31). After the delay, the parental strain developed normally and the colony displayed the typical cohesive properties when disrupted (Fig. 31). In contrast to the expectation that OAA addition might restore the ability of the *mdh* mutant to wrinkle, the *mdh*::Tn*5*P mutant failed to wrinkle in the presence of OAA, even after 77 hours of growth (Fig. 31). Given the delayed biofilm results obtained for the parent, it would not have been surprising had the *mdh* mutant exhibited a further delay compared to the no addition control, but a complete lack of wrinkling was unexpected. Lastly, I disrupted the colony formed by the *mdh* mutant with a toothpick at 77 h. I found that the adherence to the plate that I observed in the no addition control was fully abolished in the presence of OAA (Fig. 31). Together, these data first suggest that, at the amount I used, OAA does not make a positive contribution to biofilm formation, but rather caused increased delays and decreased biofilm formation. Second, these data suggests that, if adhesion, like cohesion (Ray, Driks et al., 2015), depends on Syp PS, then exposure to OAA causes a decrease in Syp PS production.

The impact of other carbon sources on wrinkled colony formation by the *mdh*::Tn*5*P mutant strain

It was somewhat surprising that we would see evidence of a decrease in PS production in the *mdh*::Tn*5*P mutant strain with the addition of OAA, a TCA intermediate

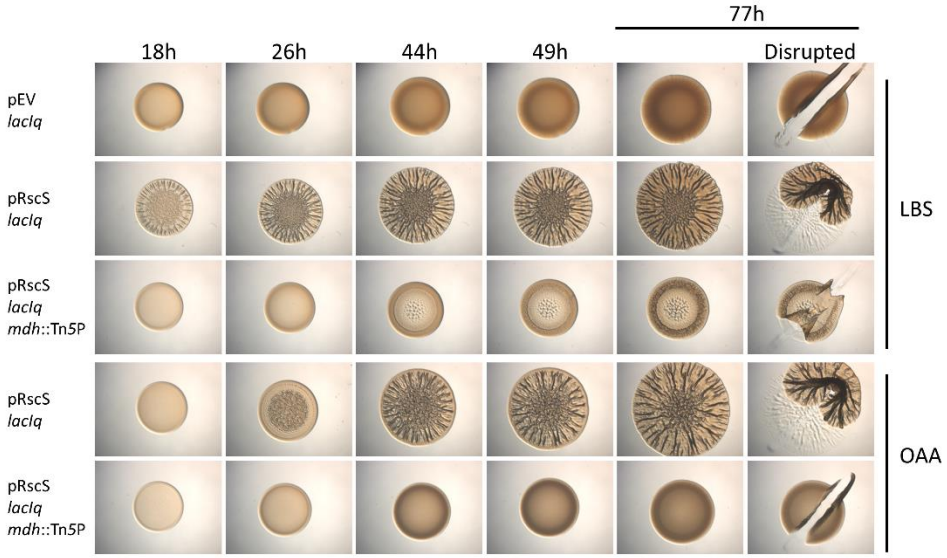

Figure 31 - The biofilm phenotypes of the parental and *mdh* mutant strains in the presence of OAA. The ability of the Mdh product, OAA, to rescue the biofilm defect of the *mdh*::Tn*5*P mutant strain was assessed using the wrinkled colony assay. Compared to growth in LBS, the parental strains carrying pJMO34 were delayed in wrinkled colony formation (18 h and 26 h). When exposed to OAA the *mdh*::Tn*5*P mutant strain was completely inhibited in both the development of colony morphology (divoting) and agar adherence. The empty vector, pEV, is pJMO33. The RscS plasmid, pRscS, is pJMO34. This figure is representative of at least 2 independent experiments.

that can serve as an input to the gluconeogenic (GNG) pathway and, thus, polysaccharide production. Therefore, I asked whether the addition of GNG end-products more proximal to PS biosynthesis, *i.e.*, further along the GNG pathway, would cause a similar decrease in cell-surface adhesion in the *mdh* mutant strain. Specifically, I inoculated the *mdh* mutant strain onto medium supplemented with 0.2% glucose or glucose-6-phosphate (G6P) and assessed colony morphology and adhesion. When grown in the presence of these two carbon sources, the parent strain exhibited phenotypes similar to those observed when grown in OAA: a moderate delay in wrinkling yet a normal wrinkling pattern and strong cell-cell cohesion when disrupted at 77 h (Figs. 31 & 32). The response of the *mdh*::Tn*5*P mutant to glucose and G6P was also similar to its response to OAA: these carbon sources fully disrupted both the divoting and, more strikingly, colony adhesion observed in their absence (Figs. 31 & 32). These data suggest that the addition of gluconeogenic carbon sources inhibits biofilm formation in general. Furthermore, these data suggest that the addition of these carbon sources can result in a decrease in Syp PS production. Quantification of Syp PS production will need to be conducted in these strains under these conditions to verify this hypothesis.

Finally, to determine if the responses I observed were specific to GNG carbon sources, I tested whether other available nutrients (Methods and Materials), when supplemented at 0.2%, modulated biofilm formation of the *mdh*::Tn*5*P mutant strain. The addition of the nitrogen source ammonium chloride accelerated the onset of colony edge wrinkling in the mutant strain, which was best observed at the 44 h time point (Fig. 33). Two of the other nutrients tested, glutamine and glutamic acid, resulted in an increased amount of wrinkling (Fig. 33). The addition of glutamic acid increased the intensity of

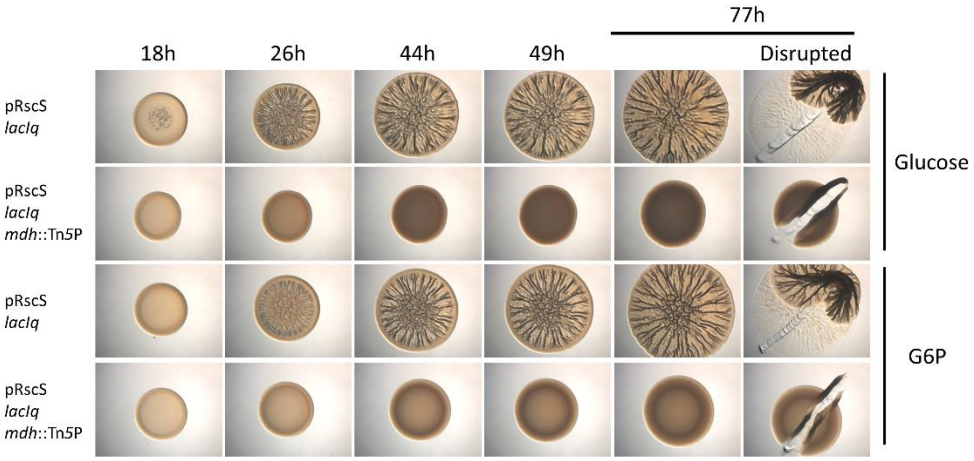

Figure 32 - The biofilm phenotypes of the parental and *mdh* mutant strains in the presence of Glucose and G6P. The ability of additional gluconeogenic end products, glucose and G6P, to inhibit the divoting and adhesion phenotypes of the *mdh*::Tn*5*P mutant strain was assessed using the wrinkled colony and toothpick assays. Compared to growth in LBS (Fig. 31), the parental strain was delayed in wrinkled colony formation when grown in both glucose and G6P. When exposed to glucose and G6P the *mdh*::Tn*5*P mutant strain was completely inhibited in both the development of colony morphology (divoting) and agar adherence. The RscS plasmid, pRscS, is pJMO34. This figure is representative of at least 2 independent experiments.

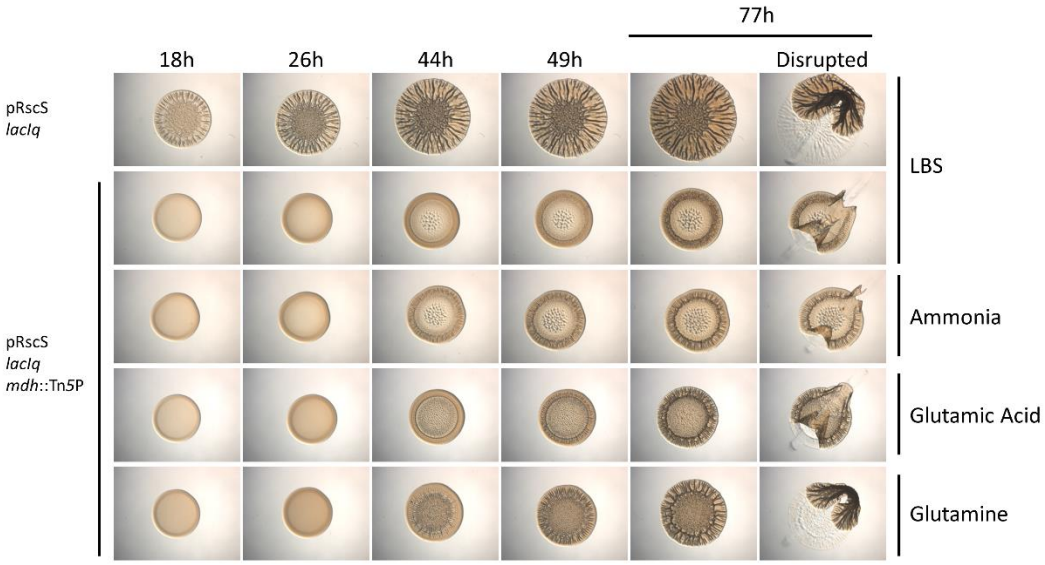

Figure 33 - The biofilm phenotypes of the *mdh* mutant strain in the presence of ammonia, glutamic acid, and glutamine. To assess whether the response of the *mdh*::Tn*5*P mutant strain to GNG end products (Figs. 31 & 32) was specific to the GNG end products, the *mdh*::Tn*5*P mutant was grown on additional nutrient sources and the biofilm phenotypes were assessed using the wrinkled colony and toothpick assays. Compared to growth in LBS, the *mdh*::Tn*5*P mutant strain exhibited an increase in edge wrinkling and center divoting when grown in ammonia and glutamic acid respectively. When grown in the presence of glutamine, the *mdh*::Tn*5*P mutant strain exhibited a restoration of WT biofilm phenotypes after a delay. The RscS plasmid, pRscS, is pJMO34. This figure is representative of at least 2 independent experiments.

the divoting at the center of the colony, which can be best seen at the 44 h time point (Fig. 33). Finally, the addition of glutamine resulted in a transition from a divoting center to a wrinkling center. Furthermore, glutamine addition caused a loss of cell-surface adhesion (Fig. 33). These data suggest that *mdh*::Tn*5*P mutant strain is somehow defective in glutamine or nitrogen regulation, though this has not been tested directly. Additionally, these data seem to show a correlation between the divoting phenotype and the agar adhesion phenotype. The connection between the two remains an area of interest. Finally, these data support my finding that the loss of adhesion when grown in the presence of GNG end-products is, in fact, specific to those carbon sources and not a general defect in biofilm formation caused by the supplementation of any additional nutrients in the medium.

Summary

In my screen for mutants with defects in wrinkled colony formation, I identified a mutant with a Tn*5*P insertion within the *mdh* gene. Investigations into the role of *mdh* in wrinkled colony formation could not rule out a role for malate accumulation, but did not support a role for OAA depletion as a cause of the defects. Further investigation suggested that increases in the concentrations of certain GNG substrates, intermediates, and end-products (OAA, G6P , and glucose) decreased the production of the Syp PS in the *mdh* mutant strain, while the addition of some GlnA products and byproducts (especially glutamine) promoted normal wrinkled colony formation. Of special interest was the ability of glutamine addition to restore both near-normal wrinkling and cell-cell cohesion.

The role of *pck* on wrinkled colony formation by *V. ficsheri*

Introduction

Two of the smooth mutants I collected in my screen contained insertions within the GNG pathway gene, *pck*. Pck removes carbon from the TCA cycle by catalyzing the decarboxylation and phosphorylation of OAA into PEP linked to the hydrolysis of GTP to GDP (Fig. 9). In the following section, I describe the phenotype of the *pck* mutant and test a number of hypotheses that could explain why the loss of Pck function could contribute to a loss of biofilm formation by *V. fischeri*.

The *pck*::Tn*5*P mutant strains

From my screen of wrinkled colony defective mutants, I isolated two independent mutants with insertions in *pck* (*VF_2478*). One mutant strain contained the Tn*5*P insertion between bases 2,775,405 and 2,775,406 on chromosome I with the Tn*5*P promoter oriented in the same direction as *pck* transcription (*pck*::Tn*5*P-forward) (Fig. 34A). The second *pck* mutant strain had the Tn*5*P insertion positioned between bases 2,775,455 and 2,775,456 with the Tn*5*P promoter oriented opposite to *pck* transcription (*pck*::Tn*5*P-reverse) (Fig. 34B). While the parent strain formed wrinkled colonies within 18 h, the *pck* mutant strains failed to form wrinkled colonies: the mutant colonies remained smooth even after 77 h of growth (Fig. 35, data not shown).

Based on the different orientations of Tn*5*P insertion, it seemed highly unlikely that the smooth phenotypes of the two *pck* mutant strains were caused by expression of neighboring genes from the Tn*5*P promoter. Indeed, I found no differences in wrinkled colony formation when the two strains were grown in the absence or presence of IPTG (Fig. 36). Based on these findings, I conclude that the two mutant strains are unable to

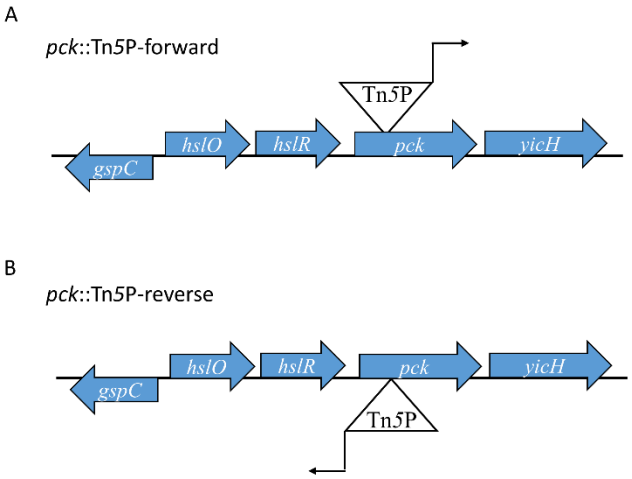

Figure 34 - The location and orientation of the Tn*5*P insertions in the *pck* mutant strains. The insertion in *pck*::Tn*5*P-forward is located in *pck* on chromosome I between bases 2,775,405 and 2,775,406 with the A1/34 promoter oriented in the direction of *pck* transcription. The insertion in *pck*::Tn*5*P-reverse is located in *pck* on chromosome I between bases 2,775,455 and 2,775,456 with the A1/34 promoter oriented opposite of *pck* transcription.

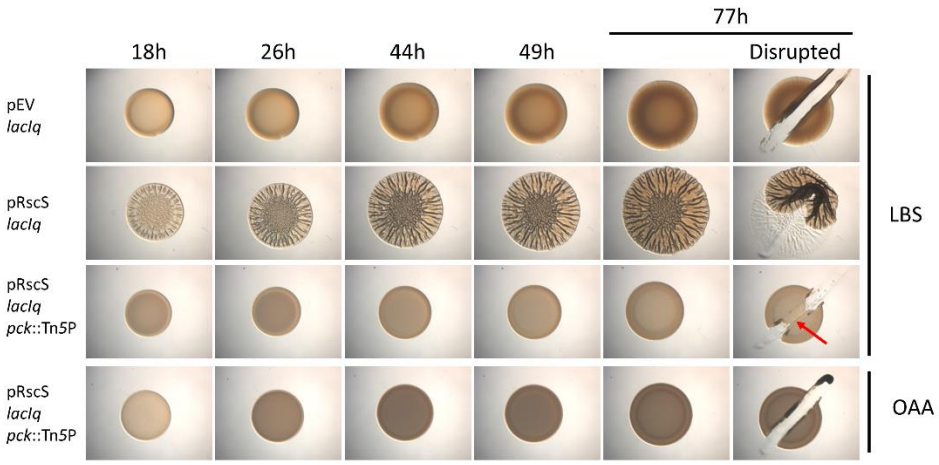

Figure 35 - The biofilm phenotype of the *pck*::Tn*5*P-forward mutant strain. The ability of the *pck*::Tn*5*P-forward mutant strain to wrinkle was assessed using the wrinkled colony and toothpick assays. A parental strain carrying an empty vector (pJMO33) does not exhibit wrinkling or any colony architecture even after 77 h when grown on LBS. Parental strains carrying an *rscS* overexpression vector (pJMO34) have begun to wrinkle by 18 h and maintain a wrinkled morphology. The *pck*::Tn*5*P mutant strain carrying pJMO34 does not develop colony morphology at advanced timepoints but does exhibit a agar adherence phenotype at the center of the colony when disrupted at 77 h. When the *pck*::Tn*5*P-forward mutant is grown in the presence of the Pck substrate, OAA, the mutant strain loses its adherence phenotype. The empty vector, pEV, is pJMO33. The RscS plasmid, pRscS, is pJMO34. This figure is representative of at least 2 independent experiments.

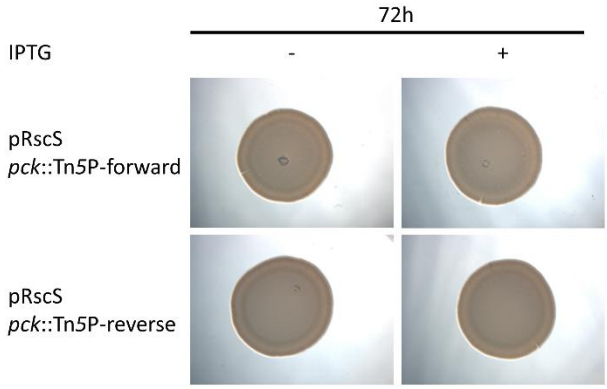

Figure 36 - The biofilm phenotypes of the *pck* mutant strains in the presence and absence of IPTG. To assess the role of the Tn*5*P promoter in the phenotype of the *pck* mutant strains, each strain was grown in the absence or presence of IPTG and assessed for the ability to form a biofilm. Both *pck*::Tn*5*P-forward and *pck*::Tn*5*P-reverse strains failed to form a biofilm and exhibited the same phenotype under both conditions. The RscS plasmid, pRscS, is pJMO34. This experiment has been conducted one time.

form wrinkled colonies due to the disruption of the *pck* gene and, thus, I conducted addition experiments primarily with the *pck*::Tn*5*P-forward mutant strain (henceforth referred to as simply *pck*::Tn*5*P).

The GNG pathway, and therefore Pck, is likely required for the biosynthesis of polysaccharide precursors utilized in Syp PS production. Thus, I first sought to identify whether there was a defect in Syp PS production. To assess the production of Syp PS, I applied the toothpick assay to colonies just after the 77 h time point. Reminiscent of the *mdh* mutant, the *pck* mutant colony also adhered to the agar surface (Fig. 35, arrow), although it didn't exhibit the divoting pattern observed with the *mdh* mutant. These results suggest that there is some Syp PS production in the *pck* mutant strain.

The role of *pck* substrate accumulation in biofilm formation

In the cell, Pck is responsible for facilitating the removal of carbon out of the TCA cycle toward gluconeogenesis. It does this by coupling the hydrolysis of GTP to the decarboxylation and subsequent phosphorylation of OAA into phosphoenolpyruvate (PEP) (Fig. 9). Therefore, in the *pck* mutant strain, there is likely either an accumulation of OAA, or OAA continues around the TCA cycle. If an accumulation of OAA plays a role in the inability of the mutant to form a wrinkled colony, the addition of OAA to a wild-type strain should have a similar effect. I performed this work as part of my investigation of the *mdh* mutant strain, and found that OAA caused only a moderate delay in wrinkled colony formation of the parent (Fig. 31). When I assessed the *pck* mutant, I found that it lost the agar adherence phenotype when exposed to OAA, like the *mdh* mutant (Fig. 35). Together, these data suggest that the accumulation of OAA may inhibit

adhesion and cohesion by the *pck*::Tn*5*P mutant strain, an effect that is amplified by the addition of OAA to the growth medium.

The effect of GNG end-products on the ability of the *pck* mutant to form wrinkled colonies

Based on the nature of Pck's role in GNG and potentially polysaccharide production, I next asked whether a hypothetical decrease in PS production could be complemented by the addition of carbon sources more proximal to PS precursors. If the *pck* mutant strain is unable to effectively perform GNG due to an inability to feed that pathway with carbon from the TCA cycle, then the addition of carbon sources that do not have to be processed by Pck to be converted into PS precursors, namely glucose and G6P, should compensate for this defect and promote the formation of wrinkled colonies. To test this hypothesis, I inoculated the *pck*::Tn*5*P mutant strain on medium supplemented with 0.2% glucose or G6P and assessed the wrinkled colony formation. The parent strain, as I observed previously (Fig. 32), exhibited a slight delay in wrinkled colony formation upon the addition of glucose and G6P, then continued to develop normal colony morphology. When exposed to either glucose or G6P, the *pck*::Tn*5*P mutant no longer adhered to the agar surface (Fig. 37, center of spots)—likely indicating a reduction in Syp PS—and did not exhibit any notable increase in cohesion. Growth with the other carbon sources tested, including succinate (Fig. 37), citrate, and glutamine, resulted in in no significant phenotype changes. I conclude that a simple decrease in availability of PS precursors in the *pck* mutant cannot account for its smooth colony phenotype.

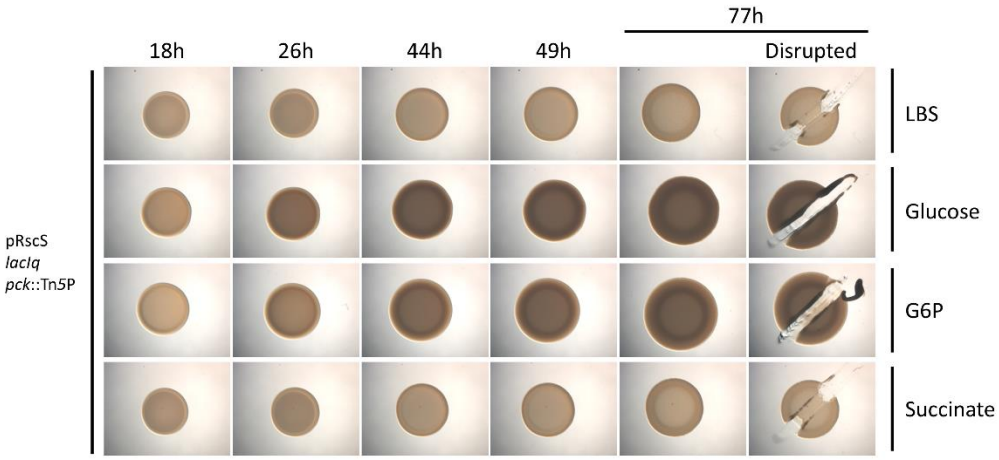

Figure 37 - The biofilm phenotypes of the *pck* mutant strain in the presence of glucose, G6P, and succinate. To assess whether the *pck* mutant strain's GNG defect was restricting the strain's ability to produce polysaccharide, the *pck*::Tn*5*P mutant was grown in the presence of carbon sources that do not have to be processed by Pck, and biofilm phenotypes were assessed. Similar to when it was grown in the presence of OAA (Fig. 35), when grown in both glucose and G6P, the *pck*::Tn*5*P mutant lost its adherence phenotype and did not wrinkle at advanced timepoints. The response of the *pck* mutant is specific to the addition to these carbon sources as the addition of other nutrients, such as succinate, did not result in a phenotypic change compared to growth on LBS. The RscS plasmid, pRscS, is pJMO34.This figure is representative of at least 2 independent experiments

Summary

In my screen for mutant with defects in wrinkled colony formation, I identified a mutant with a Tn*5*P insertion within the *pck* gene. Investigations into the role of *pck* in wrinkled colony formation supported a potential role for OAA accumulation but could not rule out a role for PEP depletion as PEP addition was not tested. Investigations into the role of Syp PS production and GNG in the *pck* mutant's smooth phenotype uncovered a minor agar attachment phenotype that could be inhibited by the addition of GNG substrates, intermediates, and products but not others. These experiments thus support the hypothesis that these carbon sources play an inhibitory role in biofilm formation by *V. fischeri*.

The role of *sdhE* in wrinkled colony formation by *V. fischeri*

Introduction

One of the smooth mutants I collected contained an insertion within *VF_2096*, which was annotated as a hypothetical protein. My subsequent bioinformatic analysis of this gene suggested that it encodes a homolog of the *E. coli* protein succinate dehydrogenase subunit E (SdhE), a member of the TCA and ETS complex succinate dehydrogenase (SDH) (Fig. 5). In *E. coli*, SdhE serves as a cytosolic protein that delivers the FAD co-factor to the membrane associated SdhCDAB complex, thereby activating its enzymatic activity (McNeil, Clulow et al., 2012, McNeil and Fineran, 2013). In addition, SdhE has been shown to activate the reverse reaction, fumarate to succinate, via FAD delivery to the fumarate reductase (FRD) complex (McNeil, Hampton et al., 2014). In the following section, I describe the phenotype of the *sdhE* mutant and test a number of

hypotheses that could explain why the loss of function of the SDH complex (or FRD complex) could contribute to the defect in biofilm formation by *V. fischeri*.

VF_2096::Tn*5*P mutant strains are defective for wrinkled colony formation

From my screen of wrinkled colony defective mutants, I isolated one mutant with an insertion in *VF_2096*. The Tn*5*P insertion was positioned on chromosome I between bases 2,333,206 and 2,333,207 with the Tn*5*P promoter oriented in the same direction as *VF_2096* transcription (Fig. 38). Downstream and overlapping is a second gene, *VF_2095*, that encodes a hypothetical protein. In a time course assay of wrinkled colony formation, I found that, while the parent formed wrinkled colonies after 18 h, the *VF_2096*::Tn*5*P mutant strain exhibited a severe defect in wrinkled colony formation, with mutant colonies just beginning to show structure at 77 h (Fig. 39). However, rather than wrinkling like the wild-type, the colonies formed divots similar to those of the *mdh* mutant strain (Fig. 30). Also, like the *mdh* and *pck* mutant strains, the *VF_2096*::Tn*5*P mutant strain adhered to the agar at the center of the colony (Fig. 39). These results suggest a role for *VF_2096* in biofilm formation by *V. fischeri*.

VF_2096 is *sdhE*

My bioinformatic analysis of the *VF_2096* amino acid sequence identified significant identity with *E. coli* SdhE, including all catalytic, stabilizing, and conserved as described by McNeil and Fineran (Fig. 40) (McNeil and Fineran, 2013). I thus sought to confirm that the identity of *VF_2096* as *sdhE*. If *VF_2096* were *sdhE*, the *sdhE* mutant strain should grow poorly when succinate is provided as the sole carbon source. To test this hypothesis, I grew both the parent and the *VF_2096*::Tn*5*P mutant strain in minimal medium broth containing succinate and observed growth. After growth overnight in

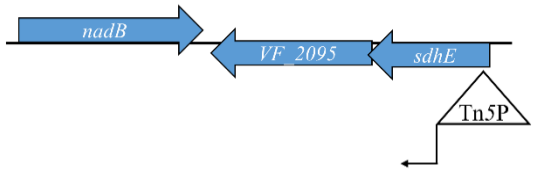

Figure 38 - The location and orientation of the Tn*5*P insertion in the *sdhE* mutant strain. The insertion in *sdhE*::Tn*5*P is located in *sdhE* on chromosome I between bases 2,333,206 and 2,333,207 with the A1/34 promoter oriented in the direction of *sdhE* transcription.

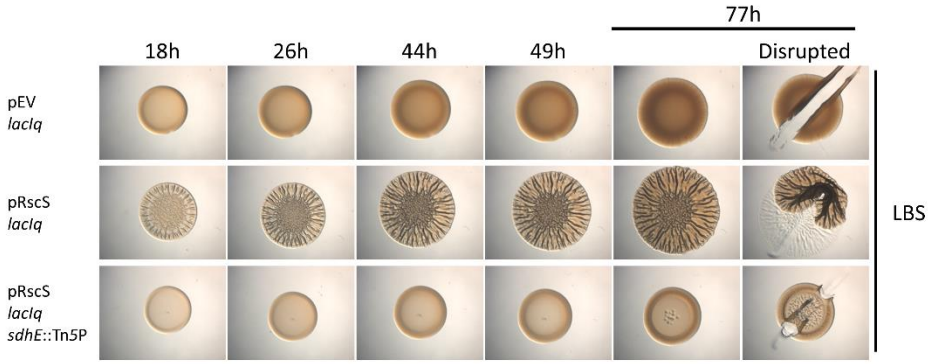

Figure 39 - The biofilm phenotype of the *sdhE*::Tn*5*P mutant strain. The ability of the *sdhE*::Tn*5*P mutant strain to wrinkle was assessed using the wrinkled colony and toothpick assays. A parental strain carrying an empty vector (pJMO33) does not exhibit wrinkling or any colony architecture even after 77 h when grown on LBS. Parental strains carrying an *rscS* overexpression vector (pJMO34) have begun to wrinkle by 18 h and maintain a wrinkled morphology. The *sdhE*::Tn*5*P mutant strain carrying pJMO34 develops a slight divoting colony morphology at advanced timepoints and adheres to the agar when disrupted at 77 h. The empty vector, pEV, is pJMO33. The RscS plasmid, pRscS, is pJMO34. This figure is representative of at least 3 independent experiments.

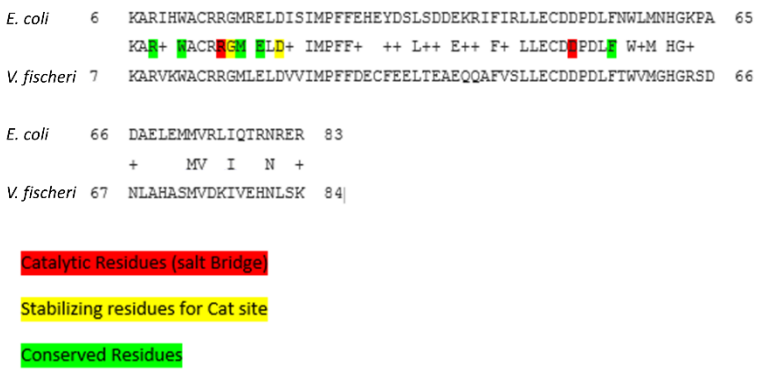

Figure 40 - Amino acid alignment of *V. fischeri* and *E. coli* SdhE proteins. Previous study of the *E. coli* SdhE protein identified a number of catalytic (Red) and stabilizing residues (Yellow) for the function of the protein, as well as a number of other residues conserved various SdhE proteins found in other species of bacteria (Green) (McNeil, 2013). Alignment of the *V. fischeri* SdhE polypeptide chain next to the *E. coli* SdhE reveals that all catalytic, stabilizing, and conserved residues are present in the *V. fischeri* SdhE.

either rich medium (LBS) or minimal medium + succinate, the parental strain was turbid in both, signifying growth. The *VF_2096*::Tn*5*P mutant strain, however, grew only in the rich medium (data not shown). This confirms that *VF_2096* has a role in succinate metabolism, and further supports its identity as *sdhE* in *V. fischeri*, and will henceforth be referred to as such.

sdhE is required for wrinkled colony formation

Based on the position and orientation of the Tn*5*P insertion (Fig. 38), it was possible that the Tn could be exhibiting polar effects on the downstream gene *VF_2095*. Indeed, analysis by McNeil and Fineran (McNeil and Fineran, 2013) demonstrated that both *sdhE* and its overlapping gene (*VF_2095*) are conserved in many organisms, suggesting that the downstream gene may have a linked function. Because disruption of *VF_2095*, *sdhE*, or both genes together could be the cause of the biofilm phenotype, I first investigated which of the two genes was required for wrinkled colony formation. If the loss of *sdhE* mediates the loss of wrinkled colony formation in the *sdhE*::Tn*5*P mutant strain, an in-frame deletion mutant of *sdhE* would also result in the smooth phenotype. To test this hypothesis, I generated an in-frame unmarked deletion of *sdhE* and assessed that strain for its ability to form a biofilm. The Δ*sdhE* strain exhibited a severe biofilm defect similar to the Tn mutant (Fig. 41). These data confirm a role for *sdhE* in biofilm formation by *V. fischeri*.

While I have shown a role for *sdhE* in the process of wrinkled colony formation, my experiments thus far don't rule out a role for the linked *VF_2095*. If *VF_2095* does have a role in biofilm formation, deletion or disruption of this gene alone would also result in a defect in biofilm formation. To test this hypothesis, I generated an in-frame

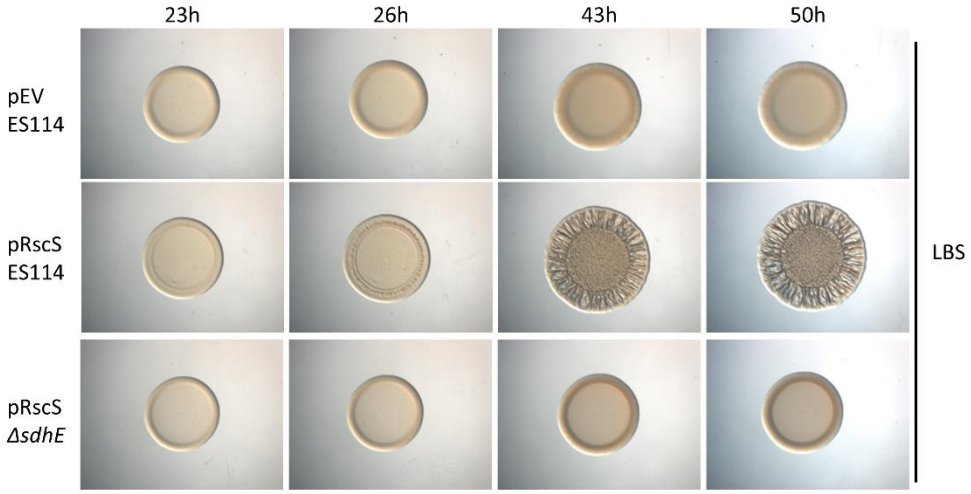

Figure 41 - The biofilm phenotype of a Δ*sdhE* mutant strain. A mutant carrying an unmarked in-frame deletion of *sdhE* exhibits the biofilm defect of the transposon mutant. The empty vector, pEV, is pKV282. The RscS plasmid, pRscS, is pARM7. This experiment has been conducted one time.

unmarked deletion of the *VF_2095* gene and assessed wrinkled colony formation. At the times assessed, the intensity of wrinkling in the Δ*VF_2095* strain was indistinguishable from that of the parent strain (Fig. 42). While the onset of wrinkling was not captured in the strains, it appears that the role of *VF_2095* in wrinkled colony formation is minimal if at all.

Mutants of *sdhE* have a similar phenotype to mutants of *sdhC*

As noted previously, SdhE is a promiscuous protein with known roles in the activation of SDH as well as FRD. I thus wondered if the requirement for SdhE depended on its role in the SDH complex or was due to one of its other functions. I hypothesized that, if the wrinkled colony phenotype of the *sdhE* mutant were due to its role in the SDH complex, then its mutant phenotype should be comparable to that of a mutant defective specifically for the SDH complex (e.g., *sdhC*). If, instead, the defect of the *sdhE* mutant were greater than that of the *sdhC* mutant strain, then SdhE may be impacting multiple enzymes or complexes such as FRD. I thus compared the biofilm phenotypes of the *sdhE*::Tn*5*P mutant to an *sdhC*::Tn*5* mutant that the Visick lab possesses. I found that, while the *sdhC* and *sdhE* mutants both exhibited biofilm defects compared to a parent strain, the phenotypes of the two mutants differed somewhat: the *sdhE* mutant had a greater defect in the development of the divoting colony morphology (Fig. 43). Clearly, these data demonstrate that a functioning SDH complex is required for the development of normal biofilms, but the greater defect of the *sdhE* mutant suggests that SdhE may provide an FAD co-factor to another protein required to promote biofilm formation. Experiments testing this hypothesis have not been conducted.

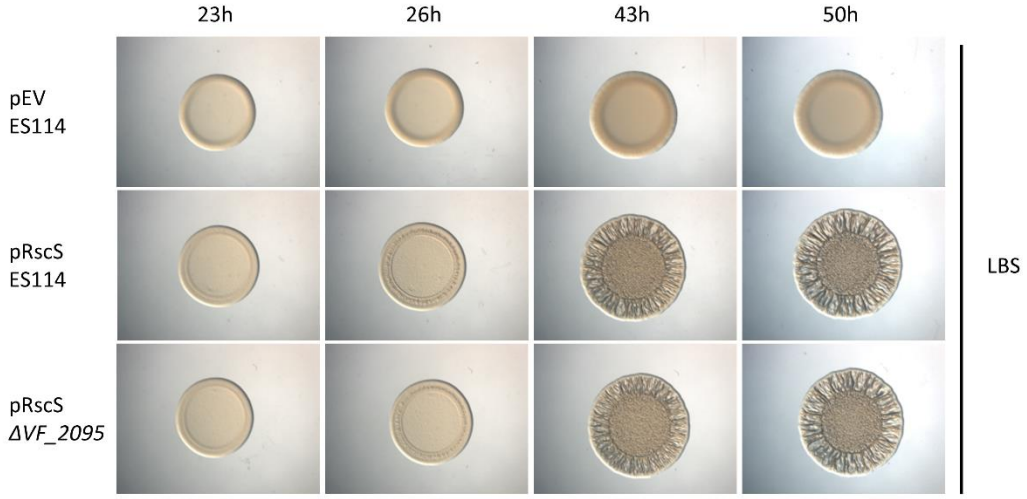

Figure 42 - The biofilm phenotype of a Δ*VF_2095* mutant strain. To rule out a role for *VF_2095*, the gene directly downstream of *sdhE*, in the biofilm defect, an unmarked in-frame deletion mutant of *VF_2095* was assessed for biofilm formation using the wrinkled colony assay. *V. fischeri* strains lacking *VF_2095* appear identical to the parental strain. The empty vector, pEV, is pKV282. The RscS plasmid, pRscS, is pARM7.This experiment has been conducted one time.

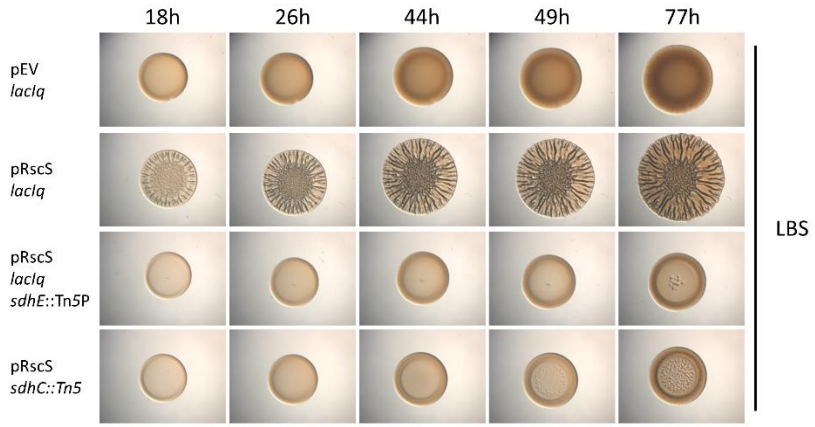

Figure 43 - A comparison of the biofilm phenotypes of the *sdhE*::Tn*5*P and *sdhC*::Tn*5* mutant strains. To gain insight on the potential promiscuity of the SdhE protein, the biofilm phenotype of the *sdhE*::Tn*5*P mutant strain was compared to that of an *sdhC*::Tn*5* mutant strain using a wrinkled colony assay. Both *sdh* mutant strains exhibit a severe defect in wrinkled colony formation with the *sdhC*::Tn*5* mutant strain also exhibiting divoting at the center of its colonies. However, the *sdhC*::Tn*5* mutant strain begins to develop divoting earlier than the *sdhE*::Tn*5*P mutant strain (49 h and 77 h respectively). The empty vector, pEV, is pJMO33. The RscS plasmid, pRscS, is pJMO34.This figure is representative of at least 2 independent experiments.

The role of SDH substrate accumulation in biofilm formation

One reason for the defect in biofilm formation by the *sdhE* (and *sdhC*::Tn*5*) mutant strain could be the accumulation of the SDH substrate, succinate. If the *sdh* phenotype is mediated by the accumulation of succinate, the addition of succinate to the parent strain should delay or inhibit wrinkled colony formation. To test this possibility, I inoculated the parent strain on medium containing 0.2% succinic acid and assessed wrinkled colony formation. No significant changes were observed in wrinkling by the parent strain at the time points captured. However, there appeared to be a slight increase in the divoting of the *sdhE* mutant strain when grown in the presence of succinate; divoting occurred at 49 h in presence of succinate instead of at 77 h in its absence (Fig. 44). The rationale for this experiment is predicated on the assumption that the TCA cycle is cycling "clockwise" and SdhE is primarily functioning to activate SDH. However, the TCA cycle could also be cycling counterclockwise, with SdhE activating the FRD complex. In such a situation, succinate, the product of FRD, would be depleted and these data could be interpreted to mean that the addition of succinate suppresses the defect. To further test this possibility, I repeated the experiment with the *sdhC*::Tn*5* mutant strain, which should be deficient only for SDH activity. If the *sdhC*::Tn*5* mutant strain is "blind" to succinate, then it is likely that the primarily role of SdhE is to activate FRD. However, when grown with succinate, the *sdhC*::Tn*5* mutant strain also exhibited an earlier appearance of divoting, with this architecture appearing at 44 h rather than 49 h (Fig. 44). These data suggest that the defect of the *sdhE* mutant is not caused by an accumulation of the SDH substrate succinate and could indicate that the presence of succinate promotes the formation of biofilms in *V. fischeri*.

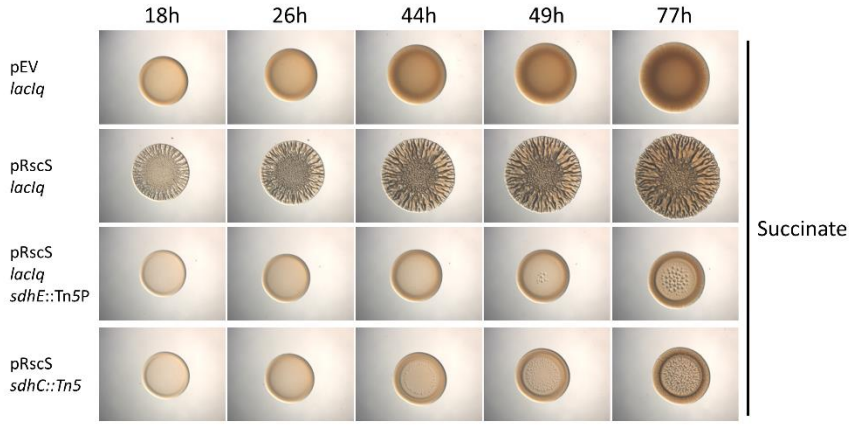

Figure 44 - A comparison of the biofilm phenotypes of the *sdhE*::Tn*5*P and *sdhC*::Tn*5* mutant strains in the presence of succinate. To gain insight on the potential promiscuity of the SdhE protein, the biofilm phenotype of the *sdhE*::Tn*5*P mutant strain was compared to that of an *sdhC*::Tn*5* mutant strain using a wrinkled colony assay. Both *sdh* mutant strains exhibit a severe defect in wrinkled colony formation with the *sdhC*::Tn*5* mutant strain also exhibiting divoting at the center of its colonies. However, the *sdhC*::Tn*5* mutant strain begins to develop divoting earlier than the *sdhE*::Tn*5*P mutant strain (49 h and 77 h respectively). The empty vector, pEV, is pJMO33. The RscS plasmid, pRscS, is pJMO34.This figure is representative of at least 2 independent experiments.

The role of SDH product loss in biofilm formation

An alternative reason for the defect in biofilm formation by the *sdhE* mutant strain could be a loss of the SDH product, fumarate. If the *sdhE* mutant phenotype is mediated by the loss of fumarate, the addition of fumarate to the mutant strain would partially or fully restore wrinkled colony formation. To test this possibility, I examined wrinkled colony formation by the *sdhE* mutant and its parent in the presence and absence of 0.2% fumaric acid. Unfortunately, the addition of fumarate to the medium inhibited growth of *V. fischeri* (data not shown). It thus remains possible that the loss of the fumarate product could contribute to the biofilm defect observed for the *sdhE* mutant strain or that the addition of fumatate at that concentration is toxic to the cells, similar to the effect of malate.

The effect of a variety of carbon sources on *sdhE* mutant strain wrinkling

I next assessed the impact of a variety of other nutrients (Materials and Methods) on the phenotype of the *sdhE* mutant. Succinate, glutamic acid, and ammonia had no noticeable effect on the biofilm phenotypes of the sdhE mutant strain. Similar to what I have observed with other mutant strains, the addition of glucose, G-6-P, and OAA abrogated the formation of secondary structures, i.e., divots (Fig. 45A). Interestingly, there was a reproducible difference when comparing the agar adhesion phenotypes of the *sdhC* and *sdhE* mutant strains: colonies of the *sdhE* mutant strain could be dislodged as a single unit when grown in OAA while colonies of the *sdhC* mutant could be similarly dislodged when grown in glucose and G6P (Fig. 45B). There were also differences in the response of the *sdhE* and *sdhC* mutant strains to serine: the addition of 0.2% serine promoted wrinkling, especially along the outside edge of the spots, of the *sdhC* mutant

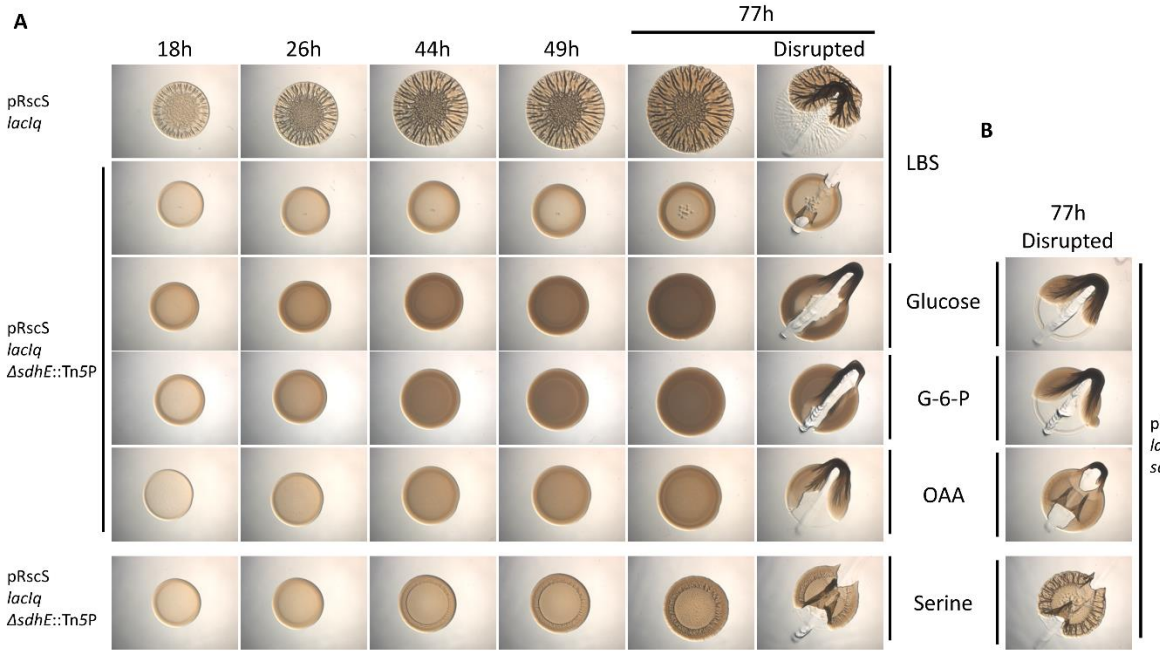

Figure 45 - The biofilm phenotypes of the *sdh* mutant strains in the presence of GNG carbons and serine. To assess whether the addition of other nutrient sources would alter the phenotypes of the *sdh* mutant strains the *sdhE*::Tn*5*P and *sdhC*::Tn*5* mutant strains were grown on LBS supplemented with a variety of nutrient sources and assessed for biofilm formation using a wrinkled colony assay. The addition of GNG carbon sources generally inhibited both the divoting and adherence phenotypes of the *sdhE* and *sdhC* mutant strains, however, a consistently different phenotype of weak adherence occurred: when the *sdhE*::Tn*5*P mutant was grown in glucose and G6P or the *sdhC*::Tn*5* mutant was grown in OAA, a greater portion of the spot adhered to the plate. Growth of the two mutants in serine promoted wrinkling of the colony edges. The RscS plasmid, pRscS, is pJMO34. This figure is representative of at least 2 representative images.

but not the *sdhE* mutant (Fig. 45). The reasons for these different responses and the mechanisms that drive them are unclear, but these phenotypes lend support to the hypothesis that the SDH complex plays a role in biofilm formation and suggests that SdhE may play a role in biofilm formation beyond activation SDH.

The role of *sdhE* in growth

Disruption of SDH, a complex that functions in both the TCA cycle and ETS, is likely to have effects on the growth rate of mutant strains. Indeed, when examining liquid sub-cultures, I noted that the turbidity of the Δ*sdhE* strain was consistently lower than that of its parent. To quantify this possible growth defect, I inoculated Δ*sdhE* mutant and its parent in LBS and monitored growth as described in Methods and Materials. Growth data showed that the two strains remained at relatively similar optical densities at 600 nm (OD_{600}) until they reached an OD_{600} of about 1.5. Then, the growth rate of the parent strain continued in exponential growth while growth of the Δ*sdhE* strain seemed to plateau early at an OD_{600} of around 1.75 (Fig. 46A). However, after prolonged (overnight) growth, the Δ*sdhE* strain reached almost the same OD_{600} as its parent (Fig. 46B). I hypothesize that the Δ*sdhE* strain is inefficient in generating ATP through the ETS and the TCA cycle, but remains able to use non-aerobic means for growth.

Squid colonization by the *sdhE* mutant strain

A majority of *V. fischeri* biofilm mutants are defective in initiating colonization of the squid host. One exception, the *bmpABC* mutant, failed to form wrinkled colonies, but still produced Syp PS and was competent to colonize the squid (Ray, 2015). While the Δ*sdhE* strain has severe defects in wild-type biofilm formation, the cells appear, based on the agar adherence and divoting patterns, able to produce Syp PS. However, it is

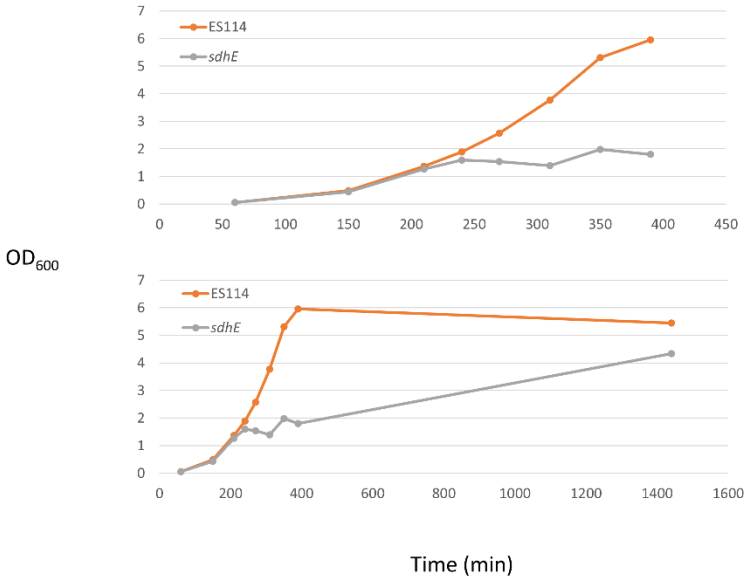

Figure 46 - Growth curve of the *sdhE* mutant strain. The growth rate of the *sdhE* mutant strain was assessed by assessing the OD throughout one day, and then once the following morning after growth overnight. This experiment has been conducted one time.

unknown whether the strain produces enough PS to colonize the squid, and/or whether it is defective in additional unknown processes required to initiate colonization. To assess whether the biofilm defect of the *sdhE* mutant strain correlated with defects in the ability of the strain to colonize its host, I exposed freshly hatched squid to wild-type and Δ*sdhE* strains and evaluated colonization as described in Materials & Methods. My data showed that there was 10-fold decrease in the number of Δ*sdhE* cells present in the squid compared to the parent (Fig. 47). This moderate 10-fold decrease may be meaningful, as a 10-fold colonization defect would likely be much more exaggerated in a competitive environment. Alternatively, the defect could also be due to the known growth defect of the *sdhE* mutant. Additional experimentation will need to be conducted to gain more insight.

The role of *sdhE* in bioluminescence

During the colonization experiments, I noted that when I evaluated luminescence, an indirect measure of colonization, squid exposed to the Δ*sdhE* strain emitted no detectable light, a result that suggested that they were uncolonized. However, as described above, these squid were clearly colonized. This observation thus seemed to indicate that the Δ*sdhE* strain was defective for bioluminescence. Indeed, it has been a reported that *E. coli sdhE* mutants have a defect in the production of quorum sensing molecules, though luminescence was, naturally, never tested (McNeil, Clulow et al., 2012). To assess a possible bioluminescence defect more directly, I measured luminescence of the Δ*sdhE* mutant and its parent in culture. The level of luminescence exhibited by the parent strain indicated that luminescence was activated by an OD_{600} of about 0.9. While the *sdhE* mutant strain reached that OD_{600}, it never reached that level of

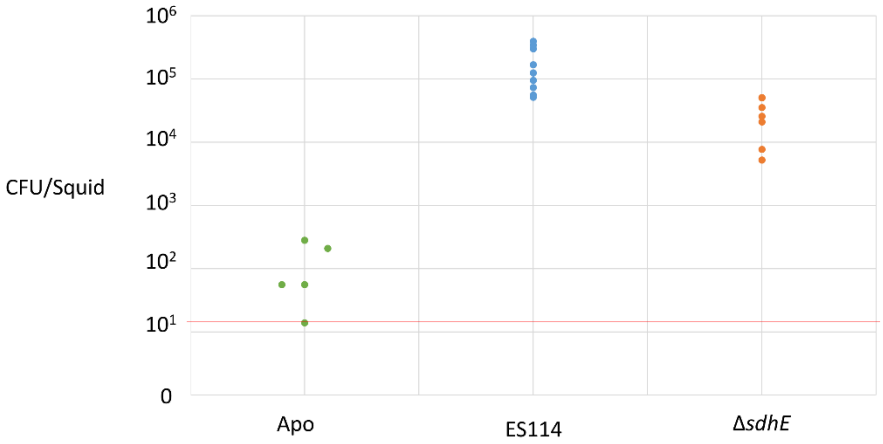

Figure 47 - Colonization phenotype of the Δ*sdhE* mutant strain. Juvenile squid were exposed to either wild-type or Δ*sdhE V. fischeri* overnight or placed in sterile seawater. After 18 h animals were sacrificed, homogenated. Squid homogenates were inoculated onto SWT medium and incubated at 28°C. *V. fischeri* colonies were counted the following day and CFU/squid was calculated. The limit of detection (14 CFU/squid) is indicated by a red line. This experiment has been conducted one time.

luminescence (Fig. 48). Additionally, while the *sdhC* mutant strain was able to grow to an OD of 1.2, its light output was only 15% of its WT counterpart at the same OD. These preliminary data suggest that the luminescence defect of the *sdhE* mutant strain is likely caused by a loss of function of the SDH complex, and that an intact SDH is required for bioluminescence. These results may also indicate that while the Δ*sdhE* is able to colonize juvenile animals, it will exhibit a persistence defect commensurate with other luminescence mutants.

Summary

In my screen for mutant with defects in wrinkled colony formation, I identified a mutant with a Tn*5*P insertion within the *sdhE* gene. Investigations into the role of *sdhE* in wrinkled colony formation confirmed a role for SDH and suggested a role for another target of SdhE activation. Additional experiments demonstrated that an intact SDH is required for wild-type growth, bioluminescence, and probably colonization as the *sdhE* mutant strain exhibits a defect in both growth and luminescence, as well as a 10-fold defect in squid colonization. Further work will be needed to determine whether the defect in colonization is due to its growth phenotype or to a genuine defect in colonization initiation.

The role of Na^+-NQR and electron transport in wrinkled colony formation by *V. fischeri*

Introduction

Two of the smooth mutants I collected contained insertions within the *nqrA* gene and an undetermined *nqr* gene (*nqr*). These genes encode proteins that make up the Na^+-translocating NADH:quinone Reductase (Na^+-NQR) complex. Na^+-NQR is predicted to

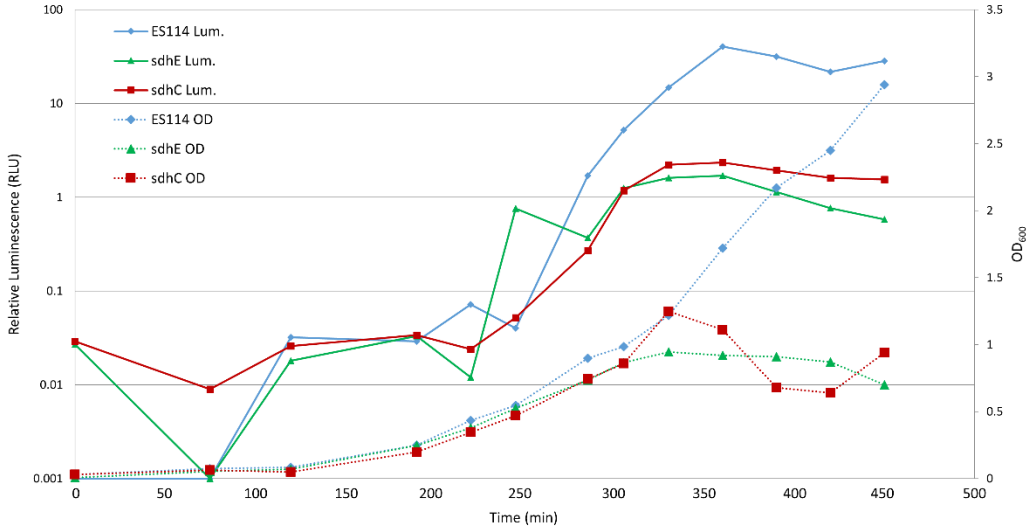

Figure 48 - Bioluminescence of the *sdhE* and *sdhC* mutant strains. The Δ*sdhE* mutant strain exhibited an apparent bioluminescence defect during squid colonization experiments. To assess whether there was a defect of bioluminescence in culture, and whether this defect was due to either a defect in SDH or an alternate target of SdhE, the bioluminescence of both the Δ*sdhE* and *sdhC*::Tn*5* mutant strains were assessed. This figure is representative of at least 2 independent experiments.

serve as Complex I of the Electron Transport System (ETS) in *V. fischeri* where it utilizes the energy released in the redox reaction of NADH to QH_2 to pump Na^+ ions out of the cell. In the following section, I describe the phenotype of the *nqr* mutants and test a number of hypotheses that could explain why a loss of function in Na^+-NQR could contribute to a defect in biofilm formation by *V. fischeri*.

The *nqrA*::Tn*5*P and *nqr*::Tn*5*P mutant strains

From my screen of wrinkled colony-defective mutants, I isolated two independent mutants with insertions within the genes of the *nqr* locus, a 6 gene locus positioned on chromosome I that encodes the structural proteins of Na^+-NQR. The Tn*5*P insertion disrupting *nqrA* was positioned between bases 792,504 and 792,505 with the Tn*5*P promoter oriented in the orientation opposite to *nqrA* transcription (Fig. 49A). Identifying the location of the Tn*5*P insertion disrupting the second *nqr* gene was complicated by multiple poor sequencing results. However, sequencing data suggest that the Tn*5*P was inserted within *nqrB* with the Tn*5*P promoter oriented in the opposite direction to *nqrB* transcription (Fig. 49B). Due to this ambiguity, this mutant will be referred to as *nqr*::Tn*5*P. A time course evaluation of wrinkled colony formation revealed that the *nqrA*::Tn*5*P mutant strain was both severely delayed and defective: while the parent formed wrinkled colonies within 18 h, the mutant colony began to show signs of divoting only after 44 h of growth (Fig. 50A). In addition to these phenotypes, the *nqrA*::Tn*5*P mutant strain exhibited a very tight adherence to the agar surface (Fig. 50A). The adherence phenotype exhibited by the *nqr* mutant strains is far greater than the adherence displayed by the previous mutant strains, as even the edges could not be moved from the agar surface. Indeed, this adherence phenotype occurred at very early times (*e.g.*, 10 h)

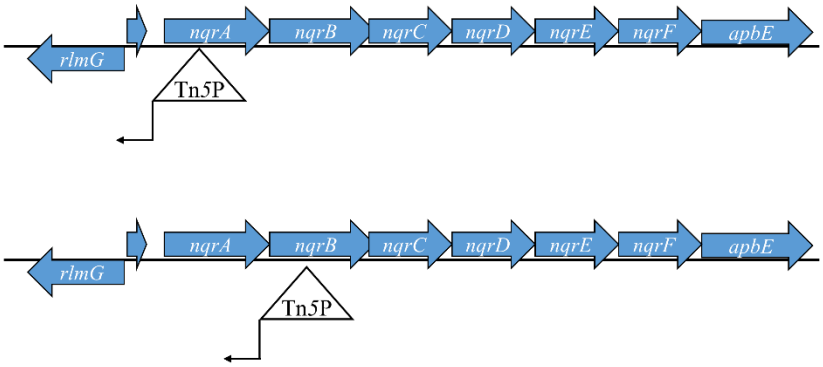

Figure 49 - The location and orientation of the Tn*5*P insertions in the *nqr* mutant strains. The insertion in *nqrA*::Tn*5*P is located in *nqrA* on chromosome I between bases 792,504 and 792,505 with the A1/34 promoter oriented opposite of *nqrA* transcription. The insertion in *nqr*::Tn*5*P is located within *nqr*, possibly *nqrB* as depicted, on chromosome I with the A1/34 promoter oriented opposite of *nqr* transcription.

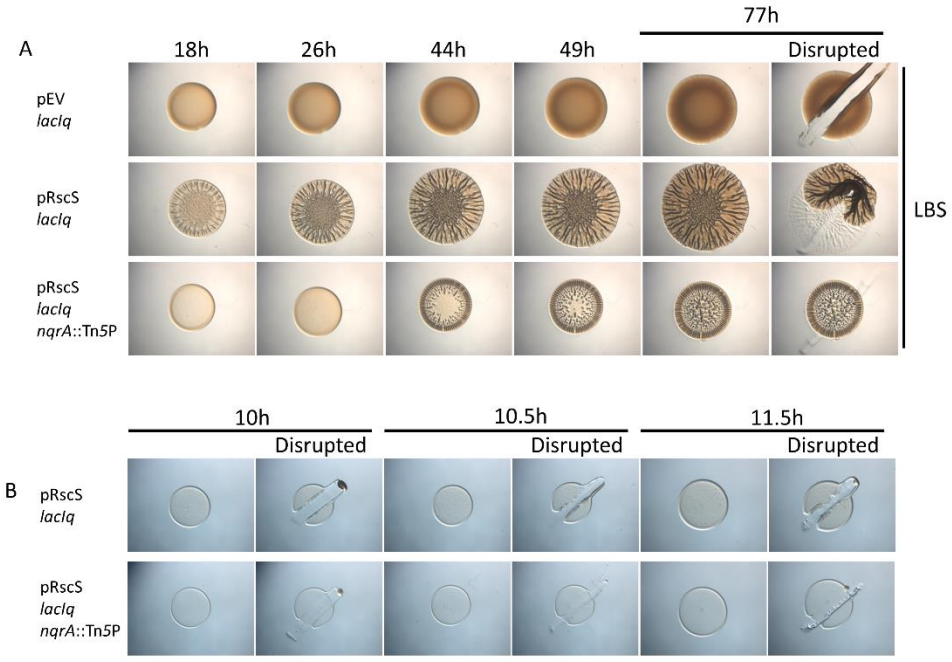

Figure 50 - The biofilm phenotype of the *nqrA*::Tn*5*P mutant strain. The ability of the *nqrA*::Tn*5*P mutant strain to wrinkle was assessed using the wrinkled colony and toothpick assays. **A)** A parental strain carrying an empty vector (pJMO33) does not exhibit wrinkling or any colony architecture even after 77 h when grown on LBS. Parental strains carrying an *rscS* overexpression vector (pJMO34) have begun to wrinkle by 18 h and maintain a wrinkled morphology. The *nqrA*::Tn*5*P mutant strain carrying pJMO34 first develops regular wrinkling around its edge (not captured in this timecourse, see Fig. 51 26h) then develops a severe divoting colony morphology. The *nqrA*::Tn*5*P tightly adheres to the agar when disrupted at 77 h: not even the edge is disrupted by the toothpick. **B)** To assess the onset of agar adherence the *nqrA* mutant was assessed at earlier timepoints. At 10.5 h the *nqrA* mutant has adhered to the agar surface. At this same time, the parental strain has begun to exhibit some cohesion. The empty vector, pEV, is pJMO33. The RscS plasmid, pRscS, is pJMO34. This figure is representative of at least 2 independent experiments.

(Fig. 50B). Therefore, I will refer to this extreme phenotype as the *nqr* attachment phenotype. In the following sections, I will further describe the phenotype of the *nqrA*::Tn*5*P and *nqr*::Tn*5*P mutant strains and investigate specific hypotheses as to how disruption of these genes cause a defect in biofilm formation.

The role of *nqr* in biofilm formation and *nqr* attachment

Though the phenotypes of the *nqrA*::Tn*5*P and *nqr*::Tn*5*P mutant strains are similar (Fig. 51), it was still unclear whether the phenotype is driven by the disruption of the *nqr* genes, or by the Tn*5*P promoter or polar effects on downstream genes. If there is a role of either of those mechanisms in the failure of the mutants to form a wild-type biofilm or the exhibition of the *nqr* attachment phenotype, then these phenotypes should be lost in a strain containing an unmarked in-frame deletion of *nqrA*. To test this, I generated an in-frame, unmarked deletion of *nqrA* and assessed biofilm formation of the resulting mutant. Whereas the colony formed by the parent began wrinkling at 18 h and was easily disrupted at 77 h, the Δ*nqrA* mutant phenocopied the *nqrA*::Tn*5*P mutant: the colonies exhibited the delayed divoting and attachment phenotypes (Fig. 52) and looked exactly like the *nqrA*::Tn*5*P mutant strain. I attempted to complement the *nqrA* deletion, however, I was unable to clone the *nqrA* gene. In spite of my failure to complement the defect, these results suggest that the mutant phenotypes are due to the disruption of *nqrA* (and *nqr*) and not to the Tn*5*P promoter or polar effects.

The role of Syp PS production in the *nqr* mutant phenotype

Disruption of the *nqr* locus should have an effect on the electron transport system and sodium transport and, thus, should alter the membrane potential of the cell. Because of this possibility, the question arose as to whether the *nqr* attachment phenotype was a

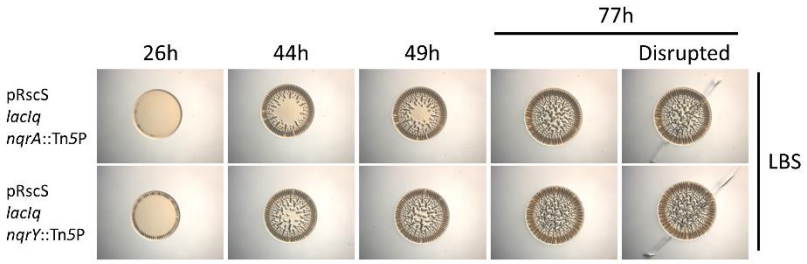

Figure 51 - A comparison of the *nqrA*::Tn*5*P and *nqr*::Tn*5*P biofilm phenotypes. The similarity of the *nqrA* and *nqr* mutant strains was assessed using the wrinkled colony and toothpick assays. Both mutants exhibit similar phenotypes with the development of regular wrinkling at the edges of the colony and the formation of divots at the center of the colony. The development of these phenotypes appears to happen slightly faster in the *nqr* mutant strain. Both mutants adhere to the agar surface when disrupted with a toothpick. The RscS plasmid, pRscS, is pJMO34. This figure is representative of at least 2 independent experiments.

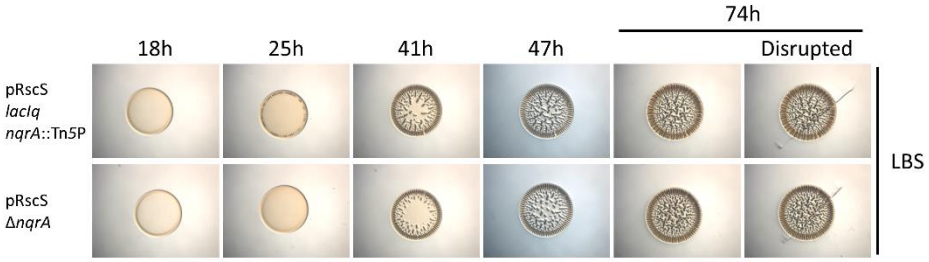

Figure 52 - A comparison of the *nqrA*::Tn*5*P and Δ*nqrA* biofilm phenotypes. To rule out a role for promoter and polar effects, the *nqrA* gene was deleted from the chromosome and assessed for the ability to form a biofilm using the wrinkled colony and toothpick assays. Both the *nqrA*::Tn*5*P and Δ*nqrA* mutants exhibit similar phenotypes with the development of regular wrinkling at the edges of the colony and the formation of divots at the center of the colony. The development of these phenotypes appears to be slightly delayed in the Δ*nqrA* mutant strain but is indistinguishable by 47 h. Both mutants adhere to the agar surface when disrupted with a toothpick. The RscS plasmid, pRscS, is pJMO34. This figure is representative of at least 2 independent experiments.

biofilm phenotype at all, *i.e.*, would the cells exhibit some or all of the *nqr* associated phenotypes in the absence of *rscS* overexpression and biofilm induction? If any of the associated phenotypes were independent of the induction of biofilm formation, then the absence of the *rscS* plasmid would not result in a loss of the phenotype. To address this question, I evaluated the biofilm and attachment phenotypes of the Δ*nqrA* mutant strain carrying an empty vector. I found that this strain exhibited no phenotypes (Fig. 53), save a growth defect which is likely the result of a dysfunctional ETS. These results suggest that some *rscS*-dependent factor is required for the *nqr* associated phenotypes and confirms that the phenotypes are biofilm associated.

RscS controls both Syp PS production and the production of the Bmp matrix proteins (Yip, Geszvain et al., 2006, Ray, Eddy et al., 2013). Thus, I next asked if disruption of either the *syp* locus or of the three *bmp* genes abrogated the *nqr*-associated phenotypes. To do so, I generated *rscS*-overexpressing strains that were defective for both *nqr* and either *syp* (Δ*sypC*, Δ*sypK*, or Δ*sypQ*) or *bmp* (Δ*bmpA* Δ*bmpB* Δ*bmpC*) and evaluated development of the *nqr*-associated phenotypes. While the single *nqrA*::Tn*5*P mutant strain exhibited the *nqr*-associated phenotypes, each of the *nqrA*::Tn*5*P Δ*syp* double mutants failed to exhibit any of the phenotypes save poor growth on agar (Fig. 54). The *nqrA*::Tn*5*P Δ*bmpABC* quadruple mutant failed to form the divoting phenotype but maintained the agar attachment phenotype (Fig. 54). These results suggest that the Syp PS is required for both *nqr*-associated colony phenotypes and the Bmp proteins are required for the divoting phenotype (Ray, 2015). However, it remains unclear, at this time, what specific role the Syp PS has in the *nqr*-associated phenotypes.

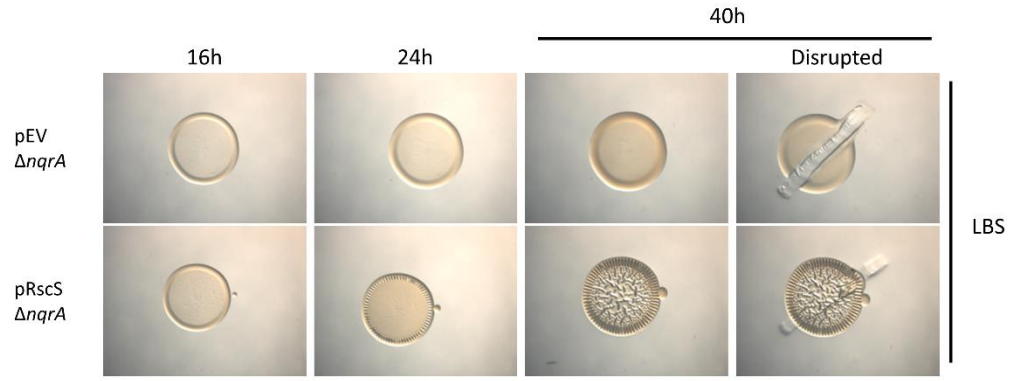

Figure 53 - The role of *rscS* overexpression in the development of the *nqr* adherence phenotype. To assess the role of *rscS* overexpression in the development of the agar attachment phenotype, adherence was assessed in a Δ*nqrA* mutant strain carrying either an empty vector (pJMO33) or the *rscS* overexpression plasmid (pJMO34) using the toothpick assay. When disrupted at 40 h, the strain carrying the empty vector does not exhibit the adherence phenotype of the *rscS* expressing strain. The empty vector, pEV, is pJMO33. The RscS plasmid, pRscS, is pJMO34. This figure is representative of at least 2 independent experiments.

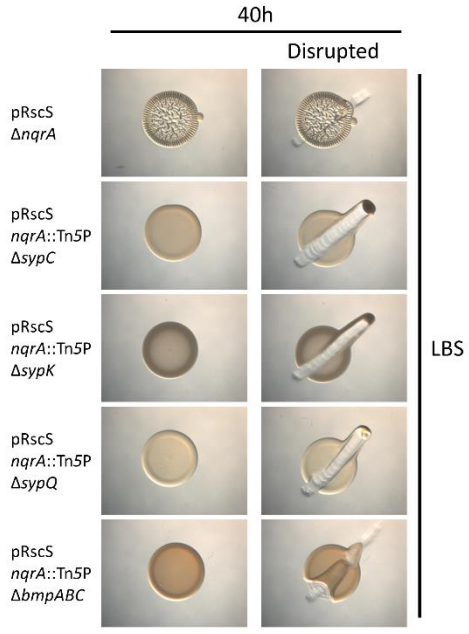

Figure 54 - The role of the *rscS* regulon in the adherence phenotype of the *nqrA* mutant strain. To assess the role of the known members of the RscS regulon in the development of the agar attachment phenotype of the *nqrA* mutant strain, adherence was assessed in *nqrA*::Tn*5*P double mutant strains also carrying deletion alleles in a number of *syp* genes (*sypC*, *sypK*, or *sypQ*) or a quadruple *nqrA*::Tn*5*P Δ*bmpABC* mutant using the toothpick assay. When the mutant strains were disrupted at 40 h mutant strains lacking the *syp* genes did not adhere to the agar surface, while the strain deleted for the *bmpABC* did adhere. The RscS plasmid, pRscS, is pJMO34. This experiment has been completed one time.

The role of Na^+-NQR substrate accumulation and product deficiency in biofilm formation

Aside from the export of Na^+ ions, Na^+-NQR consumes NADH and generates QH_2. Though these molecules are not easily supplemented in LBS medium, I hypothesized that the addition of certain carbon sources would modulate concentrations of NADH or QH_2 in the cell and could therefore be used to test the impact of these molecules on biofilm formation. For example, pyruvate generates a molecule of NADH as it is metabolized to AcCoA. Therefore, if a delay in wrinkling by the *nqrA*::Tn*5*P mutant strain is caused, in part, by an excess of NADH due to its loss of Na^+-NQR activity, the addition of pyruvate could exacerbate that defect. To test this I assessed the ability of the *nqrA*::Tn*5*P strain to form a biofilm on medium supplemented with pyruvate. While the addition of pyruvate had no effect on the development of biofilm phenotypes by the parental strain, pyruvate did have a detrimental effect on the divoting of the *nqrA* mutant: while the *nqrA*::Tn*5*P mutant strain began to exhibit wrinkling at 25 h and had developed significant divoting at 41when grown in LBS, when grown in the presence of pyruvate, the *nqrA* mutant strains did not show any divoting and only slight wrinkling through 74 h of incubation (Fig. 55A). The addition of pyruvate only had a slight negative effect on the adherence phenotype of the *nqrA* mutant strain. These data suggest that excess NADH may contribute to the delay in the formation of morphology by the *nqr* mutant strains.

As described above, loss of Na^+-NQR function should lead to a decrease in QH_2 available in the cell. I hypothesized that the generation of additional QH_2 through the metabolism of succinate by the SDH complex would promote wrinkling in the

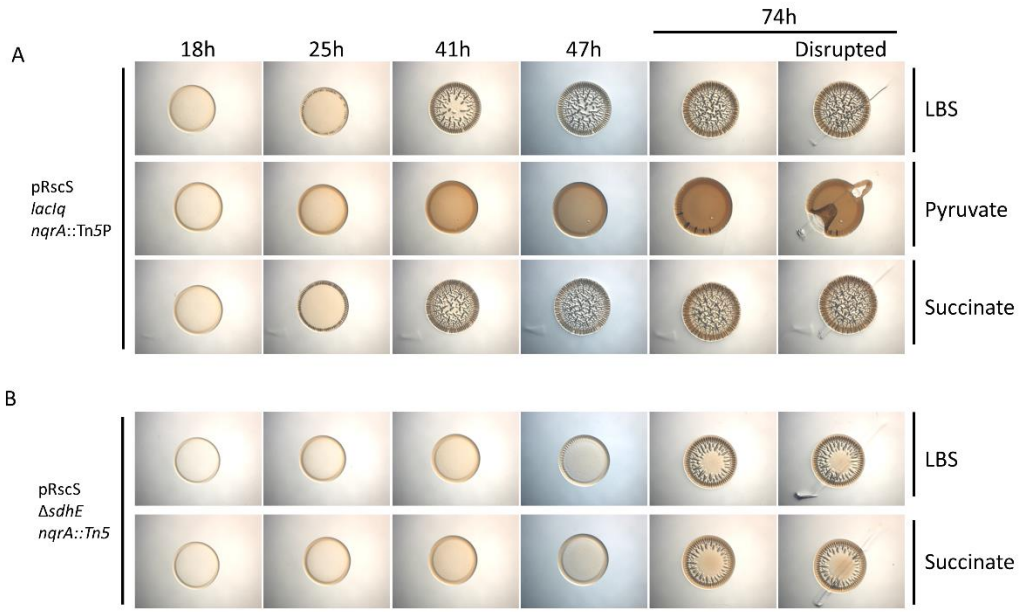

Figure 55 - The biofilm phenotype of the *nqrA* single and *nqrA sdhE* double mutant strains in the presence of carbon sources hypothesized to alter NA^+-NQR substrates and products. A) To assess the role of increased levels of NADH and QH_2 on the phenotype of the *nqrA* mutant strain, the *nqrA*::Tn*5*P mutant strain was grown in medium supplemented with 0.2% of either pyruvate or succinate and the biofilm phenotype was assessed using the wrinkled colony and toothpick assays. The addition of pyruvate to the growth medium inhibits the formation of colony morphology by the *nqrA* mutant strain. The addition of succinate to the growth medium of the *nqrA* mutant strain appears to result in a slight decrease in the time taken to form wrinkles along the edge of the colony at 25 h and an increase in the concentration of divots at 41 h. **B)** To decrease the hypothetical increase of QH_2 resulting from the addition of succinate to the *nqrA* mutant strain, the *sdhE* gene was deleted and the double mutant was grown in both the presence and absence of succinate and the biofilm phenotypes were assessed using the wrinkled colony and toothpick assays. The deletion of the *sdhE* gene results in a delay in the development of *nqrA* biofilm phenotypes compared to the *nqrA* single mutant with the double mutant showing edge wrinkling at 47 h. The addition of succinate to the growth medium results no promotion of biofilm formation and potentially a slight delay: not wrinkles have formed on the double mutant by 47 h. The RscS plasmid, pRscS, is pJMO34. This experiment has been completed one time.

nqrA::Tn*5*P mutant strain. Indeed, the addition of succinate resulted in a modest promotion of wrinkling: while the *nqrA*::Tn*5*P mutant strain began to exhibit some wrinkling at 25 h and significant divoting by 41 h when grown in LBS, in the presence of succinate the *nqrA*::Tn*5*P mutant strains developed more wrinkles along the edges by 25 h and a more fully developed divoting phenotype by 41 h (Fig. 55B). These data, along with the phenotype upon the addition of pyruvate, support a hypothesis that states wrinkling is, in part, mediated by levels of NADH and QH_2 and thus, are not necessarily caused by Na^+-NQR specifically, but rather a defect in electron transport generally.

It is unclear if the addition of succinate to the growth medium of an *nqrA*::Tn*5*P mutant strain does, in fact, cause an increase in the levels of QH_2. If it does, then the succinate-induced increase in QH_2 should be lost in an *nqrA sdhE* double mutant strain. Thus, I generated a Δ*sdhE nqrA*::Tn*5*P double mutant, inoculated it in medium supplemented with succinate, and assessed wrinkled colony formation. Consistent with the hypothesis that the addition of succinate increases the levels of QH_2 via SDH activity in the *nqrA*::Tn*5*P mutant strain, the addition of succinate in the double mutant did not promote biofilm formation (Fig. 55B). At 47 h, the double mutant strain began to show edge wrinkling when grown in LBS but showed no development at that time when inoculated in LBS + succinate. These data suggest that a defect in QH_2 generation in the *nqrA*::Tn*5*P mutant strain could be a cause for the biofilm defect. Further experimentation will need to be conducted to validate its significance.

<u>The role of assorted carbon sources in the *nqr*-associated phenotype</u>

Although no strong rationale existed, I included the *nqr* mutant in the nutrient addition experiments described in other sections above and report here that some

additions impacted the *nqr* phenotypes. The addition to the medium of G6P, glucose, OAA, pyruvate, and citrate all caused an inhibition or delay in the development of the central divoting and regular edge wrinkling phenotypes (Fig. 56A). The phenotypes resulting from the GNG carbon sources is not surprising as the addition of these carbon sources to the parental strain and all mutants tested has resulted in a general delay or inhibition of wrinkling and biofilm formation. Of note, however, is that the addition of these carbon sources did not completely inhibit the ability of the *nqrA* mutant strain to adhere to the agar surface. While it is currently unknown what mediates the adherence of some *V. fischeri* mutant strains, and especially *nqr* mutant strains, to the agar surface, the addition of the GNG substrates, intermediates, and products seems to suppress the attachment phenotype.

In addition to the general inhibition of adherence and divoting of the GNG substrates and products, the addition of citrate to the *nqrA* mutant strain resulted in a complete inhibition of divoting: while the *nqr* mutant strain had begun to exhibit wrinkling around its edge and divoting at its center by 44 h, the mutant strain never developed colony morphology by 77 h when grown in the presence of citrate (Fig. 56B). The addition of citrate to the parental strain also resulted in a slight delay in biofilm formation as well as a surprising increase in adherence to the plate. In my studies, this is the only condition I observed increased adherence by the parental strain and the first evidence of an increase in adherence by a wild-type strain overexpressing *rscS*. These results suggest that citrate may both inhibit the development of colony morphology while promoting the adherence phenotype.

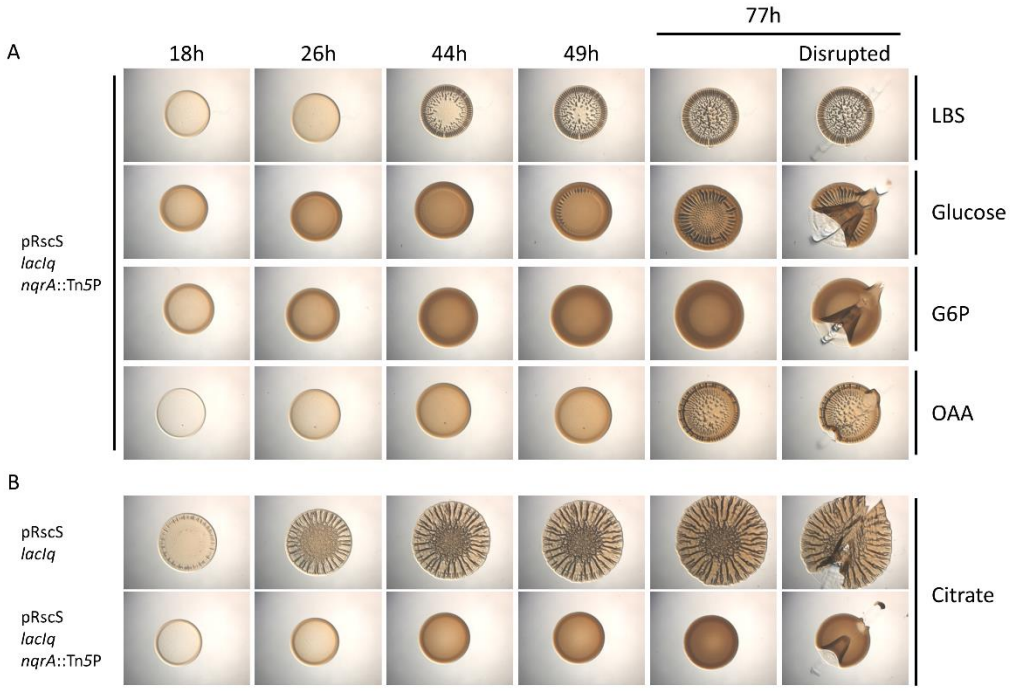

Figure 56 - The effect of GNG carbon and citrate addition to the biofilm phenotype of the *nqrA* mutant strain. The response of the *nqrA* mutant to a number of additional nutrients was assessed using the wrinkled colony and toothpick assays. **A)** The addition of GNG carbon sources, glucose, G6P, and OAA resulted in a delay in the development of morphology typical of those carbon sources. The addition of these carbons did not fully inhibit the adherence phenotype, with the addition of OAA having very little effect on the phenotype. **B)** The addition of citrate promoted increased adherence of the parental strain while completely inhibiting the formation of colony morphology by the *nqrA* mutant strain. The RscS plasmid, pRscS, is pJMO34. This figure is representative of at least 2 independent experiments.

The role of Na^+-NQR in growth

Disruption of Na^+-NQR, a key component of *V. fischeri* ATP generation, is likely to have effects on the growth rate of *V. fischeri*. Indeed, when subjectively examining liquid cultures and colonies, the turbidity and colony size of the Δ*nqrA* strain appeared to lag behind that of the parent strain. To quantitate this possible growth defect, I inoculated the Δ*nqrA* mutant and its parent in LBS and monitored growth as described in Methods and Materials. The two strains remained at the same OD_{600} during the first 60 min of growth, then the growth of the parent became exponential while growth of the Δ*nqrA* strain seemed to plateau early, around an OD_{600} of 1 (Fig. 57A). After prolonged (overnight) growth, the OD_{600} of Δ*nqrA* strain increased over two orders of magnitude, although it didn't reach that of the parent strain (Fig. 57B). These data are similar to that of the Δ*sdhE* mutant strain (Fig. 46). I hypothesize that the Δ*nqrA* mutant cells are inefficient in generating ATP through the ETS, but are able utilize non-aerobic means for growth. Cultures growing in this manner would likely exhibit a slow but steady increase in OD_{600}.

The role of *nqr* in pellicle formation

Another kind of biofilm that forms at the air/liquid interface of a static culture is called a pellicle. Wild-type *V. fischeri* strains induced to form a biofilm can form pellicles in a number of liquid media (Yip, Geszvain et al.). Based on the increased adherence phenotype of the Δ*nqrA* strain grown on agar, I next asked whether a similarly strong pellicle could form when the strain was grown in liquid. To test this possibility, I inoculated the Δ*nqrA* strain and its parent in various media in microtiter plates, and monitored pellicle formation. Specifically, I investigated pellicle formation in Hepes- and

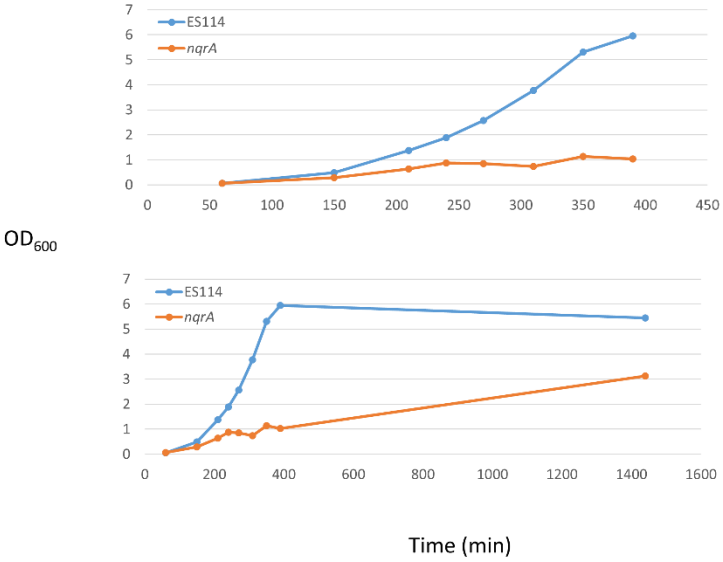

Figure 57 - Growth curve of the Δ*nqrA* mutant strain. The growth rate of the *nqrA* mutant strain was assessed by assessing the OD throughout one day, and then once the following morning after growth overnight. This experiment has been conducted one time.

Tris-buffered minimal media, and LBS and SWT complex media as well as with inoculum concentrations at an OD_{600} between 0.1 and 0.4. Unfortunately, I was not able to consistently obtain pellicles for the positive control strain, making it difficult to draw a conclusion regarding the relative strength of the *nqr* mutant pellicle. This inconsistency may be due to the use of the pJMO34 plasmid, though experiments testing this have not been conducted. However, because the *nqrA* mutant was able to form pellicles in some instances, I conclude that the Δ*nqrA* strain is not unable to form a pellicle.

The role of *nqr* in glass attachment

Another method of evaluating biofilm formation is to assess the ability of a bacterial strain to adhere to glass. While the ability of *V. fischeri* to adhere to glass is not strongly correlated with its ability to colonize squid (Shibata, Yip et al., 2012), the strong agar adherence phenotype of the Δ*nqrA* strain made it compelling to examine this phenotype. I expected that, if the Δ*nqrA* strain was simply better at adhering to all surfaces, it would exhibit an increased ability to attach to the glass tube, and thus I would observe more crystal violet staining of *nqr* mutant samples. To examine the ability of the *nqr* mutant to adhere to glass, I inoculated it and its parent into HMM-glucose, incubated the test tubes statically for 48 h, then stained them with crystal violet.

My preliminary experiment was hindered somewhat due to the strength of the pellicle that was formed by the Δ*nqrA* strain: whereas the simple addition of crystal violet to the parent cultures broke the pellicles, permitting the stain to reach the liquid below, the addition of the dye to the Δ*nqrA* cultures did not initially penetrate the pellicle. Only after repeated attempts to puncture the pellicle of the Δ*nqrA* mutant with a pipet tip was I successful in delivering the dye to the liquid below (Fig. 58A). After I added the stain, I

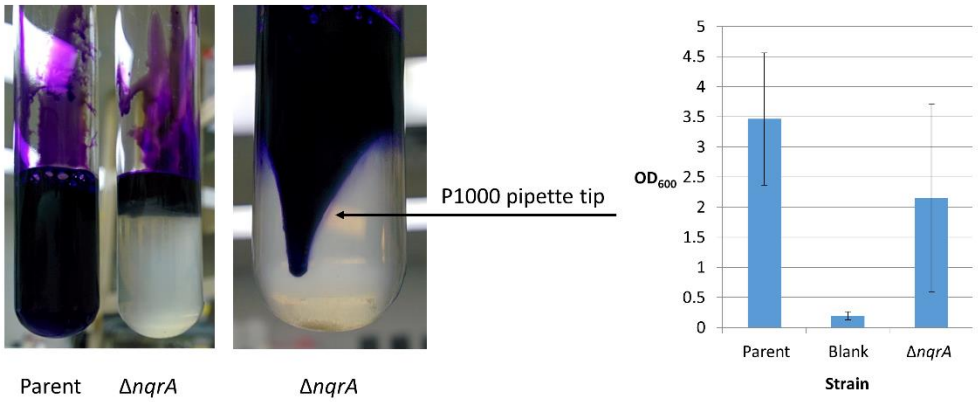

Figure 58 - Glass attachment of the *nqrA* mutant strain. Crystal violet (CV) was added to 48 h old pellicles formed in HMM by either the parent or *nqrA*::Tn*5*P strains. **A)** The addition of CV to the parent culture broke the pellicle allowing the dye to stain the liquid below the pellicle that had formed at the air-liquid interface. Unlike the parent, the addition of CV to the *nqrA* culture did not penetrate the pellicle, which was initially resistant to puncture by a pipette tip. **B)** The amount of CV recovered upon completion of the CV assay suggests that the parent strain had greater glass attachment, however, cohesion of the *nqrA*::Tn*5*P mutant was so strong (see panel A) that portions of the pellicle that were attached to the glass peeled off during the course of the wash steps. 2 technical replicates were used in this experiment. The experiment has been conducted one time.

then rinsed the test tube to remove stain that wasn't surface-associated. During these manipulations, I found that the pellicle material of the parent strain easily separated from the glass and those tubes maintained only the material positioned very close to the glass. However, the strong cell-cell interactions of the Δ*nqrA* strain caused a great deal of intact pellicle material to maintain its attachment to the glass wall such that a majority of the pellicle was not initially washed away.

As the wash steps continued, the Δ*nqrA* strain's pellicle material peeled entirely off of the glass in many places, potentially due to increased drag. This greatly decreased the amount of dyed material attached to the glass and also likely introduced high variability in amount of crystal violet ultimately recovered. Finally, I quantified the stain that remained associated with the test tube, and found that the amount of crystal violet recovered from test tube of the parent strain was greater than that of the Δ*nqrA* strain (Fig. 58B). However, given the properties of the Δ*nqrA* pellicle in this experiment, I suspect that these results don't accurately represent the phenotype of the *nqr* mutant strain. I hypothesize that the inability of the dye to penetrate the pellicle and the pellicle to resist separation from the glass walls was due to the stronger cell-cell and cell-surface associations, respectively. If the dye did not penetrate the biofilm effectively, it is unlikely that all of the glass associated-cells had an opportunity to take up the dye, which would result in a lower reading. While these preliminary results are not a good quantitative measure of the ability of the Δ*nqrA* strain to attach to glass, these data do suggest an increase in both cell-cell and cell-surface associations. Further work is needed to confirm and build upon this hypothesis.

Colonization Experiments

Based on the previous experiments, the Δ*nqrA* strain clearly has a delay in biofilm formation and an altered phenotype when it does form a biofilm. Thus, it seemed likely that the Δ*nqrA* strain would be competent to form a biofilm in the context of squid colonization. What was less obvious, however, was whether the Δ*nqrA* strain would be able to leave the biofilm and colonize the light organ of the squid due to the strong cell-cell and cell-surface associations observed in previous experiments. I hypothesized that the Δ*nqrA* strain would be unable to disperse from the biofilm and enter the light organ and, therefore, the animals would not become colonized. To test this hypothesis, I exposed juvenile squid to *V. fischeri* strains and assessed the resulting colonization. My results showed that the Δ*nqrA* strain could colonize juvenile *E. scolopes*, though at slightly lower levels compared to the parent strain (Fig. 59). However, due to the growth phenotype of the Δ*nqrA* strain, I was unable to determine whether the colonization defect is due to a defect in a particular stage of the colonization process, or a result of the growth defect.

Interestingly, while the inoculum was standardized to OD_{600} in order to expose each animal to similar concentrations of *V. fischeri* cells, a plating of a portion of the inoculum on SWT plates revealed approximately twice as many Δ*nqrA* cells in the inoculum compared to the control. *nqrA* strains when at the same OD_{600} could indicate a difference in cell size or shape; *i.e.*, the Δ*nqrA* cells could be smaller or rounder. Careful microscopic examinations and comparisons of OD_{600} and colony counts will be necessary to verify a difference in the shape and size of Δ*nqrA* cells as well as whether the growth environment, *i.e.*, static/agitated/rich/minimal, affects any noted changes.

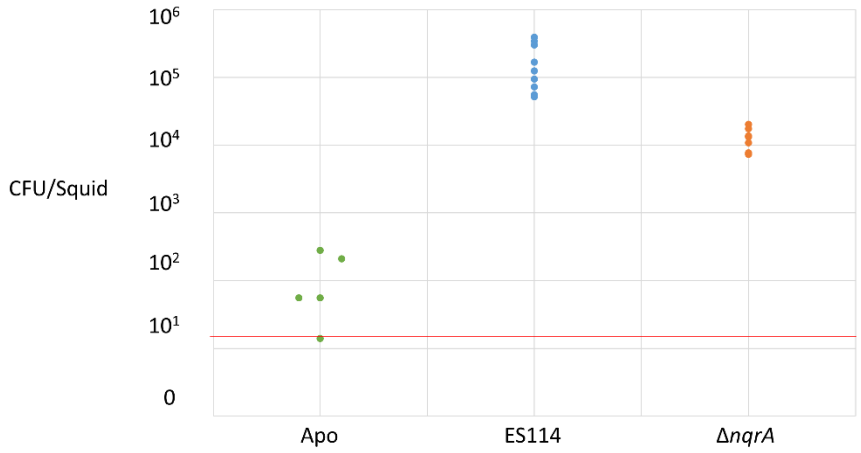

Figure 59 - Colonization phenotype of the *nqrA* mutant strain. Juvenile squid were exposed to either wild-type or Δ*nqrA V. fischeri* overnight or placed in sterile seawater. After 18 h animals were sacrificed, homoginated. Squid homogenates were inoculated onto SWT medium and incubated at 28°C. *V. fischeri* colonies were counted the following day and CFU/squid was calculated. The limit of detection (14 CFU/squid) is indicated by a red line. This experiment has been conducted one time.

The role of Na^+-NQR in bioluminescence

During colonization experiments I noted that while squid were colonized to a level that should have induced bioluminescence of the symbiont, as occurred with the Δ*sdhE* strain, no bioluminescence was detected (data not shown). This observation suggested that the Δ*nqrA* mutant strain was also defective for bioluminescence. To test this hypothesis, I inoculated the Δ*nqrA* mutant and its parent in liquid medium and monitored the strains for growth and luminescence. While the *nqrA* mutant strain exhibited a severe growth defect when grown in SWTO, consistent with what I had observed in LBS (Fig. 57), it retained the ability to activate luminescence and did so at a low cell density (Fig. 60). These preliminary data suggest that the *nqrA* mutant is capable of producing light. However, it is unclear, based on the level of light emitted from the squid, whether this strain would confer a fitness benefit to its host or whether it would even be able to persist in the light organ.

The role of the Msh and Csg pili in the *nqr* mutant phenotype

The *nqr* mutant exhibits a striking ability to adhere to the surface of the agar medium. One hypothesis that could explain this phenotype is that pilus production is upregulated in this mutant and these pili mediate attachment to the agar surface. The *V. fischeri* genome encodes 10 pili loci, most of which have not been studied in this organism (Ruby, Urbanowski et al., 2005). One, the Msh (mannose-sensitive hemagglutin) pilus, may be important for colonization by *V. fischeri* as the addition of mannose to the *V. fischeri* inoculum inhibits colonization (McFall-Ngai, Brennan et al., 1998). Of note, the Msh pilus is involved in electron transport in *Shewanella oneidensis* MR-1 (McLean, Pinchuk et al., 2008). In *E. coli*, the Csg pilus (also encoded

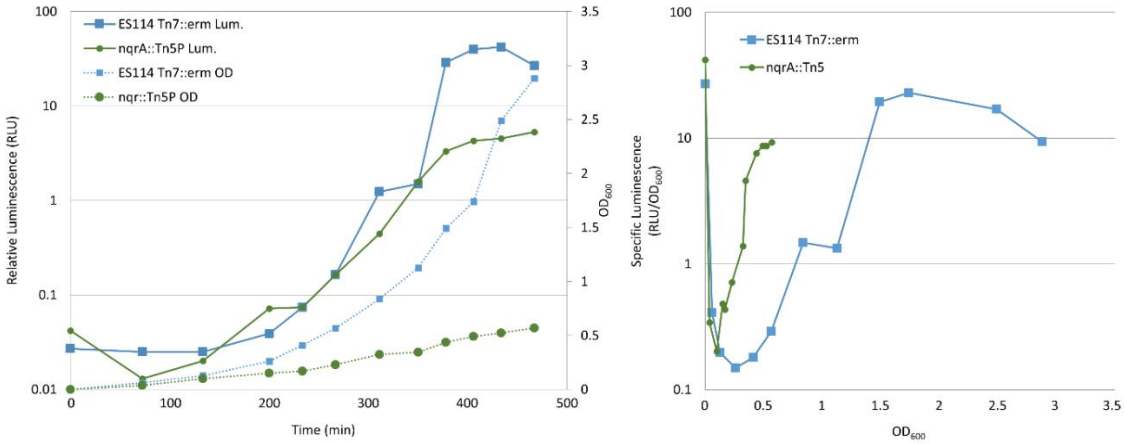

Figure 60 - Bioluminescence of the *nqrA* mutant strain. The Δ*nqrA* mutant strain exhibited an apparent bioluminescence defect during squid colonization experiments. To assess whether there was a defect of bioluminescence in culture the bioluminescence of the *nqrA* mutant strain was assessed. This experiment has been conducted one time.

by *V. fischeri*) is required for biofilm formation (Prigent-Combaret, Prensier et al., 2000, Chapman, Robinson et al., 2002). These two pili thus have potential to be involved in the *nqr* mutant phenotype. If these pili mediate the attachment phenotype of the *nqr* mutant phenotype, then the disruption of these loci in an *nqrA* mutant would abrogate the attachment of the *nqrA* mutant to the agar surface. To test this hypothesis, I generated double mutant strains possessing a Δ*nqrA* allele and either an *mshA*::Tn*5* or *csgA*::Tn*5* allele, inoculated the strains onto plates and assessed their ability to attach to agar. I found that the double mutants attached to the agar surface in a manner similar to the Δ*nqrA* mutant strain (Fig. 61). This result suggests that the agar attachment phenotype of the *nqr* mutant does not require the Msh or Csh pili. There remain a number of other pili that could be tested for a role in the *nqr* associated phenotype in a similar manner.

Summary

Investigations into the role of *nqrA*/*B* and Na^+-NQR revealed a novel attachment phenotype and a role for electron transport in the ability of *V. fischeri* to form a wrinkled colony. Biofilms formed by the Δ*nqrA* strain exhibit a severe delay as well as an altered phenotype including a surprisingly robust attachment phenotype. Growth and luminescence experiments suggested that, while the Δ*nqrA* mutant strain exhibited a growth defect, it remained capable of reaching sufficiently high cell densities to induce bioluminescence (though issues of cell size and shape may complicate those data). Finally, the Δ*nqrA* strain is capable of squid colonization, suggesting that a lack of Na^+-NQR does not significantly impact biofilm formation, dispersal, and colonization in the context of the squid host.

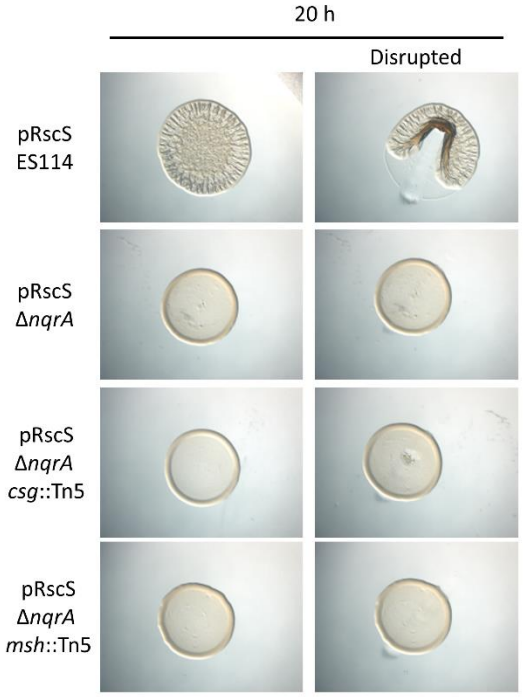

Figure 61 - The role of select pili on the adherence phenotype of the *nqrA* mutant strain. To assess the requirement of the Csg and Msh pili in the adherence phenotype, the wrinkled colony and toothpick assays were conducted on double mutants carrying either an empty vector or an *rscS* overexpressing plasmid and lacking *nqrA* and either the *csgA* or *mshA* gene. At 20 h the wild-type strain exhibits wrinkling and cohesion but not adherence, a phenotype typical of the strain. The *nqrA* mutant strain is smooth but adherent, also typical. Both the *csg* and *msh* double mutant strains mimic the phenotype of the *nqrA* mutant strain suggesting no role for the pili. The RscS plasmid, pRscS, is pJMO34. This experiment has been conducted one time.

The role of *ubiG* in wrinkled colony formation by *V. fischeri*

Introduction

One of the smooth mutants I collected contained an insertion within the ubiquinone (Q) biosynthesis pathway gene *ubiG*. As described in the literature review, the methyltransferase activity of UbiG is the final enzymatic step in the biosynthesis of Q (Fig. 11). The biosynthesis of Q is important for the cell due to the role the molecule plays in the carriage of electrons in the electron transport system (ETS). Thus, it is reasonable to assume that disruption of the Q biosynthetic pathway would also impact the ability of the cell to conduct electron transport and cause the cell to be deficient in associated activities such as ATP generation, maintenance of electrochemical gradients, and O_2 fixation. In the following section, I will describe the phenotype of the *ubiG*::Tn*5*P mutant strain and test a number of hypotheses that could explain why a loss of Q biosynthesis could impact biofilm formation.

The *ubiG*::Tn*5*P mutant strain

From my screen of wrinkled colony defective mutants, I isolated one mutant with an insertion in *ubiG* (VF_1203). The Tn*5*P insertion was positioned on chromosome I between bases 1,339,109 and 1,339,110, and the Tn*5*P was oriented opposite to *ubiG* transcription (Fig. 62). A time course assay of wrinkled colony formation revealed that the *ubiG*::Tn*5*P mutant strain exhibited a severe defect in wrinkled colony formation: whereas colonies of the parent strain began wrinkling within 18 h, the mutant colonies did not begin to show architecture until between 26 and 44 h (Fig. 63). Furthermore, rather than developing wrinkles in the center of the colony, the *ubiG*::Tn*5*P mutant strain developed the divoting pattern exhibited by a number of the other mutant strains (Fig.

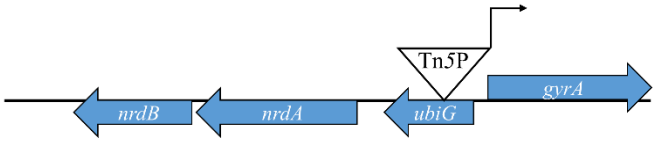

Figure 62 - The location and orientation of the Tn*5*P insertion in the *ubiG* mutant strain. The insertion in *ubiG*::Tn*5*P is located in *ubiG* on chromosome I between bases 1,339,109 and 1,339,110 with the A1/34 promoter oriented opposite of *ubiG* transcription.

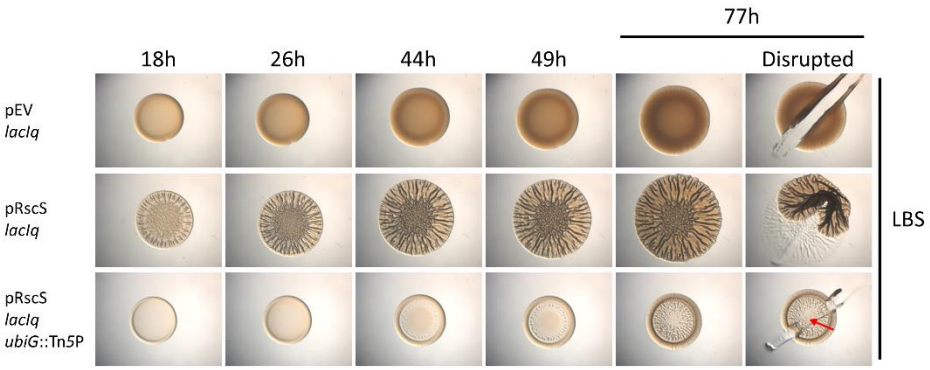

Figure 63 - The biofilm phenotype of the *ubiG*::Tn*5*P mutant strain. The ability of the *ubiG*::Tn*5*P mutant strain to wrinkle was assessed using the wrinkled colony and toothpick assays. A parental strain carrying an empty vector (pJMO33) does not exhibit wrinkling or any colony architecture even after 77 h when grown on LBS. Parental strains carrying an *rscS* overexpression vector (pJMO34) had begun to wrinkle by 18 h and maintained a wrinkled morphology. The *ubiG*::Tn*5*P mutant strain carrying pJMO34 developed a divoting colony morphology around 44 h. When disrupted at 77 h the strain adhered to the agar at its center while the edges (arrow) could be disrupted. The empty vector, pEV, is pJMO33. The RscS plasmid, pRscS, is pJMO34. This figure is representative of at least 3 independent experiments.

63). The *ubiG*::Tn*5*P mutant strain also exhibited an agar adhesion phenotype very similar to that of the *nqr* mutant strains (Fig. 63). This is, perhaps, not surprising because of connected roles of Na^+-NQR and Q. Unlike the *nqr* mutant strains which exhibited regular and adherent wrinkles (Fig. 63), the *ubiG*::Tn*5*P mutant strain exhibited a smooth edge that could be disrupted (Fig. 63, arrow). Based on the location of the Tn*5*P insertion and the gap between *ubiG* and the downstream genes, *nrdA* and *nrdB*, (Fig. 62), it is unlikely that the insertion within *ubiG* is exerting polar effects on the *nrd* operon. Additionally, the phenotype of the *ubiG*::Tn*5*P strain is unchanged in the presence and absence of IPTG (data not shown), ruling out a role for the upstream gene *gyrA* in the phenotype. These data suggest that the insertion within *ubiG* is the main, and likely only, driver of the biofilm phenotype of the *ubiG*::Tn*5*P mutant strain.

The *ubiG*::Tn*5*P mutant strains ETS defect is the primary driver of its biofilm defect

The phenotype of the *ubiG*::Tn*5*P mutant strain is most similar to that of the *nqr* mutant strains. As such, I next asked what responses the *ubiG*::Tn*5*P mutant strain would have when exposed to a number of carbon sources, and then, whether the phenotypic changes would be similar to those of the Δ*nqrA* mutant strain. Many nutrient sources such as ammonia, arginine, glutamine, glutamic acid, pyruvate and succinate induced no changes in the biofilm phenotype of the *ubiG*::Tn*5*P mutant strain. However, the addition of glucose, G6P, OAA, citrate, and serine did cause notable changes in the phenotype of the *ubiG* mutant. Similar to what I observed when exposing other mutant strains to these carbon sources, the addition of the GNG carbon sources, glucose, G6P, and OAA resulted in an abrogation of colony architecture formation (Fig. 64). In addition, these

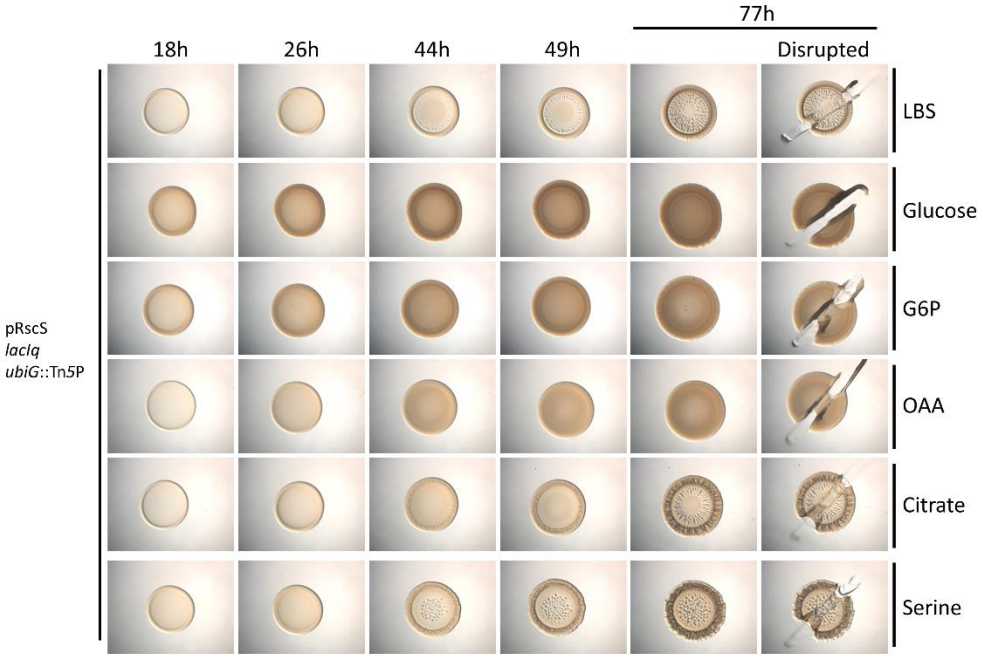

Figure 64 - The effect of various carbon sources on the biofilm phenotype of the *ubiG*::Tn*5*P mutant. The response of the *ubiG*::Th*5*P mutant to a number of different carbon sources was assessed using the wrinkled colony and toothpick assays. The addition of the GNG carbons glucose, G6P, and OAA resulted in an inhibition of morphology development as well as a decrease in adherence (with a complete inhibition of adherence with the addition of glucose). The addition of both citrate and serine to the medium resulted in the development of edge wrinkling by the *ubiG* mutant strain but did not alter the adherence phenotype. The addition of citrate delayed the formation of central divoting while the addition of serine promoted the same. The RscS plasmid, pRscS, is pJMO34. This figure is representative of at least 2 independent experiments.

carbon sources diminished the cell-surface adherence phenotype and, in the case of glucose, caused a complete disruption of adhesion. Previous research has shown that the production of the Syp PS is required for the cohesion phenotype (Ray, Driks et al., 2015). When examining the *nqr* mutant strains, I found that the production of Syp PS is also required for the adherence phenotype (Fig. 54). Therefore, the maintenance of the cohesion phenotype suggests that the decrease or loss of adhesion is not due to a loss of Syp PS production in the *ubiG*::Tn*5*P mutant strain under these conditions.

The addition of citrate and serine to the growth medium also had an effect on the wrinkling phenotype of the *ubiG*::Tn*5*P mutant strain: when grown in LBS, the *ubiG*::Tn*5*P mutant strain exhibited a smooth edge but in the presence of citrate and serine, the *ubiG*::Tn*5*P mutant strain developed a wrinkled edge (Fig. 64). These results were somewhat surprising because they diverge from what was seen when the *nqrA* mutant was grown in these conditions: the *nqrA* mutant was unchanged when grown in serine (data not shown) and the addition of citrate delayed wrinkled colony formation by the parent strain and completely inhibited the formation of architecture by the *nqrA* mutant (Fig. 56). These results demonstrate that the role of *ubiG* and Q biosynthesis in biofilm formation and further suggest a role for the ETS in biofilm formation. The differences between the responses of *ubiG* and *nqrA* mutants also suggests that Q has a role in an additional pathway or protein outside its role in Na^+-NQR activity.

Because the *ubiG* mutant strain is, presumably, unable to make Q for the carriage of electrons, a process vital for the function of Na^+-NQR and SDH, I hypothesized that the *ubiG*::Tn*5*P mutant phenotype would be similar to that of an *nqrA sdhE* double mutant. The addition of succinate and citrate had notable effects on the phenotypes of the

sdhE and *nqrA* mutant strains (Figs. 44 & 56); therefore, I asked whether the *ubiG*::Tn*5*P single mutant and the Δ*sdhE nqrA*::Tn*5*P double mutant behaved similarly when grown in these carbon sources. To test this, I grew the mutant strains in LBS supplemented with citrate and succinate and assessed colony morphology. When grown in citrate, the two strains exhibited very different phenotypes: the Δ*sdhE nqrA*::Tn*5*P double mutant strain failed to wrinkle at advanced times (Fig. 65), similar to the phenotype of the *nqrA*::Tn*5*P mutant strain (Fig. 56), but maintained its adherence to the agar surface instead of exhibiting the increase in edge wrinkling observed with the *ubiG*::Tn*5*P mutant strain (Fig. 63). However, when grown in serine, the two mutant strains exhibited similar responses: both strains began to show the development of biofilm morphology at earlier times. These results suggest that Q has a role in biofilm formation outside of its role in the ETS.

Summary

Investigations into the role of *ubiG* and Q biosynthesis supported a role for electron transport in blocking or inhibiting the development of a number of biofilm phenotypes, including the divoting phenotype as well as the agar adherence phenotype. Biofilms formed by the *ubiG* mutant strain exhibited both phenotypes. While the *ubiG* mutant strain shares a number of phenotypes with the *nqrA* mutant strain, it responds differently when exposed to citrate than the *nqrA* mutant strain, suggesting the mutant has defects in additional pathways. Finally, comparisons of the *ubiG* mutant strain with the *nqrA sdhE* double mutant strain suggested that the requirement for Q in the cell extend beyond its roles in electron carriage in the electron transport system.

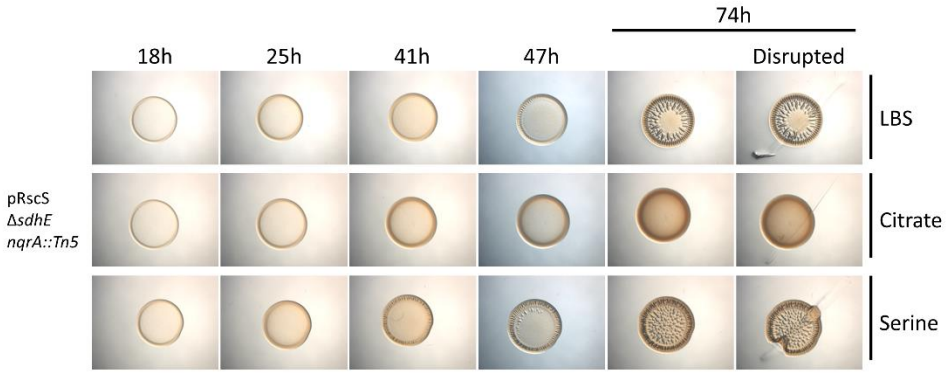

Figure 65 - The biofilm phenotype of the *sdhE nqrA* double mutant in response to citrate and serine. The response of an *nqrA sdhE* double mutant (which should presumably have a similar ETS defect as an *ubiG* mutant) to citrate and serine was assessed using the wrinkled colony and toothpick assays. The response of the *nqrA sdhE* double mutant to citrate mimics that of the *nqrA* single mutant (Fig. 56) rather than the *ubiG* mutant strain (Fig. 64) but with increased adherence. The response of the double mutant to serine mimics that of the *ubiG* mutant strain with the promotion of edge wrinkling and central divoting (Fig 64). The RscS plasmid, pRscS, is pJMO34. This experiment has been conducted one time.

CHAPTER FOUR

DISCUSSION

In this thesis, I generated new genetic tools for the random disruption and induction of genes and used them to identify a number of central metabolism genes with roles in biofilm formation by *Vibrio fischeri*. While it is logical that defects in the central metabolic pathways of an organism would exert broad effects on its physiology, the genes I have identified and the phenotypes I have described appear to have specific roles in biofilm formation rather than general roles in homeostasis. In the following section, I discuss my work and the implications it has on expanding our understanding of biofilm formation in *V. fischeri*. I make a number of conclusions regarding the role of central metabolism (CM) and the electron transport system (ETS) in biofilm formation as well as pose a number of questions that remain unanswered and a possible roadmap to obtaining the answers.

Tn*5*P, a multi-purpose transposon for use in mutagenesis experiments

To expand the reach of currently available tools for the identification of mutants with novel phenotypes, I adapted a system of transposon mutagenesis for use in *V. fischeri.* Specifically, I generated a transposon with an outward facing IPTG inducible promoter as well as a *lacI*-expressing background strain as a recipient for mutagenesis. This system combines the beneficial traits of different mutagenesis and overexpression

approaches in a single assay. For example, I showed that it can be used to identify genes whose increased OR decreased expression can result in a specific phenotype (Ondrey and Visick, 2014).

Further, I presented evidence that the Tn*5*P can insert within a gene yet express a truncated protein due to the putative RBS and start codon located within the Tn end. This tool could, therefore, help identify what parts of a disrupted protein are needed for specific functions. If desired, the Tn*5*P transposon could be engineered further to add a ribosome binding site upstream from a start codon. This would allow for better protein expression. Additional sequence could also be added to place an epitope tag at either the C- or N- terminus of a disrupted gene. The development of genetic tools for identifying genes of interest in *V. fischeri* is far from complete, but the Tn*5*P transposon represents an important step in *V. fischeri* genetics.

I then utilized the Tn*5*P to mutagenize a biofilm-forming strain of *V. fischeri* in order to identify genes that modulate the process of biofilm formation. While I screened approximately 47,000 mutant strains and identified independent insertions in a number of genes, it is apparent from the mutants that I have characterized that my mutagenesis was not saturating. For example, while I isolated mutants with independent Tn*5*P insertions within the *pck* gene, I did not isolate an insertion within the *sdhC* gene (or in the genes that encode the remaining members of the SDH and NQR complexes). In addition, I did not identify a number of other genes with previously reported defects in biofilm formation, such as *dnaJ* (Brooks, Gyllborg et al., 2014). Aside from simply being non-saturating, an explanation for this could be the differences in strain backgrounds or conditions used in my experiments relative to the experiments that yielded other mutant

strains. For example, a different method of *rscS* overexpression was used in the experiments that identified a role for *dnaJ* in biofilm formation. In addition, the amount of time I allowed for the formation of wrinkled colonies could have limited the genes that I could identify, essentially eliminating the identification of mutants that merely exhibit a delay in biofilm formation.

It was unsurprising that I identified a high proportion of genes already known to play a role in biofilm formation by *V. fischeri*, such as *rscS*, *rpoN*, and the genes of the *syp* locus. However, it was surprising that I primarily identified metabolic genes. With the knowledge that my mutagenesis was not saturating, it does seem meaningful that the genes that I did identify as having a role in biofilm formation encode proteins with closely related roles in central metabolism. However, it is unclear why I did not obtain other, seemingly equally connected, genes such as the gene for fumarase (which connects SDH and Mdh in the TCA cycle). Potentially, loss of these "missing" genes could result in growth defects that are severe enough to prevent isolation under my conditions, or whose function is redundant in some way or can be complemented in trans by other colonies.

Glutamine biosynthesis is required for biofilm formation by *V. fischeri*

Prior to this work, a role for glutamine biosynthesis in biofilm formation had not been described. Within this thesis, I described the phenotype of the *glnA* mutant strain and complemented the biofilm defect of the mutant strain by adding glutamine to the growth medium (Fig. 23). One question that remains regarding this mutant strain is why an inability to synthesize glutamine leads to a failure of the strain to form a wrinkled colony. Due to the inability of the *glnA* mutant strain to exhibit cell-cell cohesion, it is

likely that the biofilm defect is due to an inability to produce the Syp PS. What remains unknown is how glutamine intersects with the process of Syp PS production. Is the biosynthesis of glutamine required for the activation of RscS or the transcription of the *syp* locus? Or could glutamine be an important residue in a protein that links polysaccharide together within the matrix? To begin to address the question of a connection between Syp PS and glutamine, transcriptional and translational reporters could be utilized in a *glnA* mutant strain to identify where, or if, Syp PS production is inhibited. Previous work in *E. coli* has shown that glutamine residues are important for the function of amyloid fibers, and thus biofilm formation (Wang and Chapman, 2008). While a role for amyloid fibers in biofilm formation by *V. fischeri* has not been identified, it is an interesting possibility. The first step would be to identify whether *V. fischeri* produces an amyloid as part of its biofilm.

One surprising finding was that the addition of glutamine to an *mdh* mutant almost completely restored the wild-type biofilm phenotypes: growth of the *mdh*::Tn*5*P strain on medium supplemented with 0.2% glutamine greatly restored wrinkling and inhibited agar attachment (Fig. 33). These data suggested that perhaps the one of the roles of the TCA cycle in biofilm formation is to generate glutamine. Disruption in the TCA cycle will disrupt the supply of the TCA intermediate α-ketogluterate, which is the precursor to glutamine (Figs. 4 & 13). One potential reason that glutamine did not rescue other mutant strains may be that the other mutations exert additional effects on pathways adjacent to the TCA cycle, *i.e.*, in addition to their TCA defects, the *sdh* mutants also have defects in the ETS and the *pck* mutants have defects in GNG. Thus, glutamine or glucose added to a *pck* mutant strain may bypass the TCA and GNG defects respectively,

but not the additional defects, and thus biofilm formation remains blocked. Indeed, the phenotype of a *pck* mutant strain grown in the presence of glucose (Fig. 37) looks very similar to that of a *glnA* mutant in LBS (Fig. 27C). Further experiments, such as assessing the phenotype of the *pck* mutant grown in the presence of both glutamine and glucose, would provide greater insight into the validity of this hypothesis.

An additional question is whether the failure to generate glutamine impacts the ability of this strain to colonize juvenile squid. As the production of Syp PS is required for the formation of the biofilm outside of the light organ, the apparent failure of this strain to produce Syp PS (Fig. 27) suggests that the strain would unlikely be capable of initiating the colonization process. If future colonization experiments show that a *glnA* mutant strain can colonize squid, it might suggest the presence of glutamine in the squid mucus.

The role of SdhE in biofilm formation by *V. fischeri*

Previous research first identified SdhE as an activator of the SDH complex, and then as a promiscuous protein with roles in the activation of the FRD complex (McNeil, Clulow et al., 2012, McNeil, Hampton et al., 2014). My work has supported the hypotheses that SdhE has a role in SDH function as both *sdhE* and *sdhC* mutants exhibit similar phenotypes. My work has also supported the hypothesis that SdhE may have roles outside of SDH activation. First, when examining the phenotypes of the *sdhE* and *sdhC* mutant strains, I found that they had different phenotypes when exposed to different carbon sources (Figs. 44 & 45) and had different timing of biofilm structure development when grown in LBS (Fig. 43). These data suggest that, in *V. fischeri*, there is a target of SdhE outside of SDH, likely FRD. To confirm this possibility, it would be relatively

simple to generate an *frd sdhC* double mutant strain and compare the phenotype of this mutant strain to that of the *sdhE* mutant strain. If the two exhibit the same phenotypes in LBS and when exposed to different carbon sources, it would confirm that FRD activation in *V. fischeri* is mediated by SdhE.

The *sdhE* and, to a slightly lesser extent, *sdhC* mutant strains exhibited decreased bioluminescence when grown in SWTO medium (Fig. 48), a phenotype that the other ETS mutant strain (*nqrA*) did not exhibit (Fig. 60). This result suggests that the role of SDH activity in bioluminescence is outside of its role as a member of the ETS. Could decreases in TCA cycle activity (or glutamine synthesis) impact quorum sensing and bioluminescence? Previous work in *Serrtatia sp.* showed that there was a decrease in production of N-acyl homoserine lactone quorum sensing molecules by *sdhE* mutant strains (McNeil, Clulow et al., 2012), suggesting that alterations in quorum sensing could be an important area of focus for future study. Investigations into the bioluminescence phenotypes of the other central metabolism mutants (especially *mdh* and *glnA*) would be informative.

Colonization experiments with the *sdhE* mutant strain showed that the mutant was able to colonize juvenile squid, but the growth defect by the strain hindered my ability to conclude that the 10-fold colonization defect was a *de facto* defect (Fig. 47). However, it has been suggested that the primary means of growth by *V. fischeri* cells within the light organ is anaerobic. This calls in to question whether an *sdhE* mutant strain would actually have a growth disadvantage in the light organ. Perhaps an examination of the ability of the *sdhE* mutant to grow under anaerobic conditions would shed light as to whether this mutant strain would have a comparative growth defect in the light organ.

The role of Na^+-NQR in biofilm formation by *V. fischeri*

The biofilm mutants with the most unique phenotype were undoubtedly the *nqrA* and *nqr* mutant strains. Their agar attachment phenotype is unlike anything we have observed in the lab to date (Fig. 50). The factor that mediates this attachment remains unknown. The phenotype is independent of Msh or Csg pili (Fig. 61) but requires the production of the Syp PS (Fig. 54). Could the Syp PS of the Na^+-NQR strains be modified in some way that promotes increased cell-cell cohesion as well as cell-surface adherence? Additional research into the composition and structure of both wild-type and *nqr* Syp PS will need to be conducted to pursue this exciting area of inquiry.

The adherence phenotype of the other central metabolism mutant strains is less extreme, but the observation that they, too, exhibited a version of this phenotype suggests that the attachment phenotype could be a response to an inability to use the ETS. The severity of the adherence phenotypes correlates well to the proximity of the mutated gene's function to the ETS system with the *nqr* and *ubiG* mutants being the most severe (Figs. 50 & 63), followed by *sdh* (Fig. 39), *mdh* (Fig. 30), and *pck* (Fig. 35) mutants in order from most to least severe. The *glnA* mutant has very little connection to the ETS and, perhaps as a consequence, has no adherence phenotype (Fig. 27). These analyses are complicated by the additional phenotypes present in these mutant strains. While it is clear that the production of the Syp PS is required for adherence (at least of the *nqr* mutant), the phenotype is made stronger by the formation of colony architecture.

Previous research by Ray et al. showed that the development of 3-dimensional colony architecture (wrinkling) in *V. fischeri* biofilms, or "maturation" as they termed it, required the BmpA, BmpB, or BmpC proteins (Ray, Driks et al., 2015). My research

supports that conclusion and has shown that the adherence phenotype is not dependent on the Bmp proteins, but is made stronger by the presence of them (Fig. 54). I propose that a decrease in the Bmp proteins plays a role in the decrease of adherence in mutants that lose architecture (wrinkling or divoting) upon exposure to certain carbon sources (eg. Figs. 32 & 56). Previous research into *syp* and *bmp* has shown that expression of these loci are controlled by the same regulators (Ray, Eddy et al., 2013). My data, however, suggest that the addition of certain carbon sources may inhibit Bmp production while allowing Syp PS production. Future investigations into *syp* and *bmp* expression in the presence of various nutrient sources could identify conditions that promote or inhibit Bmp activity.

There is also a question as to whether the agar adherence phenotype has relevance in the context of squid colonization and symbiosis. I had originally hypothesized that an *nqr* mutant strain would be able to form a biofilm outside the light organ, but be unable to escape it due to the tendency of the mutant strain to have such strong cell-cell and cell-surface interactions. This, however, proved not to be the case since the *nqr* mutant strain was able to colonize juvenile *E. scolopes* (Fig. 59). There are a number of possible explanations for these findings. One reason for this apparent discrepancy could be that the *in vitro* experiments used an *rscS* overexpression plasmid, while no plasmid was used in colonization experiments. Perhaps, without overexpression of *rscS*, there not enough Syp PS produced to mediate the severe attachment phenotype in the course of squid colonization. Thus, it could be informative to assess the ability of an *rscS*-overexpressing *nqr* mutant to colonize squid.

Another reason why the *nqr* mutant could be able to colonize the squid could be that the amount of time that *V. fischeri* cells are present in a biofilm outside the light organ is relatively brief. It is highly possible that it takes more time for the *nqr* mutant strains to develop this strong phenotype and there simply is not enough time between biofilm formation and dispersal of cells into the light organ to cause the cells to become stuck outside the light organ. Additionally, it is possible that the mechanism that the *V. fischeri* cells use to disperse from the biofilm, which are apparently not activated in *in vitro* cultures, are sufficient to override even the strong *nqr* biofilm phenotype in the context of animal colonization. An examination of the biofilms formed by *nqr* mutant cells on the surface of the light organ could be informative as to whether these cell-cell and cell-surface associations are tighter than wild-type biofilms, as well as whether the timing of dispersal is altered.

Regardless of the role of Na^+-NQR in the initial stages of colonization, it may also play a role in later stages inside the light organ. An examination of the phenotype of *nqr* mutant cells once they are within the deep crypts of the light organ could be informative. Do animals colonized by *nqr* mutant strains exhibit a decrease in the amount of *V. fischeri* cells vented at dawn? If so, does the squid host eventually fail to thrive due to over-colonization? Such questions could shed light on certain aspects of this host microbe symbiosis. While we know a great deal about the biofilm that forms outside the light organ, we know relatively little about whether the bacteria also form a biofilm within the light organ of the squid. As mentioned above, the *nqrA* mutant strain could be a used as a tool to assess whether the RscS Syp biofilm is made within the confines of the light organ. The presence of the Syp PS is needed for the formation of the attachment

phenotype and an observation that there is decreased venting of an *nqrA* mutant strain could suggest that the strong biofilm of the *nqrA* mutant strain is being formed, and with it the production of the Syp PS.

One final intriguing factor of the Na^+-NQR mutant strain is that while it is generally dim in culture and below the threshold of bioluminescence detection when in the light organ it has an apparent increase in bioluminescence per cell (Fig. 60). It has been previously hypothesized that the ability to burn O_2 via bioluminescence is beneficial to colonized *V. fischeri* cells (Visick, Foster et al., 2000). Potentially, if colonized cells are undergoing anaerobic respiration (perhaps in response to a squid signal), bioluminescence is the only way that squid-derived O_2 can be safely reduced. This model could explain why bioluminescence mutants are quickly outcompeted by bioluminescent competent strains. If this model is accurate, the phenotypes of the *nqrA* mutant, i.e. increased luminescence per cell, anaerobic respiration, and increased surface adherence, could be similar to how colonized *V. fischeri* cells behave.

The role of gluconeogenic carbon sources on biofilm formation by *V. fischeri*

Throughout my investigations of my biofilm-defective mutants, I have shown that the addition of a number of gluconeogenic carbon sources (glucose, G6P, and OAA) to the growth medium results in a delay in wrinkled colony formation by the parent strain or a defect in the development of biofilm structure by many mutant strains (eg. Figs. 32 & 45). This was, at first, surprising as the Syp PS appears to be one of the most important requirements for the formation of wrinkled colonies, and the production of PS presumably requires the cell to generate these intermediates if it is grown on a medium comprised mainly of amino acids. The reason for this response to these carbon sources *by*

V. fischeri is, as yet, unknown, but there are a number of hypothesis which could be readily tested to bring us closer to an answer.

One such hypothesis is that there is a "sweet spot" of polysaccharide production required to produce what we consider the wild-type wrinkled colony. The addition of G6P to the medium may simply result in too much Syp PS. However, because my data show that parent strain wrinkles in the presence of these carbon sources (Fig. 28), there is clearly something else at play; the parent strain grown in the presence of G6P would likely make more PS precursors than the *pck* mutant grown in G6P.

Another possibility is that a ratio of polysaccharide to protein is required for the generation of both cohesion and the development of architecture. As shown by Ray et al., the Syp polysaccharide is not the only component in the *V. fischeri* biofilm matrix. The BmpA protein is also found in the matrix and BmpA, along with BmpB and BmpC, are required for the development of *V. fischeri*'s characteristic wrinkled colony (Ray, Driks et al., 2015). It is possible that disrupting the ratio of these components, the PS and the protein, beyond a certain point results in a wrinkled colony defect. The addition of the GNG carbons could do just that. To test this possibility, we could assess whether an increase in the expression of the *bmp* genes fully or partially diminishes the delay caused by the addition of the carbon sources. In addition to the Bmp proteins, there are likely other proteins (perhaps one that requires glutamine biosynthesis) that need to be present in an appropriate ratio.

Conclusion

My research has identified roles for central metabolism and the ETS in biofilm formation and uncovered a novel adherence phenotype. This work illustrates the level of

complexity involved in the regulation of biofilm formation by *V. fischeri* as many environmental changes result in a modulation of biofilm development. This work has also opened the door to numerous additional areas of focus for those seeking to learn more about how biofilm formation is regulated by *V. fischeri*.

REFERENCES

Alteri, C. J., S. N. Smith and H. L. Mobley (2009). "Fitness of *Escherichia coli* during urinary tract infection requires gluconeogenesis and the TCA cycle." PLoS Pathog **5**(5): e1000448.

Altura, M. A., E. A. Heath-Heckman, A. Gillette, N. Kremer, A. M. Krachler, C. Brennan, E. G. Ruby, K. Orth and M. J. McFall-Ngai (2013). "The first engagement of partners in the *Euprymna scolopes*-*Vibrio fischeri* symbiosis is a two-step process initiated by a few environmental symbiont cells." Environ Microbiol.

Bertani, G. (1951). "Studies on lysogenesis. I. The mode of phage liberation by lysogenic *Escherichia coli*." J Bacteriol **62**(3): 293-300.

Boettcher, K. J., E. G. Ruby and M. J. McFall-Ngai (1996). "Bioluminescence in the symbiotic squid *Euprymna scolopes* is controlled by a daily biological rhythm." Journal of Comparative Physiology A **179**(1): 65-73.

Bose, J. L., U. Kim, W. Bartkowski, R. P. Gunsalus, A. M. Overley, N. L. Lyell, K. L. Visick and E. V. Stabb (2007). "Bioluminescence in *Vibrio fischeri* is controlled by the redox-responsive regulator ArcA." Mol Microbiol **65**(2): 538-553.

Bose, J. L., C. S. Rosenberg and E. V. Stabb (2008). "Effects of *luxCDABEG* induction in *Vibrio fischeri*: enhancement of symbiotic colonization and conditional attenuation of growth in culture." Arch Microbiol **190**(2): 169-183.

Bowden, S. D., V. K. Ramachandran, G. M. Knudsen, J. C. Hinton and A. Thompson (2010). "An incomplete TCA cycle increases survival of Salmonella Typhimurium during infection of resting and activated murine macrophages." PLoS One **5**(11): e13871.

Brennan, C. A., M. J. Mandel, M. C. Gyllborg, K. A. Thomasgard and E. G. Ruby (2013). "Genetic determinants of swimming motility in the squid light-organ symbiont *Vibrio fischeri*." Microbiologyopen **2**(4): 576-594.

Brooks, J. F., 2nd, M. C. Gyllborg, D. C. Cronin, S. J. Quillin, C. A. Mallama, R. Foxall, C. Whistler, A. L. Goodman and M. J. Mandel (2014). "Global discovery of

colonization determinants in the squid symbiont *Vibrio fischeri*." Proc Natl Acad Sci U S A **111**(48): 17284-17289.

Casutt, M. S., T. Huber, R. Brunisholz, M. Tao, G. Fritz and J. Steuber (2010). "Localization and function of the membrane-bound riboflavin in the Na+-translocating NADH:quinone oxidoreductase (Na+-NQR) from Vibrio cholerae." J Biol Chem **285**(35): 27088-27099.

Cecchini, G., I. Schroder, R. P. Gunsalus and E. Maklashina (2002). "Succinate dehydrogenase and fumarate reductase from *Escherichia coli*." Biochim Biophys Acta **1553**(1-2): 140-157.

Chandra, H., S. F. Basir, M. Gupta and N. Banerjee (2010). "Glutamine synthetase encoded by glnA-1 is necessary for cell wall resistance and pathogenicity of Mycobacterium bovis." Microbiology **156**(Pt 12): 3669-3677.

Chapman, M. R., L. S. Robinson, J. S. Pinkner, R. Roth, J. Heuser, M. Hammar, S. Normark and S. J. Hultgren (2002). "Role of *Escherichia coli* curli operons in directing amyloid fiber formation." Science **295**(5556): 851-855.

Darnell, C. L., E. A. Hussa and K. L. Visick (2008). "The putative hybrid sensor kinase SypF coordinates biofilm formation in *Vibrio fischeri* by acting upstream of two response regulators, SypG and VpsR." J Bacteriol **190**(14): 4941-4950.

Dassler, T., T. Maier, C. Winterhalter and A. Bock (2000). "Identification of a major facilitator protein from Escherichia coli involved in efflux of metabolites of the cysteine pathway." Mol Microbiol **36**(5): 1101-1112.

Davidson, S. K., T. A. Koropatnick, R. Kossmehl, L. Sycuro and M. J. McFall-Ngai (2004). "NO means 'yes' in the squid-vibrio symbiosis: nitric oxide (NO) during the initial stages of a beneficial association." Cell Microbiol **6**(12): 1139-1151.

Deloney-Marino, C. R. and K. L. Visick (2012). "Role for cheR of Vibrio fischeri in the Vibrio-squid symbiosis." Can J Microbiol **58**(1): 29-38.

DeLoney-Marino, C. R., A. J. Wolfe and K. L. Visick (2003). "Chemoattraction of *Vibrio fischeri* to serine, nucleosides, and N-acetylneuraminic acid, a component of squid light-organ mucus." Appl Environ Microbiol **69**(12): 7527-7530.

DeLoney, C. R., T. M. Bartley and K. L. Visick (2002). "Role for phosphoglucomutase in *Vibrio fischeri-Euprymna scolopes* symbiosis." J Bacteriol **184**(18): 5121-5129.

Donlan, R. M. and J. W. Costerton (2002). "Biofilms: survival mechanisms of clinically relevant microorganisms." Clin Microbiol Rev **15**(2): 167-193.

Dunlap, P. V. and A. Kuo (1992). "Cell density-dependent modulation of the Vibrio fischeri luminescence system in the absence of autoinducer and LuxR protein." J Bacteriol **174**(8): 2440-2448.

Flemming, H. C. and J. Wingender (2010). "The biofilm matrix." Nat Rev Microbiol **8**(9): 623-633.

Franke, I., A. Resch, T. Dassler, T. Maier and A. Bock (2003). "YfiK from *Escherichia coli* promotes export of O-acetylserine and cysteine." J Bacteriol **185**(4): 1161-1166.

Gonidakis, S., S. E. Finkel and V. D. Longo (2011). "Lifespan extension and paraquat resistance in a ubiquinone-deficient *Escherichia coli* mutant depend on transcription factors ArcA and TdcA." Aging (Albany NY) **3**(3): 291-303.

Graf, J. and E. G. Ruby (1998). "Host-derived amino acids support the proliferation of symbiotic bacteria." Proc Natl Acad Sci U S A **95**(4): 1818-1822.

Hase, C. C. and B. Barquera (2001). "Role of sodium bioenergetics in *Vibrio cholerae*." Biochim Biophys Acta **1505**(1): 169-178.

Herrero, M., V. de Lorenzo and K. N. Timmis (1990). "Transposon vectors containing non-antibiotic resistance selection markers for cloning and stable chromosomal insertion of foreign genes in gram-negative bacteria." J Bacteriol **172**(11): 6557-6567.

Ho, S. N., H. D. Hunt, R. M. Horton, J. K. Pullen and L. R. Pease (1989). "Site-directed mutagenesis by overlap extension using the polymerase chain reaction." Gene **77**(1): 51-59.

Hussa, E. A., C. L. Darnell and K. L. Visick (2008). "RscS functions upstream of SypG to control the *syp* locus and biofilm formation in *Vibrio fischeri*." J Bacteriol **190**(13): 4576-4583.

Hussa, E. A., T. M. O'Shea, C. L. Darnell, E. G. Ruby and K. L. Visick (2007). "Two-component response regulators of *Vibrio fischeri*: identification, mutagenesis, and characterization." J Bacteriol **189**(16): 5825-5838.

Iverson, T. M., C. Luna-Chavez, G. Cecchini and D. C. Rees (1999). "Structure of the *Escherichia coli* fumarate reductase respiratory complex." Science **284**(5422): 1961-1966.

Jones, B. W. and M. K. Nishiguchi (2004). "Counterillumination in the Hawaiian bobtail squid, *Euprymna scolopes* Berry (Mollusca: Cephalopoda)." Marine Biology **144**(6): 1151-1155.

Keseler, I. M., J. Collado-Vides, A. Santos-Zavaleta, M. Peralta-Gil, S. Gama-Castro, L. Muniz-Rascado, C. Bonavides-Martinez, S. Paley, M. Krummenacker, T. Altman, P. Kaipa, A. Spaulding, J. Pacheco, M. Latendresse, C. Fulcher, M. Sarker, A. G. Shearer, A. Mackie, I. Paulsen, R. P. Gunsalus and P. D. Karp (2011). "EcoCyc: a comprehensive database of Escherichia coli biology." Nucleic Acids Res **39**(Database issue): D583-590.

Kim, S. H., S. Ramaswamy and J. Downard (1999). "Regulated exopolysaccharide production in *Myxococcus xanthus*." J Bacteriol **181**(5): 1496-1507.

Kitagawa, M., T. Ara, M. Arifuzzaman, T. Ioka-Nakamichi, E. Inamoto, H. Toyonaga and H. Mori (2005). "Complete set of ORF clones of *Escherichia coli* ASKA library (a complete set of *E. coli* K-12 ORF archive): unique resources for biological research." DNA Res **12**(5): 291-299.

Koch, E. J., T. Miyashiro, M. J. McFall-Ngai and E. G. Ruby (2014). "Features governing symbiont persistence in the squid-vibrio association." Mol Ecol **23**(6): 1624-1634.

Koropatnick, T. A., J. T. Engle, M. A. Apicella, E. V. Stabb, W. E. Goldman and M. J. McFall-Ngai (2004). "Microbial factor-mediated development in a host-bacterial mutualism." Science **306**(5699): 1186-1188.

Lanzer, M. and H. Bujard (1988). "Promoters largely determine the efficiency of repressor action." Proc Natl Acad Sci U S A **85**(23): 8973-8977.

Le Roux, F., J. Binesse, D. Saulnier and D. Mazel (2007). "Construction of a *Vibrio splendidus* mutant lacking the metalloprotease gene *vsm* by use of a novel counterselectable suicide vector." Appl Environ Microbiol **73**(3): 777-784.

Lichtenstein, C. and S. Brenner (1982). "Unique insertion site of Tn*7* in the *E. coli* chromosome." Nature **297**(5867): 601-603.

Lyell, N. L., A. K. Dunn, J. L. Bose, S. L. Vescovi and E. V. Stabb (2008). "Effective mutagenesis of *Vibrio fischeri* by using hyperactive mini-Tn*5* derivatives." Appl Environ Microbiol **74**(22): 7059-7063.

Mah, T. F. (2012). "Biofilm-specific antibiotic resistance." Future Microbiol **7**(9): 1061-1072.

Mandel, M. J., A. L. Schaefer, C. A. Brennan, E. A. Heath-Heckman, C. R. Deloney-Marino, M. J. McFall-Ngai and E. G. Ruby (2012). "Squid-derived chitin oligosaccharides are a chemotactic signal during colonization by *Vibrio fischeri*." Appl Environ Microbiol **78**(13): 4620-4626.

McCann, J., E. V. Stabb, D. S. Millikan and E. G. Ruby (2003). "Population Dynamics of *Vibrio fischeri* during Infection of *Euprymna scolopes*." Applied and Environmental Microbiology **69**(10): 5928-5934.

McFall-Ngai, M., C. Brennan, V. Weis and L. H. Lamarcq (1998). Mannose adhesin-glycan interactions in the *Euprymna scolopes*-*Vibrio fischeri* symbiosis. New developments in marine biotechnology. L. G. Y. and H. H. O. New York, Springer**:** 273-276.

McFall-Ngai, M. and M. K. Montgomery (1990). "The anatomy and morphology of the adult bacterial light organ of *Euprymna scolopes* Berry (Cephalopoda: Sepiolidae)." Biol Bull **179**: 332-339.

McFall-Ngai, M. J. and E. G. Ruby (1991). "Symbiont recognition and subsequent morphogenesis as early events in an animal-bacterial mutualism." Science **254**(5037): 1491-1494.

McLean, J. S., G. E. Pinchuk, O. V. Geydebrekht, C. L. Bilskis, B. A. Zakrajsek, E. A. Hill, D. A. Saffarini, M. F. Romine, Y. A. Gorby, J. K. Fredrickson and A. S. Beliaev (2008). "Oxygen-dependent autoaggregation in *Shewanella oneidensis* MR-1." Environ Microbiol **10**(7): 1861-1876.

McNeil, M. B., J. S. Clulow, N. M. Wilf, G. P. Salmond and P. C. Fineran (2012). "SdhE is a conserved protein required for flavinylation of succinate dehydrogenase in bacteria." J Biol Chem **287**(22): 18418-18428.

McNeil, M. B. and P. C. Fineran (2013). "Prokaryotic assembly factors for the attachment of flavin to complex II." Biochim Biophys Acta **1827**(5): 637-647.

McNeil, M. B., H. G. Hampton, K. J. Hards, B. N. Watson, G. M. Cook and P. C. Fineran (2014). "The succinate dehydrogenase assembly factor, SdhE, is required for the flavinylation and activation of fumarate reductase in bacteria." FEBS Lett **588**(3): 414-421.

Meganathan, R. (2001). "Ubiquinone biosynthesis in microorganisms." FEMS Microbiol Lett **203**(2): 131-139.

Millikan, D. S. and E. G. Ruby (2003). "FlrA, a σ^{54}-dependent transcriptional activator in *Vibrio fischeri*, is required for motility and symbiotic light-organ colonization." J Bacteriol **185**(12): 3547-3557.

Millikan, D. S. and E. G. Ruby (2004). "*Vibrio fischeri* flagellin A is essential for normal motility and for symbiotic competence during initial squid light organ colonization." J Bacteriol **186**(13): 4315-4325.

Morris, A. R., C. L. Darnell and K. L. Visick (2011). "Inactivation of a novel response regulator is necessary for biofilm formation and host colonization by *Vibrio fischeri*." Mol Microbiol **82**(1): 114-130.

Morris, A. R. and K. L. Visick (2013). "The response regulator SypE controls biofilm formation and colonization through phosphorylation of the *syp*-encoded regulator SypA in *Vibrio fischeri*." Mol Microbiol **87**(3): 509-525.

Norsworthy, A. N. and K. L. Visick (2015). "Signaling between two interacting sensor kinases promotes biofilms and colonization by a bacterial symbiont." Mol Microbiol **96**(2): 233-248.

Nyholm, S. V. and M. J. McFall-Ngai (1998). "Sampling the light-organ microenvironment of *Euprymna scolopes*: description of a population of host cells in association with the bacterial symbiont *Vibrio fischeri*." Biol Bull **195**(2): 89-97.

Nyholm, S. V., E. V. Stabb, E. G. Ruby and M. J. McFall-Ngai (2000). "Establishment of an animal-bacterial association: recruiting symbiotic vibrios from the environment." Proc Natl Acad Sci U S A **97**(18): 10231-10235.

Nyholm, S. V., J. J. Stewart, E. G. Ruby and M. J. McFall-Ngai (2009). "Recognition between symbiotic *Vibrio fischeri* and the haemocytes of *Euprymna scolopes*." Environ Microbiol **11**(2): 483-493.

O'Shea, T. M., A. H. Klein, K. Geszvain, A. J. Wolfe and K. L. Visick (2006). "Diguanylate cyclases control magnesium-dependent motility of *Vibrio fischeri*." J Bacteriol **188**(23): 8196-8205.

Ondrey, J. M. and K. L. Visick (2014). "Engineering *Vibrio fischeri* for inducible gene expression." Open Microbiol J **8**: 122-129.

Osteras, M., T. M. Finan and J. Stanley (1991). "Site-directed mutagenesis and DNA sequence of *pckA* of Rhizobium NGR234, encoding phosphoenolpyruvate carboxykinase: gluconeogenesis and host-dependent symbiotic phenotype." Mol Gen Genet **230**(1-2): 257-269.

Peyer, S. M., M. S. Pankey, T. H. Oakley and M. J. McFall-Ngai (2014). "Eye-specification genes in the bacterial light organ of the bobtail squid *Euprymna scolopes*, and their expression in response to symbiont cues." Mech Dev **131**: 111-126.

Pollack-Berti, A., M. S. Wollenberg and E. G. Ruby (2010). "Natural transformation of *Vibrio fischeri* requires *tfoX* and *tfoY*." Environ Microbiol **12**(8): 2302-2311.

Poon, W. W., R. J. Barkovich, A. Y. Hsu, A. Frankel, P. T. Lee, J. N. Shepherd, D. C. Myles and C. F. Clarke (1999). "Yeast and rat Coq3 and *Escherichia coli* UbiG polypeptides catalyze both O-methyltransferase steps in coenzyme Q biosynthesis." J Biol Chem **274**(31): 21665-21672.

Prigent-Combaret, C., G. Prensier, T. T. Le Thi, O. Vidal, P. Lejeune and C. Dorel (2000). "Developmental pathway for biofilm formation in curli-producing *Escherichia coli* strains: role of flagella, curli and colanic acid." Environ Microbiol **2**(4): 450-464.

Proctor, L. M. and R. P. Gunsalus (2000). "Anaerobic respiratory growth of *Vibrio harveyi*, *Vibrio fischeri* and *Photobacterium leiognathi* with trimethylamine N-oxide, nitrate and fumarate: ecological implications." Environ Microbiol **2**(4): 399-406.

Ray, V. A., A. Driks and K. L. Visick (2015). "Identification of a novel matrix protein that promotes biofilm maturation in *Vibrio fischeri*." J Bacteriol **197**(3): 518-528.

Ray, V. A., J. L. Eddy, E. A. Hussa, M. Misale and K. L. Visick (2013). "The *syp* enhancer sequence plays a key role in transcriptional activation by the σ^{54}-dependent response regulator SypG and in biofilm formation and host colonization by *Vibrio fischeri*." J Bacteriol **195**(23): 5402-5412.

Ray, V. A. and K. L. Visick (2012). "LuxU connects quorum sensing to biofilm formation in *Vibrio fischeri*." Mol Microbiol.

Reyes-Prieto, A., B. Barquera and O. Juarez (2014). "Origin and evolution of the sodium -pumping NADH: ubiquinone oxidoreductase." PLoS One **9**(5): e96696.

Romling, U., M. Gomelsky and M. Y. Galperin (2005). "C-di-GMP: the dawning of a novel bacterial signalling system." Mol Microbiol **57**(3): 629-639.

Ruby, E. G. and L. M. Asato (1993). "Growth and flagellation of *Vibrio fischeri* during initiation of the sepiolid squid light organ symbiosis." Arch Microbiol **159**(2): 160-167.

Ruby, E. G. and M. J. McFall-Ngai (1999). "Oxygen-utilizing reactions and symbiotic colonization of the squid light organ by *Vibrio fischeri*." Trends Microbiol **7**(10): 414-420.

Ruby, E. G. and K. H. Nealson (1977). "A luminous bacterium that emits yellow light." Science **196**(4288): 432-434.

Ruby, E. G., M. Urbanowski, J. Campbell, A. Dunn, M. Faini, R. Gunsalus, P. Lostroh, C. Lupp, J. McCann, D. Millikan, A. Schaefer, E. Stabb, A. Stevens, K. Visick, C. Whistler and E. P. Greenberg (2005). "Complete genome sequence of *Vibrio*

fischeri: a symbiotic bacterium with pathogenic congeners." Proc Natl Acad Sci U S A **102**(8): 3004-3009.

Sadykov, M. R., T. Hartmann, T. A. Mattes, M. Hiatt, N. J. Jann, Y. Zhu, N. Ledala, R. Landmann, M. Herrmann, H. Rohde, M. Bischoff and G. A. Somerville (2011). "CcpA coordinates central metabolism and biofilm formation in *Staphylococcus epidermidis*." Microbiology **157**(Pt 12): 3458-3468.

Septer, A. N., Y. Wang, E. G. Ruby, E. V. Stabb and A. K. Dunn (2011). "The haem-uptake gene cluster in *Vibrio fischeri* is regulated by Fur and contributes to symbiotic colonization." Environ Microbiol **13**(11): 2855-2864.

Shibata, S. and K. L. Visick (2012). "Sensor kinase RscS induces the production of antigenically distinct outer membrane vesicles that depend on the symbiosis polysaccharide locus in *Vibrio fischeri*." J Bacteriol **194**(1): 185-194.

Shibata, S., E. S. Yip, K. P. Quirke, J. M. Ondrey and K. L. Visick (2012). "Roles of the structural symbiosis polysaccharide (*syp*) genes in host colonization, biofilm formation, and polysaccharide biosynthesis in *Vibrio fischeri*." J Bacteriol **194**(24): 6736-6747.

Singh, P., J. F. Brooks, 2nd, V. A. Ray, M. J. Mandel and K. L. Visick (2015). "CysK plays a role in biofilm formation and colonization by *Vibrio fischeri*." Appl Environ Microbiol **81**(15): 5223-5234.

Stabb, E. and D. Millikan (2009). Is the *Vibrio fischeri-Euprymna scolopes* symbiosis a defensive mutualism? Defensive mutualism in microbial symbiosis. J. F. J. White and M. S. Torres. Boca Raton, Taylor and Francis**:** 85-98.

Stabb, E. and K. L. Visick (2013). *Vibrio fischeri*: A Bioluminescent Light-Organ Symbiont of the Bobtail Squid *Euprymna scolopes*. The Prokaryotes – Prokaryotic Biology and Symbiotic Associations. E. Rosenberg, E. F. DeLong, E. Stackebrandt, S. Lory and F. Thompson, Springer**:** 497-532.

Stabb, E. V., K. A. Reich and E. G. Ruby (2001). "*Vibrio fischeri* genes *hvnA* and *hvnB* encode secreted NAD(+)-glycohydrolases." J Bacteriol **183**(1): 309-317.

Stabb, E. V. and E. G. Ruby (2002). "RP4-based plasmids for conjugation between *Escherichia coli* and members of the Vibrionaceae." Methods Enzymol **358**: 413-426.

Steuber, J., P. Halang, T. Vorburger, W. Steffen, G. Vohl and G. Fritz (2014). "Central role of the Na+-translocating NADH:quinone oxidoreductase (Na+-NQR) in sodium bioenergetics of Vibrio cholerae." Biol Chem **395**(12): 1389-1399.

van der Rest, M. E., C. Frank and D. Molenaar (2000). "Functions of the membrane-associated and cytoplasmic malate dehydrogenases in the citric acid cycle of *Escherichia coli*." J Bacteriol **182**(24): 6892-6899.

Visick, K. L., J. Foster, J. Doino, M. McFall-Ngai and E. G. Ruby (2000). "*Vibrio fischeri lux* genes play an important role in colonization and development of the host light organ." J Bacteriol **182**(16): 4578-4586.

Visick, K. L., K. P. Quirke and S. M. McEwen (2013). "Arabinose induces pellicle formation by *Vibrio fischeri*." Appl Environ Microbiol **79**(6): 2069-2080.

Visick, K. L. and E. G. Ruby (1997). New genetic tools for use in the marine bioluminescent bacterium *Vibrio fischeri*. Bioluminescence and Chemiluminescence. J. W. Hastings, L. J. Kricka and P. E. Stanley. New York, John Wiley and Sons**:** 119-122.

Visick, K. L. and L. M. Skoufos (2001). "Two-component sensor required for normal symbiotic colonization of *euprymna scolopes* by *Vibrio fischeri*." J Bacteriol **183**(3): 835-842.

Wang, X. and M. R. Chapman (2008). "Sequence determinants of bacterial amyloid formation." J Mol Biol **380**(3): 570-580.

Wang, Y., Y. S. Dufour, H. K. Carlson, T. J. Donohue, M. A. Marletta and E. G. Ruby (2010). "H-NOX-mediated nitric oxide sensing modulates symbiotic colonization by *Vibrio fischeri*." Proc Natl Acad Sci U S A **107**(18): 8375-8380.

Waters, C. M. and B. L. Bassler (2005). "Quorum sensing: cell-to-cell communication in bacteria." Annu Rev Cell Dev Biol **21**: 319-346.

Wei, S. and R. Young (1989). "Development of symbiotic bacterial bioluminescence in a nearshore cephalopod, *Euprymna scolopes*." Mar Bio **103**: 541-546.

Whistler, C. A. and E. G. Ruby (2003). "GacA regulates symbiotic colonization traits of *Vibrio fischeri* and facilitates a beneficial association with an animal host." J Bacteriol **185**(24): 7202-7212.

Wier, A. M., S. V. Nyholm, M. J. Mandel, R. P. Massengo-Tiasse, A. L. Schaefer, I. Koroleva, S. Splinter-Bondurant, B. Brown, L. Manzella, E. Snir, H. Almabrazi, T. E. Scheetz, F. Bonaldo Mde, T. L. Casavant, M. B. Soares, J. E. Cronan, J. L. Reed, E. G. Ruby and M. J. McFall-Ngai (2010). "Transcriptional patterns in both host and bacterium underlie a daily rhythm of anatomical and metabolic change in a beneficial symbiosis." Proc Natl Acad Sci U S A **107**(5): 2259-2264.

Wolfe, A. J., D. S. Millikan, J. M. Campbell and K. L. Visick (2004). "*Vibrio fischeri* σ^{54} controls motility, biofilm formation, luminescence, and colonization." Appl Environ Microbiol **70**(4): 2520-2524.

Wolfe, A. J. and K. L. Visick (2010). Roles of Diguanylate Cyclases and Phosphodiesterases in Motility and Biofilm Formation in *Vibrio fischeri*. The Second Messenger, Cyclic-Di-GMP. A. J. Wolfe and K. L. Visick. Washington, DC, ASM Press**:** 186-200.

Yankovskaya, V., R. Horsefield, S. Tornroth, C. Luna-Chavez, H. Miyoshi, C. Leger, B. Byrne, G. Cecchini and S. Iwata (2003). "Architecture of succinate dehydrogenase and reactive oxygen species generation." Science **299**(5607): 700-704.

Yip, E. S., K. Geszvain, C. R. DeLoney-Marino and K. L. Visick (2006). "The symbiosis regulator *rscS* controls the *syp* gene locus, biofilm formation and symbiotic aggregation by *Vibrio fischeri*." Mol Microbiol **62**(6): 1586-1600.

Yip, E. S., B. T. Grublesky, E. A. Hussa and K. L. Visick (2005). "A novel, conserved cluster of genes promotes symbiotic colonization and σ-dependent biofilm formation by *Vibrio fischeri*." Mol Microbiol **57**(5): 1485-1498.

VITA

Jakob was born in Syracuse, NY on February 8, 1984 to Sali Honess-Ondrey and Jeffrey Ondrey. After graduating high school, Jakob spent 5 years serving as a medic in the U.S. Army. In May 2010, Jakob received a B.S. in biology from North Park University in Chicago. During his undergraduate studies at North Park, he worked as a lab assistant for the microbiology course and was involved in a research project involving the prevalence of *Borrelia burgdorferi* in Chicago area ticks.

In August 2010, Jakob entered graduate school at Loyola University Chicago under the Integrated Program in Biomedical Science. He completed his masters work in the laboratory of Karen Visick, where he studied the genetic regulation of biofilm formation by *Vibrio fischeri*.

Upon successful completion of his M.S., Jakob will work in the Special Infectious Diseases Laboratory at Ann & Robert H. Lurie Children's Hospital of Chicago.